Volume 70C
Number 1
Jan.–Mar. 1966

Engineering and Instrumentation

U.S. DEPARTMENT OF COMMERCE

SECTION C

JOURNAL OF RESEARCH

NATIONAL BUREAU OF STANDARDS

Journal of Research

of the

National Bureau of Standards

C. Engineering and Instrumentation

JAN.–MAR. • 1966

VOLUME • 70C

NUMBER • 1

Editor: Martin Greenspan

Associate Editors: G. F. Montgomery, R. V. Smith

Publication dates:
Feb. 15, May 15, Aug. 15, Nov. 15, 1966

JOURNAL OF RESEARCH

The National Bureau of Standards Journal of Research reports research and development in the fields of activity shown at right. Also included from time to time are survey articles on topics closely related to the Bureau's scientific and technical program.

The Journal is published in three separate sections as follows:

A. Physics and Chemistry

Contains papers of interest primarily to scientists working in these fields. Issued six times a year. Annual subscription: domestic, $5.00; foreign, $6.00. Single copy, $1.00.

B. Mathematics and Mathematical Physics

Presents studies and compilations designed mainly for the mathematician and the theoretical physicist. Issued quarterly. Annual subscription: domestic, $2.25; foreign, $2.75. Single copy, 75¢.

C. Engineering and Instrumentation

Reports research and development results of interest chiefly to the engineer and the applied scientist. Issued quarterly. Annual subscription: domestic, $2.75; foreign, $3.50. Single copy, 75¢.

The National Bureau of Standards is a principal focal point in the Federal Government for assuring maximum application of the physical and engineering sciences to the advancement of technology in industry and commerce. Its responsibilities include development and maintenance of the national standards of measurement, and the provisions of means for making measurements consistent with those standards; determination of physical constants and properties of materials; development of methods for testing materials, mechanisms, and structures, and making such tests as may be necessary, particularly for government agencies; cooperation in the establishment of standard practices for incorporation in codes and specifications; advisory service to government agencies on scientific and technical problems; invention and development of devices to serve special needs of the Government; assistance to industry, business, and consumers in the development and acceptance of commercial standards and simplified trade practice recommendations; administration of programs in cooperation with United States business groups and standards organizations for the development of international standards of practice; and maintenance of a clearinghouse for the collection and dissemination of scientific, technical, and engineering information. The scope of the Bureau's activities is suggested in the following listing of its three Institutes and their organizational units.

Institute for Basic Standards. Applied Mathematics. Electricity. Metrology. Mechanics. Heat. Atomic Physics. Physical Chemistry. Laboratory Astrophysics.* Radiation Physics. Radio Standards Laboratory:* Radio Standards Physics; Radio Standards Engineering. Office of Standard Reference Data.

Institute for Materials Research. Analytical Chemistry. Polymers. Metallurgy. Inorganic Materials. Reactor Radiations. Cryogenics.* Materials Evaluation Laboratory. Office of Standard Reference Materials.

Institute for Applied Technology. Building Research. Information Technology. Performance Test Development. Electronic Instrumentation. Textile and Apparel Technology Center. Technical Analysis. Office of Weights and Measures. Office of Engineering Standards. Office of Invention and Innovation. Office of Technical Resources. Clearinghouse for Federal Scientific and Technical Information.**

*Located at Boulder, Colo. 80301.
**Located at 5285 Port Royal Road, Springfield, Va. 22171.

U.S. DEPARTMENT OF COMMERCE
John T. Connor, Secretary
NATIONAL BUREAU OF STANDARDS
A. V. Astin, Director

Order all publications from the Superintendent of Documents
U.S. Government Printing Office, Washington, D.C., 20402.

Use of funds for printing this publication approved by the Director of the Bureau of the Budget (June 19, 1961).

JOURNAL OF RESEARCH of the National Bureau of Standards—C. Engineering and Instrumentation
Vol. 70C, No. 1, January–March 1966

Coulometric Calibration of Microvolumetric Apparatus*

George Marinenko and John K. Taylor

(October 13, 1965)

Coulometric titration provides a simple and accurate means to calibrate microvolumetric apparatus such as burets, micropipets, and syringes. The apparatus to be calibrated is caused to deliver a solution of known concentration into an electrolysis cell where it is analyzed coulometrically. By the method described, volumes ranging from 300 μl to 1 μl have been calibrated with relative standard deviation of 0.03 to 3 percent, respectively.

Key Words: Constant-current coulometry, microburet calibrations, volume calibrations.

1. Introduction

Recent advances in the development of microvolumetric apparatus have benefited analysis in several ways. By use of solutions of ordinary analytical concentration and small volumes (10^{-3} to 10^{-6} ml), ultramicroanalysis of extremely small amounts of materials down to 10^{-12} g may be achieved [1, 2].[1] Furthermore, the use of concentrated reagents in microvolumetric amounts improves conventional titrimetric procedures by minimizing dilution effects on end-point determinations.

In order to conduct quantitative work with small volumes, however, it is necessary to have reliable methods for their calibration. Existing methods [2, 3] are essentially the same as have been used for macrovolumetric apparatus, for example, weighing the amount of a liquid of known density contained in or delivered by the apparatus. Unfortunately, this technique loses reliability when small volumes are concerned due to evaporative losses and liquid-transfer problems.

Titrimetric methods for calibration of small volumes have been suggested by Kirk [2]. However, he states that such procedures are inherently less accurate than weight calibration because all errors in the buret, in the end point, and in the concentration of the solution are included in the calibration.

The high precision of coulometric titrations [4, 5, 6] makes possible their use in volumetric calibrations. The method involves preparing a standard solution, dispensing a nominal volume of it with the volumetric apparatus to be tested, coulometrically determining the amount of reagent dispensed, and calculating the volume of reagent delivered.

2. Method

Primary standard potassium dichromate (NBS Standard Material 136b) is especially useful for the purpose of this method. It is stable in air, requires only superficial drying, and is highly soluble in water. Furthermore, it has been coulometrically assayed to a high degree of precision [6]. Accordingly, normal solutions can be readily prepared, corresponding to one microequivalent per microliter of solution.

The titration procedure is essentially that described in an earlier paper [6]. Briefly, it consists in the constant-current generation of Fe(II) at a platinum cathode in a solution 2 *M* in sulfuric acid and 0.5 *M* in ferric ammonium sulfate. The generated Fe(II) in turn reduces an equivalent amount of the dichromate. The end point is determined amperometrically (+0.85 V applied to a 1 cm^2 platinum indicator electrode, with reference to a saturated calomel electrode).

The coulometric cell used for high-precision calibrations consists of two electrode chambers separated by a two-compartment connecting tube. However, cells providing isolation of the anode in a glass tube whose bottom is a sintered-glass disk are satisfactory for the present purpose.

Polyethylene tubing drawn to a fine capillary opening is attached to the tips of the burets to be calibrated. Such tips provide a much smaller orifice than found on ordinary burets, thus minimizing interdiffusion of titrant with the solution when the tip is immersed, a procedure which is necessary for precise calibrations.

3. Results

The reliability of the coulometric method is illustrated with results obtained for the calibration of three typical volumetric instruments as follows:

A. An electrically driven positive-displacement buret (0.33 ml capacity) equipped with a revolution counter graduated to 0.01 microliter. The stainless

*This paper represents the results of an investigation undertaken during the spring of 1964 and presented at the Pittsburgh Conference on Analytical Chemistry and Applied Spectroscopy, Pittsburgh, Pa., March 1, 1965. While preparing the present manuscript, the publication "Coulometric Calibration of Micropipettes" by Gary D. Christian, Microchemical Journal 9, 16 (1965), has appeared which is similar in some respects.

[1] Figures in brackets indicate the literature references at the end of this paper.

steel piston has a nominal diameter of 0.099+in. The delivery tip is provided with a three-way stopcock so that the buret can be refilled in operating position.

B. A manual positive-displacement buret similar to the one described by Scholander [8]. The micrometer screw for volumetric read-out is subdivided in 0.2 μl intervals.

C. A 10 μl syringe subdivided in 0.1 μl intervals.

Results obtained for the calibration of buret A are given in table 1. The 300 μl graduation was also calibrated by the gravimetric method. Five determinations indicated the correction factor to be 1.0017, $s=0.0009$, which is in good agreement with the coulometrically determined value. Unfortunately, gravimetric calibrations are difficult if not impossible for samples much smaller than this.

TABLE 1. *Results for calibration of buret A*

Nominal volume delivered, μl	No. of determinations	Correction factor
		Volume, found/volume, nominal
300	3	1.0018, $s=0.0003$
100	8	1.0010, $s=$ .0015
50	3	1.0031, $s=$ .0021
20	3	1.0011, $s=$ .0013
10	3	1.005, $s=$ .002
5	5	1.008, $s=$ .003
1	7	1.002, $s=$ .034

An attempt was made to use buret A without immersing its tip but rather by collecting the fractional drop remaining on the tip by means of a glass rod. Results for 1- and 10-μl samples showed calibrations in agreement with those shown in table 1, but the standard deviations were about twice as large as those found with the immersion technique.

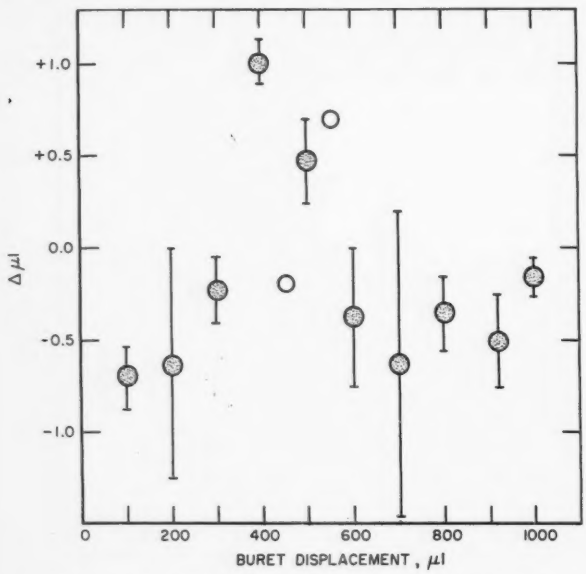

FIGURE 1. *Calibration of 100 μl aliquots delivered by different intervals of the piston displacement of buret B.*

○, Gravimetric values.
●, Coulometric values.
Average values are plotted. The vertical bars show the range of the individual measurements.

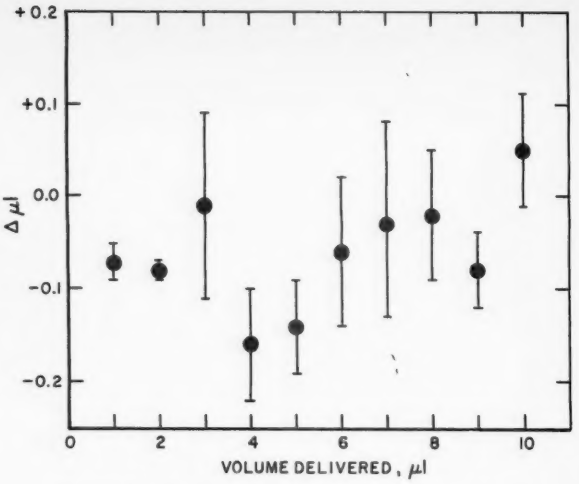

FIGURE 2. *Coulometric calibration of a 10-μl syringe.*
Average values are plotted. The vertical bars show the range of the individual measurements.

Results for the calibration of buret B at 100-μl intervals are shown in figure 1. The 0–100 μl interval was calibrated six times for which the correction -0.69 μl $s=0.17$ μl was found. Duplicate calibrations were made at all other intervals and the average values are plotted.

The open circles in the figure represent results of calibration of the 350 to 450 and the 450 to 550 μl intervals by a specially developed gravimetric procedure [9].

The results for duplicate calibrations of the 10-μl syringe, buret C, are shown in figure 2. In this case, the syringe was not mounted permanently in the cell. Rather, after adjusting to an initial reading, the needle was rinsed with distilled water, after which it was immersed in the cell for delivery of the volume indicated. The results no doubt indicate deviations from calibration as well as imprecision in delivering specified volumes with this type of equipment.

4. Discussion

The results of this investigation demonstrate the reliability of coulometric calibration of volumetric apparatus. For moderately small volumes (e.g., 300 μl), values comparable with gravimetric procedures are obtained. The coulometric method is specially useful for calibration of small volumes where weighing of calibrating liquids such as water and methylene iodide is impaired by evaporative losses and where weighing of mercury may be objectionable because of the drastically different physical properties of water and mercury.

The precision of the coulometric method appears to be limited by the sensitivity of the end-point determination. The present work was carried out with an 100-ml electrolytic cell, designed for high-precision measurements with amounts of 10 to 20 milli-

equivalent of materials [6]. In that application, an end-point uncertainty of about 0.01 microequivalent was noted which is comparable with the volumetric precision of the calibrations reported here. Some increase in precision of microcalibrations would undoubtedly be realized by the use of electrolysis cells of smaller capacity.

For work of the highest precision, the use of a standard such as potassium dichromate is preferred to establish the concentration of the calibrating solution. However, other solutions could be used provided that they were carefully standardized.

(Paper 70C1–165)

5. References

[1] I. P. Alimarin and M. N. Petrikova, Zavodsk. Lab. **24,** 29 (1958).
[2] P. L. Kirk, Quantitative Ultramicroanalysis (John Wiley & Sons, Inc., New York, N.Y., 1950).
[3] A. A. Benedetti-Pichler, Introduction to the Microtechnique of Inorganic Analysis (John Wiley & Sons, Inc., New York, N.Y., 1942).
[4] J. K. Taylor and S. W. Smith, J. Res. NBS **63A** (Phys and Chem), No. 2, 153 (1959).
[5] G. Marinenko and J. K. Taylor, J. Res. NBS **67A** (Phys and Chem), No. 1, 31 (1963).
[6] G. Marinenko and J. K. Taylor, J. Res. NBS **67A** (Phys and Chem), No. 5, 453 (1963).
[7] Handbook of Chemistry and Physics, 36th ed. (Chemical Rubber Publishing Co., Cleveland, Ohio, 1954–55).
[8] P. F. Scholander, Science **95,** 177 (1942).
[9] A. Johnson, NBS Metrology Division (212.31), private communication.

JOURNAL OF RESEARCH of the National Bureau of Standards—C. Engineering and Instrumentation
Vol. 70C, No. 1, January–March 1966

Effect of Temperature and Notch Geometry on the Tensile Behavior of a Titanium Alloy

William D. Jenkins and William A. Willard

(September 2, 1965)

A comprehensive study was made of the effects of notch geometry on the mechanical behavior of a duplex-annealed titanium-8 aluminum-1 molybdenum-1 vanadium alloy within the temperature range 75 to 1200 °F (297 to 921 °K). Yield strength, tensile strength, and true stress at fracture increased with increase in notch depth and decrease in notch angle and temperature. The maximum strength (tensile and yield) properties were obtained for the cylindrical specimens having a root radius of 0.01-inch. Generally, the increase in tensile properties was accompanied by a decrease in reduction of area values. The microstructures and the initiation and propagation of fracture of the specimens were affected by the notch geometry and test temperature.

Key Words: Notch geometry, tensile behavior, elevated temperature, titanium alloys, fracture, stress concentration, notch strength.

1. Introduction

Although many papers have been published describing the influence of notch geometry on the mechanical behavior of metals, only limited data are available from which consistent interpretations can be made when unnotched and notched cylindrical specimens having circular cross section are used. Brown and coworkers [1] [1] have recently made an extensive literature survey of high temperature properties of notched specimens. Geil and Carwile [2, 3] and Geil [4] have made comprehensive studies on the behavior of titanium alloys and the mechanisms of deformation of stainless steel at low temperatures. The present study was undertaken as a part of a general program designed to evaluate fundamental factors affecting flow, fracture, and ductility of metals at elevated temperatures.

2. Material, Specimens, and Test Procedures

The experimental program included short-time tensile tests at 75 to 1200 °F (297 to 921 °K) on unnotched and notched cylindrical specimens of a duplex-annealed Ti-8 Al-1 Mo-1 V alloy.

The test specimens were prepared from bars obtained from a single heat of the titanium alloy. The bars were supplied by the manufacturer in the form of 1-in. rounds in the hot-rolled and annealed condition. The chemical composition of the alloy is given in table 1.

TABLE 1. *Chemical composition (percentage by weight) of the alloy used* [a]

Titanium	90.4
Aluminum	7.7
Molybdenum	1.0
Vanadium	0.7
Iron	.08
Carbon	.01
Hydrogen	.0094
Oxygen	.0628
Nitrogen	.0022

[a] Analysis made at the National Bureau of Standards.

The bars were cut into lengths, each about 6.5-in. and annealed at 1750 °F (1226 °K) for 1 hr and air-cooled. This was followed by a stabilizing anneal for 8 hr at 1050 °F (838 °K). The specimens were then air-cooled. This process, called duplex annealing, is recommended by the manufacturer for obtaining a good combination of properties at high temperatures.

Each unnotched specimen had a 2-in. gage length and a gage diameter of 0.357 in. The reduced section was finished by grinding and polishing in the axial direction.

Each of the notched specimens had a circumferential V-notch of a predetermined notch angle and a root radius at the midpoint of the specimen. The root diameters were held constant at 0.357 in. while the diameters of the reduced sections were varied to produce notch depths of 10, 30, 50, 70, or 85 percent.[2] The different combinations of notch angles, notch depths, and root radii used in this investigation are shown in table 2.

[1] Figures in brackets indicate the literature references at the end of this paper.

[2] Notch depth $= \frac{D^3 - d^3}{D^3} \times 100\%$
where D = reduced diameter
d = diameter at root of notch.

TABLE 2. *Notched specimens*

Notch angle	Notch depth	Root radius	Elastic stress concentration factor	Figure numbers where data are plotted			
				Yield strength	Tensile strength	Notch strength / Tensile strength	Reduction of area
Degrees	*Percent*	*inch*					
0	50	0.01	3.9	4A	5A	7D	8A
30	50	.01	3.9	4A	5A	.....	8A
60	50	.01	3.9	4A, 4B, 4C	5A, 5B, 5C	7B, 7C	8A, 8B, 8C, 9A
90	50	.01	3.7	4A	5A	7D	8A
150	50	.01	2.2	4A	5A	7D	8A
60	10	.01	2.6	4B	5B	7B	8B, 9A
60	30	.01	3.5	4B	5B	7B	8B, 9A
60	70	.01	4.2	4B	5B	7B	8B, 9A
60	85	.01	4.2	4B	5B	7B	8B, 9A
60	10	.10	1.4	6A	6B	7A	9B
60	30	.10	1.6	6A	6B	7A	9B
60	50	.10	1.6	4C, 6A	5C, 6B	7A, 7C	8C, 9B
60	70	.10	1.6	6A	6B	7A	9B
60	85	.10	1.7	6A	6B	7A	9B
60	50	.003	6.7	4C	5C	7C	8C
60	50	.50	1.1	4C	5C	7C	8C

Notch geometries were selected to produce stress concentration factors [3] [5] varying from 1.1 (60° notch angle, 0.5-in. root radius, 50 percent notch depth) to 6.7 (60° notch angle, 0.003-in. root radius, 50 percent notch depth) as shown in table 2. Photographs of an unnotched specimen and several notched specimens are shown in figure 1. Representative microstructures of the material after duplex annealing are shown in figure 2. The microstructure indicates the existence of equiaxed alpha with stringers of Widmanstatten structure composed of alpha and beta. The presence of alpha (predominantly) and beta (small amounts) was confirmed by x-ray analysis of the samples.

[3] Stress concentration factor is equal to the ratio of the maximum normal stress to the nominal normal stress. It is directly proportional to notch depth and inversely proportional to notch angle and root radius.

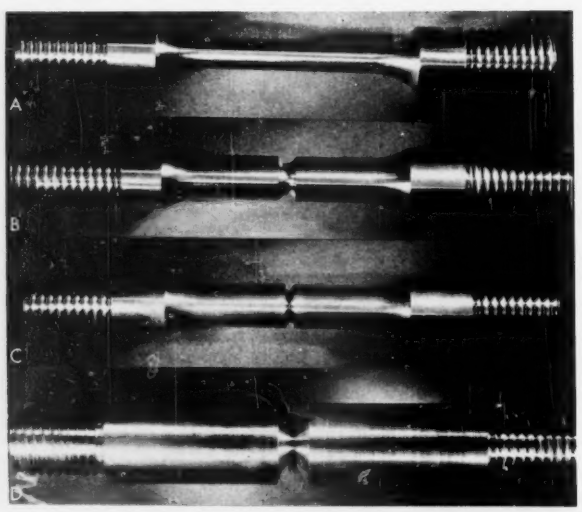

FIGURE 1. *Photographs, showing appearance of specimens before testing.* ×1/2

	Notch angle	Notch depth	Root radius
	Degrees	*Percent*	*Inch*
A	Unnotched	.....	.....
B	60	50	0.1
C	60	50	.01
D	60	85	.01

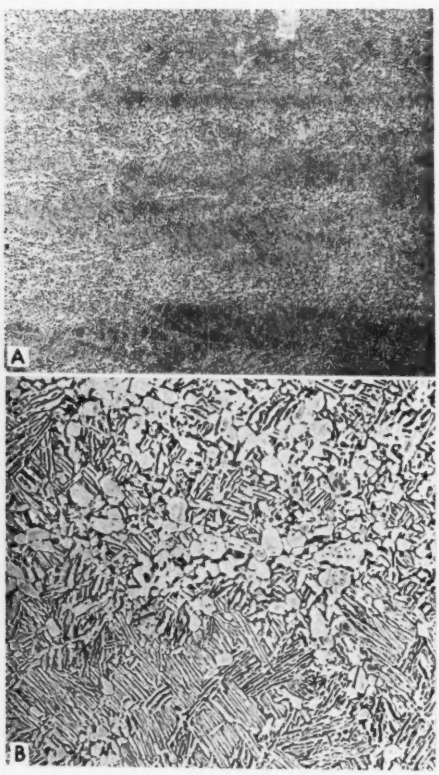

FIGURE 2. *Microstructure of the Ti-8 Al-1 Mo-1 V alloy after duplex-annealing.*

Longitudinal sections. Etched in a solution containing 3 ml HF, 6 ml HNO_3, and 100 ml H_2O. A, ×55. B, ×275.

Each tensile specimen was heated in air in a tube furnace to the desired temperature (above 75 °F), held for 1 hr, and tested at temperature. The movement of the crosshead of a hydraulic machine was controlled to produce the same rate of strain for all the specimens tested to fracture. This rate was about 1 percent per minute.

3. Results and Discussion

Some of the tensile properties of both the notched and unnotched specimens are shown in figures 3 to 12. The data are average values obtained from tests on different specimens tested under the same conditions. Yield strength values for the unnotched specimens were calculated by the 0.2 percent offset method. Yield strength values for the notched specimens were based on the stress at the first observable occurrence of plastic deformation. These values were further confirmed by load-time observations made throughout the tests. True stress at fracture values were calculated by dividing the load at fracture by the cross-sectional area of the specimens after fracture.

A small yield point drop was observed for all unnotched specimens tested at 75 and 300 °F (297 and 422 °K). The difference in stress between the upper and lower yield points was approximately 300 psi. At 600 and 800 °F (588 and 699 °K), no discontinuous flow was evident. At 1000 and 1200 °F (811 and 921 °K) wavy stress-strain curves of the type generally associated with extensive recovery or recrystallization were observed after the attainment of maximum load conditions.

The influence of temperature on tensile strength, yield strength and elongation of the unnotched specimens is shown in figure 3. The slope of the strength-temperature curve increases with increase in temperature up to 700 °F (644 °K). Thereafter this slope decreases as the temperature is increased. Apparently, the mechanisms associated with deformation of the alloy change near 700 °F as indicated by the rapid increase in the slope of the elongation-temperature curve. The possibility of changes in active slip systems in commercially pure titanium has also been mentioned [6] as a probable cause of this phenomenon.

The effect of notch geometry on yield and tensile strength of specimens tested at different temperatures is shown in figures 4 and 5. The shapes of the yield strength curves (fig. 4) are similar to those of the corresponding tensile strength curves (fig. 5). Although little or no plastic deformation is associated with the yield strength values, plastic deformation with its accompanying strain hardening effects plays an important part in the determination of the tensile strength of the alloy.

The increase of elastic stress concentration factor is a cause for the increase in both the yield and tensile strength. However, increase in notch depth (figures 4B and 5B) is a more effective strengthener than decrease in notch angles or root radius. For example, decreasing the notch angle from 150 to 0° had practically no effect on the strength values between 600

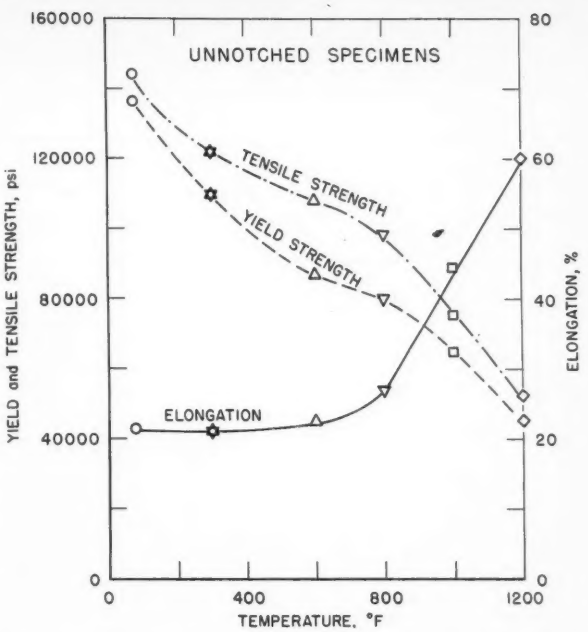

FIGURE 3. *Effect of temperature on tensile strength, yield strength and elongation of unnotched specimens.*
Each symbol (circle, triangle, etc.) designates the same test temperature in all figures except figure 10.

and 1200 °F (figs. 4A and 5A). Curves describing the effect of root radius on strength values (figs. 4C and 5C) indicate that an intermediate value of root radius exists for which the strength is a maximum. This relationship is more pronounced as the temperature is decreased. Although strength values generally increased with increase in notch depth, the sigmoidal shape of the strength-notch depth curves (figs. 4B and 5B) indicate the existence of a notch depth for which the rate of change of strength with notch depth is a maximum.

Another series of tests were run on specimens having a different root radius from those described in figures 4B and 5B to ascertain whether the conclusions drawn from one group of specimens were generally applicable when only one variable in the notch geometry was changed. The results shown in figure 6 were obtained on notched specimens having elastic stress concentration factors varying from 1.4 (10 percent notch depth) to 1.7 (85 percent notch depth) whereas data shown in figures 4B and 5B are for specimens having elastic stress concentration factors from 2.7 (10 percent notch depth) to 4.2 (85 percent notch depth).

Tensile and yield strength values for specimens having an 0.10-in. root radius (fig. 6A and B) were consistently lower than corresponding values for the specimens having an 0.01-in. root radius (figs. 4B and 5B). A general trend of increase in strength with increase in notch depth was observed for both notch geometries; however, the shapes of the curves at 600 and 800 °F were markedly affected by the increase in root radius from 0.01 to 0.10-in. That is, the specimens, having the 0.1-in. root radius, show a continuous

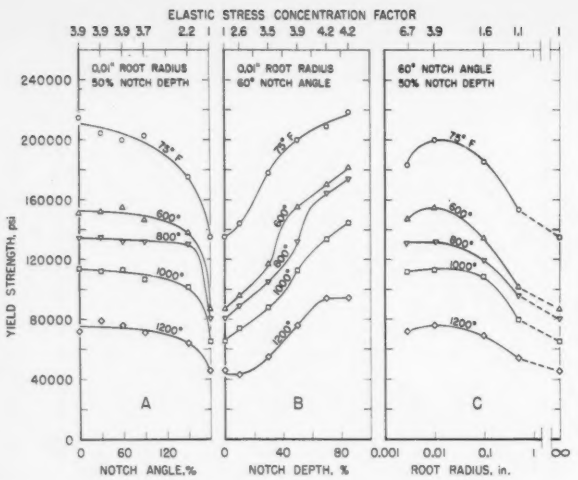

FIGURE 4. *Effect of notch angle, notch depth, and root radius on the yield strength of specimens tested at different temperatures.*
Data at 180-deg notch angle, zero percent notch depth, and infinite root radius indicate values for unnotched specimens.

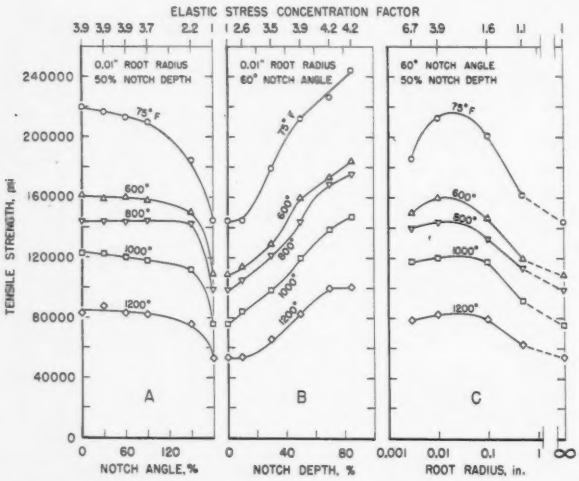

FIGURE 5. *Effect of notch angle, notch depth, and root radius on the tensile strength of specimens tested at different temperatures.*
Data at 180-deg notch angle, zero percent notch depth and infinite root radius indicate values for unnotched specimens.

increase in strength, at a decreasing rate, with increase in notch depth at these temperatures (fig. 6A and B); whereas, the corresponding curves for the specimens having an 0.01-in. radius have a sigmoidal shape (figs. 4B and 5B).

True stress at fracture increased with increase in notch depth and with decrease in test temperature as shown in figure 6C. These data give further evidence that, even at high temperatures and large strains, work hardening and fracture strength are dependent on the initial stress concentration factor.

One means of assessing the notch sensitivity of a metal is by calculating the ratio (R) of the tensile strength of the notched specimen to the tensile strength of the unnotched specimen at the same temperature. The effect of temperature on these ratios is shown in figure 7. For most of the specimens, the value appeared to be the highest at 1000 °F. Furthermore, it was more dependent on notch depth (ND) than on notch angle (NA) or root radius (RR). For an equal range of notch depths the spread in values is greater as the root radius is decreased (fig. 7A and B). However, there is a limiting value of root radius between 0.003 and 0.1-in. at which the "R" values begin to decrease with decrease in root radius (fig. 7C).

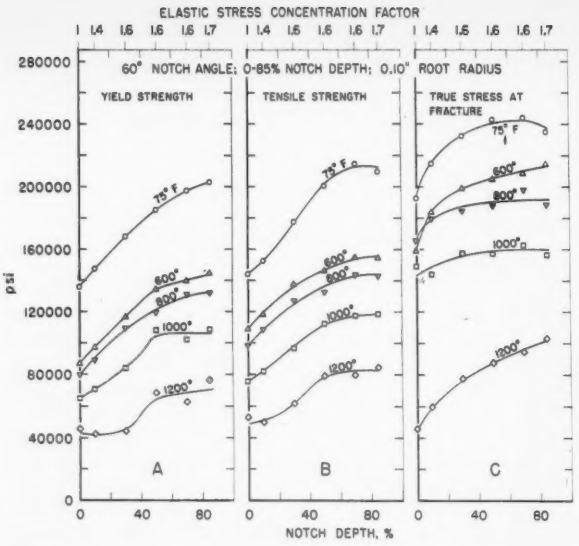

FIGURE 6. *Effect of notch depth on yield strength, tensile strength, and true stress at fracture of specimens having a 60-deg notch angle and 0.10-in. root radius.*
Data at zero percent notch depth indicate values for unnotched specimens.

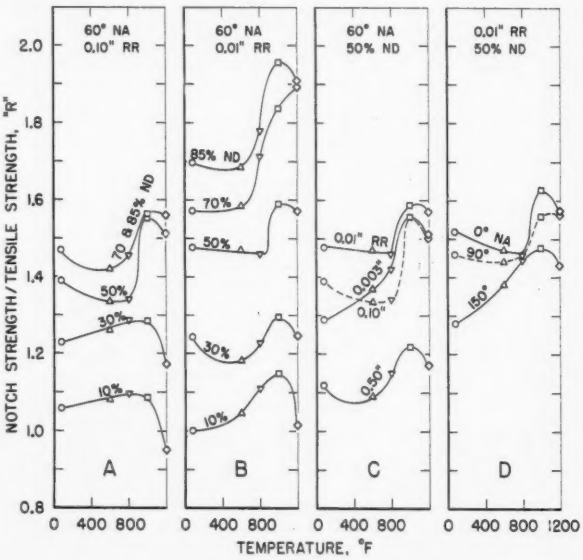

FIGURE 7. *Effect of temperature on the notch strength-tensile strength ratio (R) of specimens having various notch geometries.*

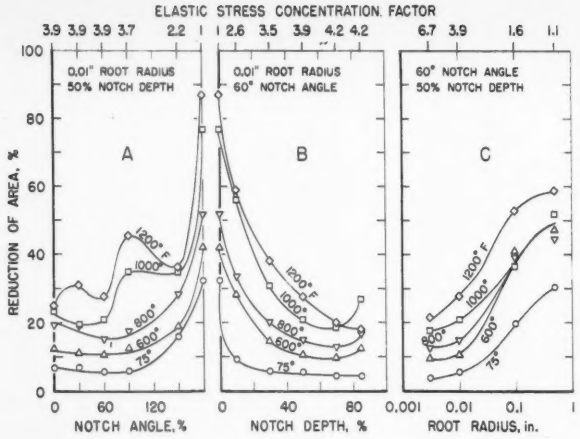

FIGURE 8. *Effect of notch angle, notch depth, and root radius on the reduction of area values of specimens tested at different temperatures.*
Data at 180-deg notch angle and zero percent notch depth indicate values for unnotched specimens.

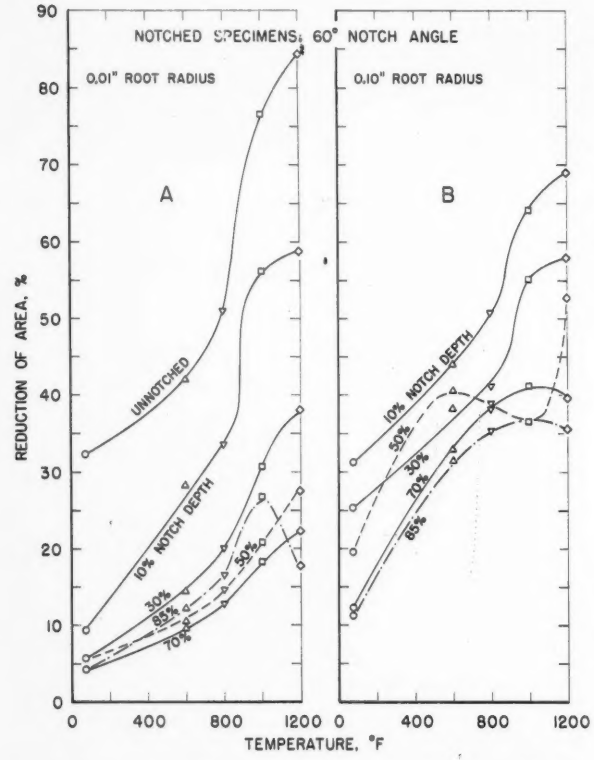

FIGURE 9. *Relation of temperature to reduction of area values for notched specimens having various notch depths.*
A—0.01-in. root radius; B—0.10-in. root radius.
Reduction of area values for unnotched specimens are included for comparison purposes.

The "R" values for 30 and 60° notch angles are not included in figure 7D as they lie between those for the zero and 90° notch angles. This is rather expected as, within limits, the angles have little effect on the stress concentration factors for specimens with the same notch depth, root radius, and diameter. For example, the stress concentration factor for the 90° angle specimen is 3.7 and for the 0° angle it is 3.9.

The effects of notch geometry and temperature on reduction of area values are shown in figures 8 and 9. In general, reduction of area values increased with increase in notch angle (fig. 8A) and root radius (fig. 8C) and with decrease in notch depth from 70 percent to zero (fig. 8B). The anomalies occurring at 1000 and 1200 °F (fig. 8A) are attributed to changes in recovery characteristics as the notch angles are changed. The cause of the inconsistent values for the specimens having an 85 percent notch depth is not known.

Reduction of area values increased with increase in temperature for most of the specimens having the same notch geometries as shown in figure 9. As indicated in figure 9A the presence of any notch causes some amount of embrittlement. However, increasing the root radius reduces the amount of embrittlement for all the conditions used (fig. 9B). Although duplicate tests have confirmed the test data for the 85 percent (fig. 9A) and the 50 percent notch depth specimens (fig. 9B) the reasons for the anomalies occurring at the different temperatures have not been discovered.

The relationship between true strain and true stress at fracture is shown in figure 10. True strain values in this figure are defined as $\log_e (A_0/A)$, where A_0 is the minimum cross-sectional area at the root of the notch before testing and A is the minimum area after fracture. The minima in figure 10A and the maxima in figure 10B indicate the existence of intermediate true strain values for which work-hardening is, respectively, least or most effective. This strain dependence is influenced by both temperature and stress system.

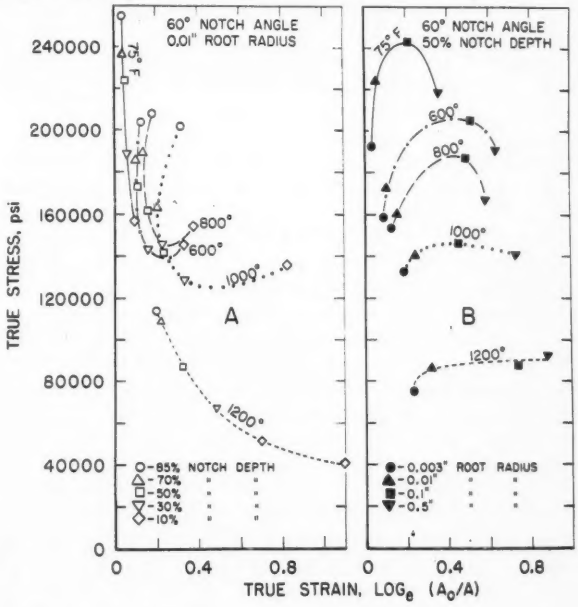

FIGURE 10. *True stress-true strain (at fracture) relations for notched specimens having (A) different notch depths and (B) different root radii.*

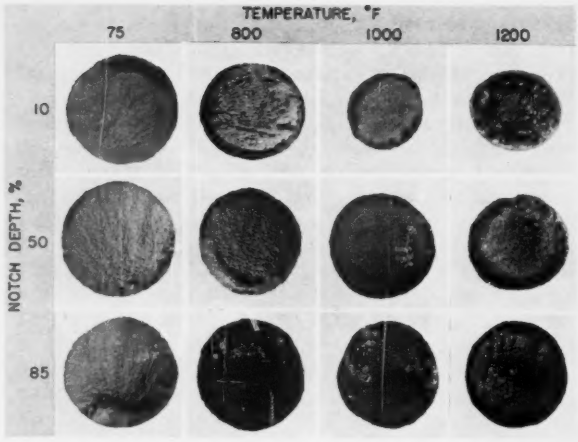

FIGURE 11. *Effect of temperature and notch depth on initiation and propagation of fracture.*
Cross sections at fracture of specimens having 60-deg. notch angle, 0.01-in. root radius. Unetched, × 2.

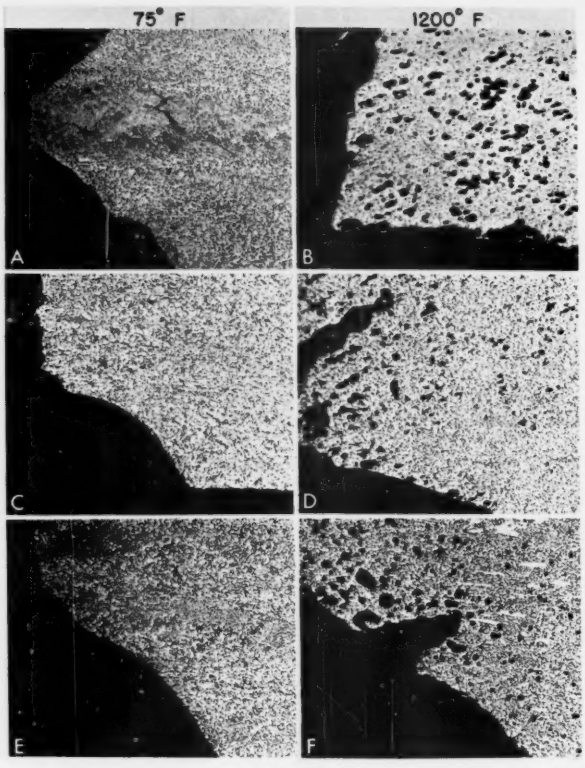

FIGURE 12. *Effect of notch depth on microstructures near root of the notch of Ti-8 Al-1 Mo-1 V specimens after fracture.*
A, B—unnotched; C, D—60° notch angle, 10 percent notch depth, 0.01 in. root radius; E, F—60° notch angle, 85 percent notch depth, 0.01-in. root radius. Longitudinal sections. Etched in a solution containing 3 ml HF, 6 ml HNO_3, and 100 ml H_2O. ×55.

4. Metallography

Geil and Carwile [3] have indicated that the position of initiation of fracture for titanium specimens was more dependent on notch geometry than on temperature within the temperature range −320 to 212 °F (77 to 373 °K). Fracture surfaces of some Ti-8 Al-1 Mo-1 V alloy specimens in the present investigation are shown in figure 11. Fracture at 75 °F was initiated at or near the root of the notch. As the temperature was increased, the point of initiation progressed towards the axis. At 1200 °F, fracture was initiated at the axis for all the specimens tested. Embrittlement effects associated with triaxiality were more predominant in the 85 percent notch depth specimens than in those with shallower notches. Furthermore, the more fully developed triaxiality conditions existed at lower temperatures for the specimens with the deeper notches. These observations indicate that, at high temperatures, the position of initiation of fracture and its mode of propagation are more dependent on test temperature than on the notch geometry.

Soltis [7] has observed that, during creep of Ti-8 Al-1 Mo-1 V alloy, voids were initiated at alpha grain boundaries in the vicinity of beta particles. In addition, Widmanstatten structure offered high resistance to deformation in smooth creep specimens of this duplex-annealed alloy. The effect of notch geometry on microstructures of specimens used in the present investigation is shown in figures 12, 13 and 14. Very few cracks were observed at the root radius of the notch (fig. 12A, C, and E) or at the axis (fig. 13A, C, and E) of the specimens tested to fracture at 75 °F. However, a number of holes and secondary cracks were observed near the surface (fig. 12B, D, and F) and near the center (fig. 13B, D, and F) of the specimens fractured at 1200 °F. The number and the size of the holes appeared to decrease as the notch depth was increased.

Several examples of the regions in which cracks or holes were formed are shown in figure 14. An isolated crack traversing an area of Widmanstatten structure is illustrated in figure 14A for an unnotched specimen fractured at 75 °F, whereas at 1200 °F the cracking was confined principally to the alpha grain boundaries (fig. 14B). A crack at the grain boundary of alpha grains that were formed from a metastable beta region in a 10 percent notch depth specimen is shown in figure 14C. Several cracks were observed in the region between alpha platelets and equiaxed alpha grains after fracture at 1200 °F (fig. 14D). Rounded holes rather than well defined cracks occurred in the regions of equiaxed alpha grain boundaries of the specimens having an 85 percent notch depth. Generally, these were observed near the regions having Widmanstatten structure (fig. 14E) in specimens tested at 75 °F while they were initiated near the vicinity of beta particles for specimens tested at 1200 °F (fig. 14F). It is apparent that both stress system and temperature had an effect on crack nucleation and growth in this alloy.

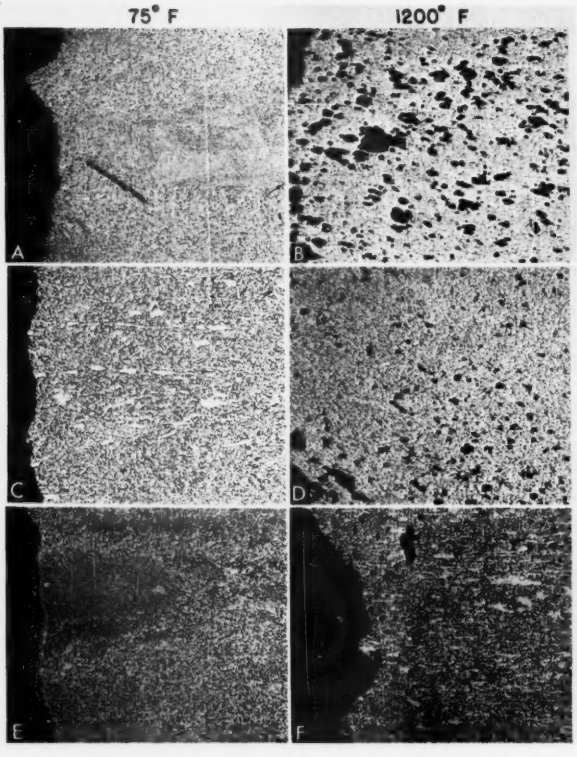

FIGURE 13. *Effect of notch depth on microstructures near axis of Ti-8 Al-1 Mo-1 V specimens after fracture.*
A, B–unnotched; C, D–60° notch angle, 10 percent notch depth, 0.01-in. root radius; E, F–60° notch angle, 85 percent notch depth, 0.01-in. root radius. Longitudinal sections Etched in a solution containing 3 ml HF, 6 ml HNO_3, and 100 ml H_2O. ×55.

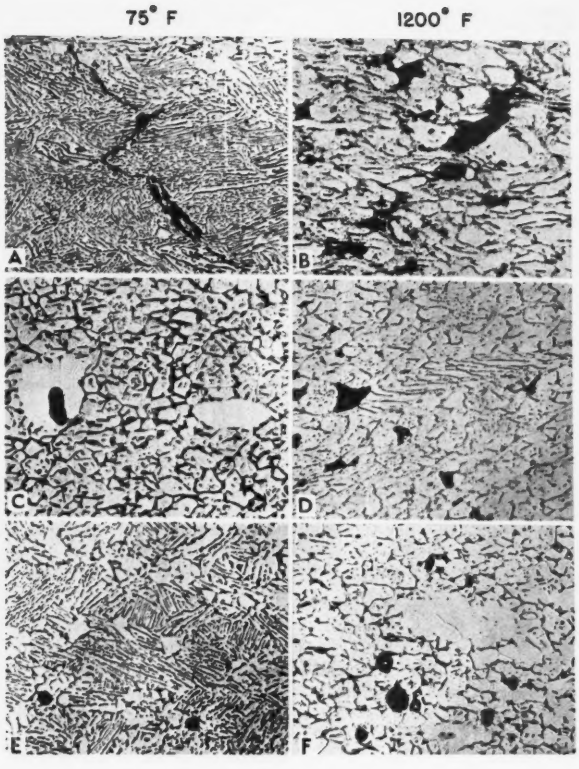

FIGURE 14. *Effect of notch depth on microstructures and crack formations in Ti-8 Al-1 Mo-1 V specimens.*
A, B–unnotched; C, E–60° notch angle, 10 percent notch depth, 0.01-in. root radius; E, F–60° notch angle, 85 percent notch depth, 0.01-in. root radius. Longitudinal sections. Etched in a solution containing 3 ml HF, 6 ml HNO_3 and 100 ml H_2O. ×275.

5. Summary

A. Short-time tensile tests were made to ascertain the effect of notch geometry and variation of temperature between 75 and 1200 °F on the mechanical behavior of a duplex-annealed Ti-8 Al-1 Mo-1 V alloy.

B. Yield and tensile strength decreased and elongation and reduction of area values usually increased with increase in temperature. Strength values generally increased and ductility decreased with decrease in notch angle and root radius and with increase in notch depth. Isolated exceptions to these general trends were observed at 1000 and 1200 °F, at 85 percent notch depth and at 0.003-in. root radius.

C. The notch strength-tensile strength ratio was the greatest at 1000 °F and was more dependent on notch depth than on root radius or notch angle.

D. Strength increased and ductility decreased with increase in elastic stress concentration factor and triaxiality. The manner in which these indicies changed was dependent on the test temperature and the parameters used in the evaluation of the data.

E. The point of initiation of fracture and its subsequent propagation were influenced by both temperature and notch geometry.

F. Only a few cracks or holes were observed for specimens tested at 75 °F; however, a large number were evident in specimens tested at 1200 °F. The number, size, shape, location, and distribution of the cracks were affected by notch geometry and temperature.

The authors are deeply grateful to H. Babb for his assistance with the metallographic examinations.

6. References

[1] W. F. Brown, S. S. Manson, G. Sachs, and J. G. Sessler, Literature survey on influence of stress concentrations at elevated temperatures, Am. Soc. Testing Mater., STP No. 260, 1 (1959).
[2] G. W. Geil and N. L. Carwile, Effect of notch geometry on tensile properties of annealed titanium at 100, 25, −78 and −196 C, Proc. Am. Soc. for Testing Mater. **59**, 985, (1959).
[3] G. W. Geil and N. L. Carwile, Fracture characteristics of notched tensile specimens of titanium and a titanium alloy, Mater. Res. Std. **1**, 16, (1961).
[4] G. W. Geil, Some effects of notch geometry and severe work-hardening on the tensile behavior of 310 stainless steel (to be published).
[5] R. E. Peterson, Stress concentration design factors (John Wiley & Sons, Inc., New York, N.Y., 1953).
[6] F. D. Rosi, F. C. Perkins, and L. L. Seigle, Mechanism of plastic flow in titanium, Trans. Am. Inst. Mining Met. Engrs. **206**, 115 (1956).
[7] P. J. Soltis, Instability and evidence of ordering in Ti-8 Al-1 Mo-1 V alloy, Trans. of the Met. Soc. of AIME **233**, 903 (1965).

(Paper 70C1–166)

JOURNAL OF RESEARCH of the National Bureau of Standards—C. Engineering and Instrumentation
Vol. 70C, No. 1, January–March 1966

Measurement Standards for Low and Medium Peak Pulse Voltages

A. R. Ondrejka* and P. A. Hudson*

National Bureau of Standards, Boulder, Colo.

(November 10, 1965)

Two systems for the measurement and standardization of peak pulse voltage have recently been developed in the Radio Standards Engineering Division of the National Bureau of Standards. Designed for use with pulses having durations as short as 10 nanoseconds, the systems represent the initial effort by NBS for establishment of standards in this field and it is expected that they will serve as the basis for a calibration service.

One of the systems is a refined, slideback voltmeter employing a solid state diode. The rise time is less than 10 nanoseconds and the instrument is useful for measurements in the range 5V to 100V as presently constructed.

The second system standardizes the output peak voltage level of pulse generators by means of cascaded zener diodes. The clipping level of the diodes is determined first by d-c voltage measurements and the system is subsequently used to generate pulses of known peak amplitudes. The rise time of the diodes is approximately 30 nanoseconds.

The accuracy of both systems is within 0.25 percent, and comparison measurements have been made between the two, and with other NBS a-c and rf (CW) voltage standards.

Key Words: Measurement, peak, pulse, pulse-limiting, slideback, standard, voltage.

1. Introduction

The use of pulse waveforms has increased significantly during recent years, resulting in a wider interest in measurement of pulse parameters. Pulses are used in a variety of applications such as high speed electronic computers, medical applications, pulse amplitude modulation of carrier waves, and for testing of broadband circuits and components. The time domain reflectometer is a good example of the latter. In addition, progress has been made in the state of the art of generation of fast-rise, short-duration pulses. Subnanosecond rise times are now common and work is progressing on picosecond rise-time pulsers.

The parameters of interest in measurements on pulses include the rise time and the peak voltage amplitude. Various types of instruments for performing these measurements are commercially available, the most common of which is the cathode ray oscilloscope. Other types include direct reading peak voltmeters which cover a wide dynamic range from a few millivolts to several kilovolts at pulse widths down to a fraction of a microsecond. The specified uncertainties of the instruments used for peak voltage measurement are generally 1 to 2 percent.

As a result of the wider application of pulse waveforms and the overall higher accuracies required in present-day measurements, the National Bureau of Standards has received requests for calibration services in the pulse parameters. It is the purpose of this paper to describe two systems for measurement and standardization of peak pulse voltage in the range 5V to 100V for pulses having durations of at least 10 nsec. These systems represent the initial efforts at NBS for establishing standards in this field and it is expected that they will serve as the basis for a calibration service.

Two independent systems were developed to allow intercomparison and thus better evaluate the absolute accuracies. One system is designed to measure the pulse voltage across its input terminals while the other generates a predetermined, accurately known, pulse voltage level. Intercomparison can then be carried out without the need for a transfer instrument.

The development of standards for pulse rise time measurement is planned for the future.

2. Principles of Operation and Design

The voltage waveform of interest here is a train of so-called "d-c" or unidirectional pulses [1].[1] That is, ideally (in the mathematical sense), the voltage excursion occurs in only one direction from the zero position. Usually the pulse width is much less than the time interval between pulses and the average voltage is small compared to the peak voltage. One of the problems is to obtain an accurate, continuous reading of a waveform whose instantaneous value is zero the greater part of the time.

*Radio Standards Engineering Division, NBS Boulder Laboratories, Boulder, Colo.

[1] Figures in brackets indicate the literature references at the end of this paper.

2.1. The Standard Measurement System

In the design of a system, for peak pulse voltage measurement, there are certain features which are necessary or desirable. Of primary importance is the system accuracy which requires that the design eliminate as many sources of error as possible even though some sacrifice in ease of operation may have to be made. Other desirable features include wide dynamic range, insensitivity to pulse duty cycle, and a continuous output reading. Since it is desired to use the system for measurements on fast-rise, short-duration pulses, it must also have an extremely broad bandwidth.

After theoretical and experimental investigation of various known measurement techniques, it was decided that a system based on the slideback principle would adequately fulfill the requirements mentioned above. Slideback voltmeters have been in use for a number of years and have been described in the literature [2, 3]. The principle involves comparing the unknown voltage to an accurately known, adjustable voltage. The circuit is arranged so that the two voltages oppose each other and null detection methods are used to indicate when the voltages are equal. For the measurement of d-c voltage, high accuracy and precision are attainable. In applying the principle to pulse voltage measurement a diode is employed to limit current drain from the d-c slideback source during the time interval between pulses. This time interval may be several orders of magnitude (e.g., 10^4) greater than the pulse width. The version used here can be described by referring to the circuit in figure 1, which is included for the purpose of illustrating the principle. In the absence of an input signal and with the d-c slideback voltage set to zero, no current flows in the circuit as evidenced by a null indication on the galvanometer. When a train of pulses (positive pulses for the circuit shown) is applied to the input, the diode becomes conducting and may be returned to its original nonconducting state by adjusting the reverse d-c (slideback) voltage until the diode is cut off and the galvanometer is again nulled. The reverse d-c bias voltage, which can be easily and accurately measured, is then equated to the peak pulse voltage.

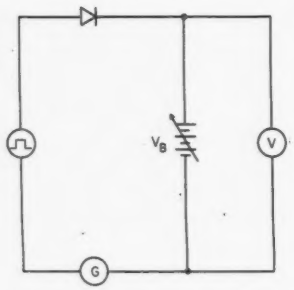

FIGURE 1. *Basic circuit of slideback principle.*

The accuracy of the system is primarily dependent on the validity of the assumption that, at a null condition, the d-c bias voltage is equal to the peak pulse voltage. The validity of this assumption is, in turn, a function of the characteristics of the diode. In an ideal diode both the back resistance and the forward conductance would be infinite while the rise time and shunt capacitance would be zero. The problem then was to choose an available diode having as nearly as possible these ideal characteristics. One of the critical characteristics is the forward conductance at low values of applied voltage. The forward conductance is important because of the finite sensitivity of the null detector. If some voltage, V_e, across the diode is required to cause a detectable current to flow, then the d-c slideback voltage, V_B, would be less than the peak pulse voltage, V_p, by an amount V_e which we have called the offset voltage. It is possible to measure the V_e of a particular diode and apply a correction. Some uncertainty would, however, be involved in this correction and, in general, it is desired to keep the correction as small as possible.

The forward diode current, I, is given approximately by the equation [4]

$$I = -I_s(\epsilon^{qv/kT} - 1) \tag{1}$$

where

I_s = reverse saturation current
q = electronic charge
v = applied voltage
k = Boltzmann's constant
T = Temperature, °K.

Thus the forward current is a function of the reverse current, I_s. This suggests the choice of certain types of point-contact diodes which have relatively large reverse currents. In the point-contact diodes tested, the reverse current did not reach a saturation value but, rather, tended to increase with increasing reverse voltage. The resultant heating effect caused changes in the forward characteristics. Thus the point-contact types were not suitable for this application. Junction diodes, on the other hand, are usually characterized by extremely low reverse currents and would not be suited because of the resulting large forward offset voltage. A diode type which is intermediate between these two is the metal-semiconductor type. In one version of this type, a gold wire is welded to n-type germanium to form a rectifying contact as in the 1N270 diode. The reverse resistance of the 1N270 is approximately 10 MΩ as compared to 1000 MΩ for typical junction types. A comparison of V–I curves for the 1N270 and a 1N4445 junction diode is shown in figure 2. The conductance of the 1N270 at the voltage levels shown is approximately 600 times greater than that of the junction type. Since conduction in metal-semiconductor diodes is by majority carriers, they have a better high frequency response (fast rise time) and in addition the shunt capacity is comparatively small. The rise time of the 1N270 is approximately 10 nsec and at present it appears to have the best overall

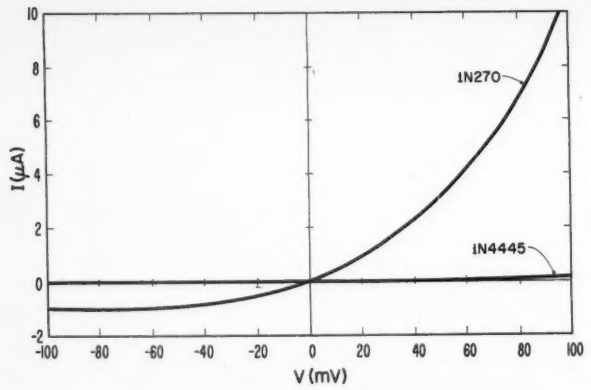

FIGURE 2. *Comparison of* V–I *characteristics of 1N270 gold bonded diode and 1N4445 junction diode.*

characteristics of the several diodes tested for this application.

Another important factor in the accuracy of the system is the means used for detecting when the diode is just at cutoff. The galvanometer detector mentioned earlier is not suitable because it responds to average current and thus suffers a considerable loss in sensitivity over that obtainable with a peak-responding detector. In addition, nulling the galvanometer would not guarantee equality between the pulse and d-c slideback voltages because of the reverse leakage current through the diode during the time interval between pulses. This current tends to reach a saturation value, I_s, of the order of 1μA (see fig. 2). The average reverse current, $\overline{I_R}$, then is given by

$$\overline{I_R} = I_s(1 - ft_p) \tag{2}$$

where f is the pulse repetition rate and t_p is the pulse duration. Typical pulse duty cycles, ft_p, range from 10^{-4} to 10^{-1} and thus $\overline{I_R}$ is equal to at least 0.9 I_s. The average forward current through the diode is given by

$$\overline{I_F} = I_p f t_p \tag{3}$$

where I_p is the peak current and a flat-top pulse is assumed. At null, $\overline{I_F} = \overline{I_R}$, and

$$I_p = \frac{I_s(1 - ft_p)}{ft_p}. \tag{4}$$

When the pulse duty cycle is 10^{-1}, for example, $I_p = 9\ I_s$, or approximately 9 μA. Referring again to figure 2, this current corresponds to 80 mV forward voltage and the peak pulse voltage must be larger than the d-c bias by this amount in order to null the galvanometer. At lower duty cycles, the pulse voltage would need to exceed the d-c bias by even greater amounts.

Due to the fact that the pulse duty cycle for narrow pulses is difficult to measure accurately and the reverse saturation current, I_s, varies with temperature, it is not practical to apply a correction for this effect.

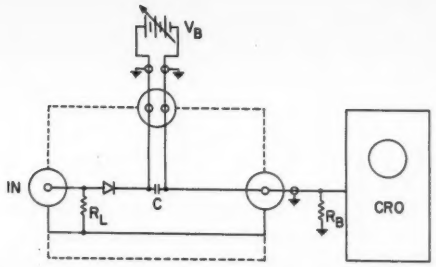

FIGURE 3. *Circuit diagram of slideback voltmeter system.*

A better detector was devised by substituting a coaxial resistor and a high gain cathode ray oscilloscope for the galvanometer. The circuit diagram of the complete measuring system is shown in figure 3. This is a peak detecting system and does not depend on average values of d-c current as previously. The CRO is set for capacitive coupling across the resistor, R_B. Pulses of current flowing through R_B are detected by the CRO and the d-c bias voltage is adjusted so that the top of the pulse just recedes into the baseline. The baseline is not affected appreciably by the reverse current[2] except for a very small differentiated pulse at the leading and trailing edges of the input pulses which is caused by the shunt capacitance of the diode.

Since the CRO detector has limited sensitivity, there will be some small forward pulse current, I_e, through the diode which is not detectable. As mentioned earlier, the voltage, V_e, which causes this current to flow is the difference (offset) between the peak pulse voltage and the d-c bias voltage. That is, $V_e = V_{\text{pulse}} - V_{\text{d-c}}$. Thus, when the d-c bias voltage has been adjusted to cause the peak of the pulse to just recede into the baseline, the diode will appear to be cutoff when in reality a small current continues to flow. It is possible to estimate the magnitude of the offset voltage by use of the *V-I* curve of figure 2 and a knowledge of the detector sensitivity. The detector sensitivity is 5 mV/cm and resolution is approximately 0.2 mm on the oscilloscope CRT which corresponds to a minimum detectable voltage of 0.1 mV. This voltage is the *IR* drop across the 50 Ω coaxial resistor, R_B, which terminates the coaxial line to the oscilloscope input and thus the minimum current is 2 μA. Referring to figure 2, it can be seen that at this current the offset voltage is 40 mV. This voltage is added to the measured d-c bias voltage as a correction. Due to thermal effects the offset voltage may vary ± 10 mV and this figure is taken as an uncertainty and it is independent of the input voltage level.

[2] It should be noted that when the bias voltage is equal to the input pulse voltage the reverse current goes to zero during the time the pulse is impressed across the diode. This interruption of the reverse current results in the generation of a small positive pulse. Since the reverse current is approximately 1 μA and the resistor is 50 Ω, the pulse voltage is 50 μV. The top of this pulse is the true baseline; however, due to the limited sensitivity of the CRO it appears only as a widening of the trace.

The detector sensitivity limits the ability of the operator to determine when the diode is just at cutoff and this is another factor which affects the accuracy of the measuring system. It was found experimentally that the random error caused by this factor alone resulted in variations in the reading of the peak pulse voltage as large as ±20 mV from the mean. In order to make a quantitative determination of this error, the standard deviation of the mean was calculated for a sample of 30 measurements made with the input voltage held constant. This value was calculated to be ±10 mV and was taken as an additional error which, again, is independent of the input pulse voltage level.

The other source of error is in the measurement of the d-c bias voltage. This measurement is made with a digital voltmeter which is accurate to within 0.05 percent of the indicated voltage. The overall system accuracy is estimated to be within 0.05 percent ±20 mV.

To complete the description of the measuring system, reference is made to figure 3. That portion of the circuit enclosed by the dashed lines is mounted in a small, round, metal container 1½ in. in diameter and 2½ in. long. The load resistor, R_L, consists of three film resistors connected in parallel. These resistors are easily removed so that R_L may be adjusted to match any generator impedance from 50 to 10,000 Ω. The parallel arrangement reduces the inductive reactance as compared to a single resistor and also increases the power dissipation capability. A second mount employing a 50 Ω coaxial resistor is used for measurements on pulses having the fastest rise times.

The slideback voltage is obtained from a battery pack containing ten 9 V batteries and one 12 V battery. Any or all of the batteries may be switched into the circuit and a 10-turn potentiometer across the 12 V battery serves as a vernier. The capacitor, C, connected across the battery serves as a path for the pulse current. Batteries cause much less distortion of the pulse than the electronically regulated supplies which were tried. The reason for the distortion by the regulated supplies has not been investigated extensively, but it is believed to be due to the filter capacitors and the frequency dependence of the internal impedance. Connection between the diode mount and the bias supply is made by means of a shielded cable. A 50 Ω cable is used to connect to the oscilloscope detector and this cable is terminated by the 50 Ω coaxial load, R_B, which is connected in parallel with the CRO input. The bandwidth of the CRO vertical amplifier is 50 MHz.

Since R_L may be as large as 10,000 Ω, the slide back system may also be used as a high impedance voltmeter. That is, it can be connected in parallel with the output of a pulse generator to measure and monitor the voltage level. The loading effect due to R_L is, in most cases, negligible.

2.2. The Standard Generating System

In order to provide a cross-check on the measuring system described above, a second independent system was developed. It was desired that the second system standardize the output level of a pulse generator to an accurately predictable value. In addition it was desirable that the output level be constant over relatively long periods of time. Intercomparison of this system and the first could then be carried out without the need for a transfer standard.

The most promising method for achieving these objectives appeared to be a circuit employing zener (reference) diodes to clip or limit the pulse generator output. The voltage level at which limiting occurred could be determined using accurately measured d-c voltage. It would then be assumed that pulse voltage limiting would occur at the same level. In order to establish the validity of this assumption, an investigation of the characteristics of zener diodes and their associated circuits was required.

The regulating action of zener diodes is now fairly well understood. This action occurs in reverse biased junction diodes when the reverse voltage, V, exceeds a certain critical value, V_c. The diode current increases extremely rapidly with $V > V_c$ causing the voltage drop across the junction to maintain a nearly constant value as shown in figure 4 [5]. The rapid increase in current is caused by an avalanche effect in the semiconductor material and is due mainly to majority (i.e., electron) carriers. Thus, the action can be fast and is highly desirable for pulse voltage limiting to avoid undue increase in the rise time of the output pulse over that of the input pulse.

A basic shunt zener regulating circuit is shown in figure 5a, with the a-c equivalent circuit of the zener junction shown in figure 5b. The junction capacitance, C_z, is of the order of a few hundred picofarads which results in the storage of charge in the junction.

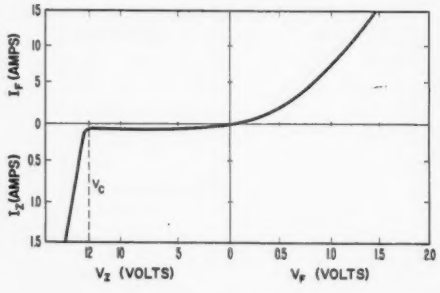

FIGURE 4. V–I *Characteristics of zener diode.*

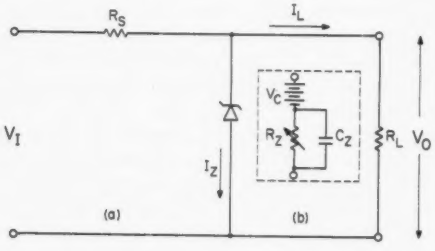

FIGURE 5 (a) *Basic zener regulating circuit;* (b) *A–C equivalent circuit of zener junction.*

This effect tends to limit the high frequency (and rise time) response. In designing the circuit for use as a d-c calibrated pulse voltage limiter, standard equations from handbooks were employed. The basic equation relating changes in output voltage, V_0, to changes in input voltage, V_i, load resistance, R_L, and temperature, T, is given by

$$dV_0 = \left(\frac{\delta V_0}{\delta V_i}\right) dV_i + \left(\frac{\delta V_0}{\delta R_L}\right) dR_L + \left(\frac{\delta V_0}{\delta T}\right) dT. \qquad (5)$$

In our application the second term in the above equation is not important because R_L is constant and $dR_L = 0$. The temperature effect on V_0 is, however, very important and required the use of diodes having low temperature coefficients. The importance of temperature coefficients is due to the fact that when calibrating V_0 using d-c voltage, the power dissipated in the junction may be several orders of magnitude greater than when the circuit is subsequently used with pulses. Temperature coefficients for the 10 and 50 W diodes used here are less than 0.1 percent/°C. It was desired to limit $\left(\frac{\delta V_0}{\delta T}\right) dT$ to 0.1 percent and hence the maximum temperature rise for a 50 W diode is 1 °C which corresponds to 1 W power dissipation in the junction. (The thermal resistance of these diodes is 1 °C/W.)

During the d-c calibration of V_0, the magnitude of V_i was adjusted so that the zener current I_z was large enough to insure good regulation (low zener impedance) and at the same time not exceed 1 W of power in the junction. In subsequently using the calibrated circuit on a pulse generator, it was assumed that $V_{i(\text{pulse})}$ could be set no closer than ± 10 percent of $V_{i(d\text{-}c)}$. It was required that the change in V_0 due to the uncertainty in $V_{i(\text{pulse})}$ be limited to 0.1 percent. Thus the value of $\frac{\delta V_0}{\delta V_i}$ in eq (5) could be no greater than 0.01 Using this information it was possible to calculate the value of the series resistor, R_s, for each diode by use of the equation

$$\frac{\delta V_0}{\delta V_i} = \frac{1}{1 + R_s\left(\frac{1}{R_Z} + \frac{1}{R_L}\right)}. \qquad (6)$$

In a typical example for a 12 V, 10 W zener and a 50 Ω load, the value of R_s is 400 Ω. The voltage drop across R_s is approximately 120 V and it must absorb 25 W of power. The same degree of regulation can be achieved with less power dissipation and voltage drop in R_s by connecting a second higher voltage zener circuit ahead of the first as shown in figure 6. The regulation required for each circuit is now only 0.1 (10 percent), and the values of R_{s_1} and R_{s_2} can be reduced to approximately 40 Ω each. The rise time of the double diode circuit is 50 nsec as compared to 30 nsec for the single diode.

Zener diodes are manufactured with breakdown voltages ranging from a few volts to well over 100 V.

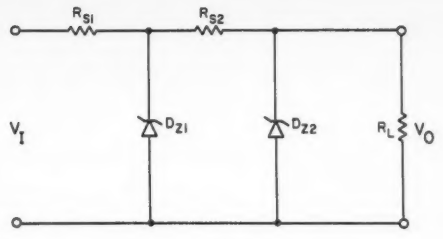

FIGURE 6. *Double zener circuit.*

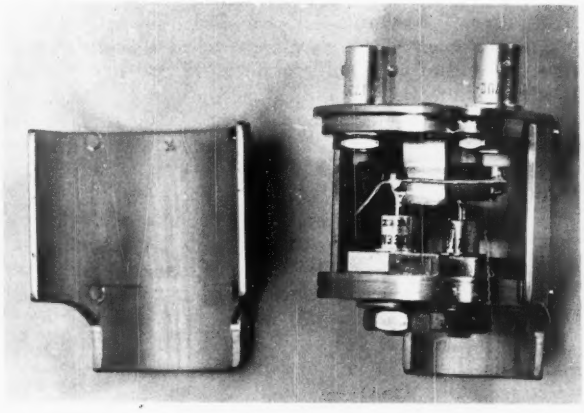

FIGURE 7. *Mount for zener diodes and resistors used in the standard generating system.*

Several circuits for various voltages in this range have been built and evaluated. In general, at the higher voltage levels it was found that the rise time could be improved by stacking several low voltage diodes in series rather than using a single high voltage unit.

Each zener circuit is mounted in a 2-in. diam by 2-in. high brass case as shown in figure 7. The performance of the circuits was improved by immersing the circuit and case in liquid nitrogen. Nitrogen is allowed to fill the case through holes in the top and bottom. This served to insure that the 0.1 percent temperature effect was not exceeded and allowed the series resistor, R_s, to be smaller in physical size.

3. Performance Characteristics and Results of Intercomparison

As mentioned earlier the estimated uncertainty of the standard measuring system using the 1N270 diode is no greater than 0.05 percent ± 20 mV. Due to the fixed 20 mV uncertainty and a maximum allowable error of 0.5 percent, the lower limit on the useful voltage range is 5 V. The upper limit of 100 V is fixed by the maximum allowed reverse voltage of the diode. The rise time of the circuit is 10 nsec and the minimum width of the peak of the pulse is 10 nsec.

794-732 O-66—2

Tests were made on the standard measurement system to determine the effect of pulse duty cycle on the accuracy. Within the limits of precision, the measuring system was found to be insensitive to duty cycle in the range 10^{-5} to 5×10^{-1}. These tests were made by varying separately both the pulse duration and the repetition rate.

In the zener circuits, as in the measuring system, the effects of varying the duty cycle were negligible. The errors in the system include the 0.1 percent due to temperature effects, the 0.1 percent due to the uncertainty in setting $V_{i(\text{pulse})}$ equal to $V_{i(\text{d-c})}$ and the 0.05 percent error in the d-c voltmeter used to measure the limiting voltage, V_0. Thus, the overall estimated accuracy is 0.25 percent.

The zener circuits may also be used to simply regulate the output of a pulse generator. In this application variations in the output amplitude of the pulse generator are reduced by a factor of 100 to 1 at the output of the zener circuit. Higher regulation can be obtained by increasing the value of the source resistor, R_s.

Comparison measurements have been made between the two systems and with the NBS a-c and CW rf voltage standards. At 100 Hz the disagreement was less than 0.1 percent, at 10 MHz and 30 MHz less than 0.3 percent, and at 100 MHz less than 2.5 percent. The uncertainty of the 100 MHz rf CW thermal voltmeter used in the comparison was approximately 1 percent.

Agreement between the standard measurement system and the standard generating system was within 0.3 percent at all voltage levels where comparison was made. These voltage levels were 6 V, 12 V, 24 V, 47 V, and 100 V.

A photograph of the console containing both standard systems is shown in figure 8.

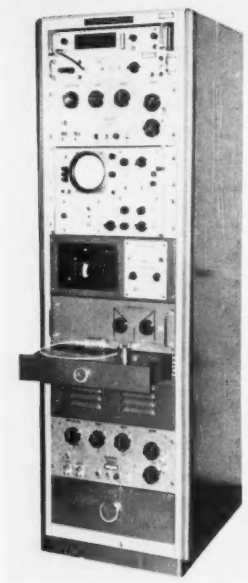

FIGURE 8. *Accessory equipment for both pulse voltage standards.* Included are the digital voltmeter, pulse generator, oscilloscope, and adjustable d-c bias supply.

(Paper 70C1–167)

4. Conclusion

The accuracies of the two systems for measurement and standardization of peak pulse voltage have been reasonably well established to be within 0.25 percent. These systems are considered an adequate basis for establishment of a calibration service for presently available commercial instruments.

Further work is planned to improve the performance characteristics of the systems and to develop new superior systems. Extension of the voltage range above the present 100 V will be an important part of this work.

5. References

[1] Standards on pulses: definition of terms, Proc. IRE, **39**, No. 6, (June 1951).
[2] F. E. Terman and J. M. Pettit, Electronic Measurements, pp. 34–36, (McGraw-Hill Book Company, 2d ed., 1952).
[3] M. C. Selby, High frequency voltage measurement, NBS Circular 481, (Sept. 1, 1949).
[4] Charles L. Alley and Kenneth W. Atwood, Electronic Engineering, p. 64, (John Wiley & Sons, Inc., New York, N.Y., 1962).
[5] Aldert Van Der Ziel, Solid State Physical Electronics, p. 287, (Prentice-Hall, Inc., 1957).

JOURNAL OF RESEARCH of the National Bureau of Standards—C. Engineering and Instrumentation
Vol. 70C, No. 1, January–March 1966

Temperature Coefficent of RF Permeability Measurement Using an Impedance Bridge as an Equality Indicating Device

A. L. Rasmussen*

National Bureau of Standards, Boulder, Colo.

(September 9, 1965)

Measurements are made on toroidal coils, without and with low-loss powdered iron samples inside, from approximately 23 to 50 °C and 300 kHz to 1.5 MHz. A high-precision Maxwell impedance bridge is used as an equality indicating device. Impedance changes of the toroidal coils are compensated by adjusting parallel capacitance and resistance standards which are external to the bridge. Data on several materials show that temperature coefficients of permeability of approximately 5×10^{-6}/°C may be evaluated.

Key Words: Equality indicating device, magnetic materials, Maxwell bridge, powdered iron materials, rf permeability, temperature coefficient, toroidal coils.

Definitions of Symbols

$(TC)_{\mu'}$ = Temperature coefficient of permeability.
$(TC)_{\mu''}$ = Temperature coefficient of the imaginary component of permeability.
μ'_T, μ''_T = Real and imaginary components of initial permeability at temperature T_2.
μ', μ'' = Real and imaginary components of initial permeability at temperature T_1.
$\Delta T = T_2 - T_1$.
ω = Angular frequency.
L_a = Equivalent air inductance of sample.
C_p, R_p = Parallel capacitance, parallel resistance to impedance Z of toroidal coil.
C_s, R_s = Parallel capacity, parallel resistance to impedance Z of toroidal coil with a sample inside.
C_e, R_e = Parallel capacity, parallel resistance to impedance Z of toroidal coil *without* a sample inside.
L_s, R_s = Toroidal coil inductance, resistance with a sample inside.
L_e, R_e = Toroidal coil inductance, resistance *without* a sample inside.
N = Number of turns of toroidal coil.
L_{space} = Equivalent inductance of space of toroidal form.
α = Coefficient of linear expansion.

1. Introduction

Magnetic materials with low-temperature coefficients of permeability are useful in stable inductors. This manuscript describes (1) a method for measuring low-temperature coefficient properties of low-loss materials, and (2) measurement results on toroidally shaped powdered iron samples.

The temperature coefficients of complex permeability, $(TC)_{\mu'}$ and $(TC)_{\mu''}$, are conventionally derived from the expressions

$$\mu'_T = \mu'[1 + (TC)_{\mu'}\Delta T], \tag{1a}$$

$$\mu''_T = \mu''[1 + (TC)_{\mu''}\Delta T], \tag{1b}$$

from which

$$(TC)_{\mu'} = \frac{\mu'_T - \mu'}{\mu'\Delta T} = \frac{(\Delta L)_{\mu'}}{\mu' L_a \Delta T}, \tag{2a}$$

$$(TC)_{\mu''} = \frac{\mu''_T - \mu''}{\mu''\Delta T} = \frac{\Delta R}{R\Delta T}, \tag{2b}$$

where $(\Delta L)_{\mu'} = (\mu'_T - \mu')L_a$. For some powdered iron materials a fractional change of permeability of the order of 10^{-6} per degree centigrade may be observed.

The accuracy of determining $(TC)_{\mu'}$ is largely dependent upon the accuracy in the determination of $(\Delta L)_{\mu'}$. Errors arise in the determination of $(\Delta L)_{\mu'}$ because (1) it is extremely small, especially for rod-shaped samples; (2) it may be masked by systematic inductance changes resulting from the movement or expansion of the wire winding, from the interaction of electric flux with the sample, etc; and (3) it may vary with the thermal cycling procedure because of magnetic aftereffect phenomena. Errors in $(TC)_{\mu''}$ are not discussed in this manuscript because of the difficulty in measuring the losses of low-loss materials. The problems related to the evaluation of $(TC)_{\mu'}$ are dis-

*Radio Standards Physics Division, NBS Boulder Laboratories, Boulder, Colo.

cussed. Dunton [1][1] gives a good discussion of specific measurement problems, some of which are related to other techniques.

Before describing the method, which is the subject of this manuscript, it is desirable to discuss briefly other methods [1–5]. A resonance method often utilized to determine inductance change involves the shift in frequency of an LC oscillator in which the inductor generally contains a rod of material surrounded by a coil subject to a temperature change. Temperature coefficients are computed after making corrections for the demagnetizing field at the ends of the sample and the inductance change of the coil alone. In another method the capacitance of a Q meter is adjusted to measure the inductance change of a toroidally shaped coil with a sample inside. A Maxwell bridge may also be used to measure directly the inductance change of toroidal coils. There are no demagnetizing field corrections. The change of inductance is larger than that for rods. Because it is difficult to determine, the coil inductance is often included in the measured temperature coefficient in the last two techniques. Dunton considers these two methods, although they are less sensitive than the LC oscillator technique, to yield better estimates of temperature coefficient and to be more suitable for the measurement of toroids. A method previously developed at the National Bureau of Standards makes use of the rf permeameter [2] [4, 6] in which a toroidal sample is measured in a small copper oven. The body and primary of the permeameter are held at room temperature by means of a water bath. The permeameter and a parallel capacitance standard are attached to an admittance bridge. Input impedance changes of the permeameter due to sample changes are compensated through adjustments of the external capacitor and the bridge conductance. Although convenient for measuring relatively high temperature coefficients, as found in some ferrite materials, this method does not yield the precision necessary for low temperature coefficient measurements.

In evaluating these methods, a measurement procedure similar to that using the rf permeameter was devised. It encompasses the convenience of using a bridge and a parallel capacitance and yields high precision. Subjected to a temperature change, the inductance changes of toroidal coils, without and with a low-loss powdered iron sample inside, are measured using a high precision Maxwell impedance bridge as an equality indicating device. The inductance changes are compensated by adjusting parallel capacitance, C_p, and parallel resistance, R_p, standards attached externally to avoid bridge errors. The circuit is shown in figure 1. The temperature and frequency ranges are approximately 23 to 50 °C and 300 kHz to 1.5 MHz, respectively. It appears that these ranges may be extended somewhat.

[1] Figures in brackets indicate the literature references at the end of this paper.

[2] The rf permeameter is a shorted section of coaxial line surrounding a primary winding which transforms the low coaxial impedance up to values which may be measured with commercially available instruments.

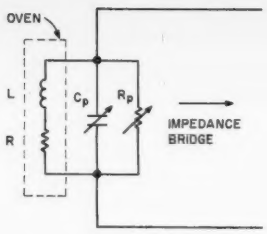

FIGURE 1. *Circuit used to measure temperature coefficient of permeability.*

2. Description of Method

Descriptions of the measurement procedure, of the equations pertinent to the method, and of the coils, bridge, standards and connectors, thermal system, and typical data follow.

2.1. Measurement Procedure

Two coils, one without and one with a sample inside, are carefully mounted in the oven. One of the coils is connected with the parallel components, C_p and R_p, to the bridge. (See fig. 1.) Although the two coils go through the thermal cycling procedure, only one is measured at a time; therefore, reference is made to the one coil being measured. This coil is thermally cycled one or more times, in 40 min intervals from an ambient temperature of ~ 23 to 50 °C and return, and then given 40 min to reach thermal equilibrium. The bridge is balanced, using its controls and the adjustable parallel capacitance and resistance standards, state 1. Additional time may be required to make certain that the frequency, temperature and bridge are adequately stable. During the rest of the procedure the capacitance and resistance standards are adjusted to compensate for any impedance change of the coil. The coil is heated to 50 °C in approximately 20 min and given approximately 40 additional minutes to reach thermal equilibrium, and the bridge is rebalanced, state 2. The coil is then cooled to ambient temperature and given approximately 40 min to reach thermal equilibrium at ambience, and the bridge is rebalanced, state 3. It requires at least 7 hr to complete a set of data on the two coils. Because of the near linearity of the temperature coefficient of permeability and the small changes observed, measurements are taken at only states 1, 2, and 3.

2.2. Equations

Each coil to be measured has an impedance of the form, $Z=R+j\omega L$, where L and R change with temperature. These changes are compensated by adjusting C_p and R_p to maintain the same impedance across the Maxwell bridge terminals.

To maintain the simplicity and accuracy of the measurements, it is necessary that

$$\omega^2 L^2 \gg R^2, \tag{3}$$

and that

$$L_{T2}^2 \approx L_{T1}^2 \tag{4}$$

and

$$[L_s - (\mu' - 1)N^2 L_a]^2 \approx L_e^2, \tag{5}$$

to within approximately 1 percent.

The impedance connected across the bridge terminals is expressed as at temperature T_1

$$R_{in} + j\omega L_{in} = \frac{1}{\frac{1}{R_{T1} + j\omega L_{T1}} + \frac{1}{R_{pT1}} + j\omega C_{pT1}}, \tag{6}$$

and, at temperature T_2,

$$R_{in} + j\omega L_{in} = \frac{1}{\frac{1}{R_{T2} + j\omega L_{T2}} + \frac{1}{R_{pT2}} + j\omega C_{pT2}}. \tag{7}$$

From these expressions, it can be shown that to a close approximation

$$\Delta L = L_{T2} - L_{T1} \approx (C_{pT1} - C_{pT2})\omega^2 L_{T1}^2 = \Delta C \omega^2 L_{T1}^2, \tag{8}$$

and

$$\Delta R = R_{T2} - R_{T1} \approx \left(\frac{1}{R_{pT1}} - \frac{1}{R_{pT2}}\right) \omega^2 L_{T1}^2 = \Delta G \omega^2 L_{T1}^2. \tag{9}$$

Considering (2) and the impedance changes of the coils, the temperature coefficients of the real and imaginary components of permeability can be expressed as

$$(TC)_{\mu'} = \frac{\Delta \mu'}{\mu' \Delta T} = \frac{\Delta L_s - \Delta L_e}{\mu' N^2 L_a \Delta T}, \tag{10}$$

and

$$(TC)_{\mu''} = \frac{\Delta R}{R \Delta T} = \frac{\Delta R_s - \Delta R_e}{R \Delta T}, \tag{11}$$

making use of the relation $(\mu' - 1) = (L_s - L_e)/N^2 L_a$ given by Danielson and Harrington [7]. In their formula, errors in permeability measurements subtract out. To obtain higher accuracy in permeability, they recommend that an air gap be introduced between the sample and the coil winding to reduce the interaction with electric flux. They used an air gap of 0.050 in. We used one greater than 0.12 in.

Equations (10) and (11) are more useful if expressed in terms of measured parameters. It can be shown that in (10) and (11)

$$\mu' N^2 La = (L_s - L_e)\mu'/(\mu' - 1) \tag{12}$$

and

$$R = R_s - R_e. \tag{13}$$

Therefore, substituting (8), (9), (12), and (13) into (10) and (11), we get

$$(TC)_{\mu'} = \frac{(\mu' - 1)\omega^2(\Delta C_s L_s^2 - \Delta C_e L_e^2)}{(L_s - L_e)\mu' \Delta T} \tag{14}$$

and

$$(TC)_{\mu''} = \frac{\omega^2(\Delta G_s L_s^2 - \Delta G_e L_e^2)}{(R_s - R_e)\Delta T}. \tag{15}$$

When samples have very low losses, $(TC)_{\mu''}$ cannot be determined accurately; therefore, such data are not presented in this paper.

Adequate resolution is obtained for the changes in the parallel capacitance standard and the coil inductance in the following way. An expression for L_a in terms of $N^2 L_{space}$ is determined for the lowest possible value of the temperature coefficient, $(TC)_{\mu' + coil}$, to be evaluated assuming $\Delta L_e = 0$.

From (8) and (10) we get

$$(TC)_{\mu' + coil} = \frac{\omega^2 \Delta C_s L_s^2}{\mu' N^2 L_a \Delta T}. \tag{16}$$

Neglecting leakage and violations of an assumption of a uniform current sheet, which subtract out in the expression of permeability, the coil inductance is

$$L_s \approx N^2(\mu' - 1)L_a + N^2 L_{space}. \tag{17}$$

Therefore,

$$(TC)_{\mu' + coil} \approx \frac{\omega^2 \Delta C_s [N^2(\mu' - 1)L_a + N^2 L_{space}]^2}{\mu' N^2 L_a \Delta T}, \tag{18}$$

and

$$\frac{\partial (TC)_{\mu' + coil}}{\partial L_a} = \frac{\omega^2 \Delta C_s N^2}{\mu' \Delta T}\left[(\mu' - 1)^2 - \frac{L_{space}^2}{L_a^2}\right] = 0, \tag{19}$$

for a maximum or minimum value of $(TC)_{\mu' + coil}$.

From (19) for a minimum, the inductance is

$$L_a \approx \frac{L_{space}}{(\mu' - 1)}. \tag{20}$$

Consequently, the minimum or lowest temperature coefficient is

$$_{min}(TC)_{\mu' + coil} \approx \frac{4\omega^2 \Delta C_s N^2 L_{space}(\mu' - 1)}{\mu' \Delta T} \tag{21}$$

and

$$N^2L_{space} \approx \frac{(TC)_{\mu'+coil}\mu'\Delta T}{4\omega^2\Delta C_s(\mu'-1)}. \quad (22)$$

To find N^2L_{space}, estimates are made for all the parameters on the right of (22) as follows:

$_{min}(TC)_{\mu'+coil}$ = lowest value to be detected
$\mu' \approx (\mu'-1)$
ΔT = range to be covered
ω = upper limit of the frequency range
ΔC_s = lowest value yielding the desired resolution in $_{min}(TC)_{\mu'+coil}$.

The following effects need to be considered in relation to the equations given: (1) the thermal expansion of the sample material and (2) the change of the self-capacitance of the coil. Considering the first, it can be shown, for $\mu_T' \approx \mu'$, that (14) is

$$(TC)_{\mu'} \approx \alpha + \frac{\mu_T' - \mu'}{\mu'\Delta T}. \quad (23)$$

Apparently the error in the true temperature coefficient due to an expansion may be large. Equation (14) is used to avoid measuring the thermal expansion. However, the temperature coefficients given by (14) or the right side of (23) are, in either case, linear and useful properties. Referring to the second problem, the computed change of self-capacitance from the expansion of the lead wires is negligible. Computed values of temperature coefficient without self-capacitance corrections do not vary appreciably with frequency regardless of the sample considered. However, the temperature coefficient of the coil inductance for a given solid wire decreases with frequency. The frequency dependence of the skin depth may affect the temperature dependence of the coil inductance.

2.3. Coils

For highest accuracy, two coils, one without and one with the sample inside, should be wound identically with wire of very uniform physical and electrical properties. Excluding any change from a sample, identical windings should result in similar impedance changes with temperature. Ideally a coil, after thermal cycling, should return to its original impedance at the initial temperature. Fused silica forms with temperature coefficient of linear expansion $\approx 5 \times 10^{-7}$/°C are used. These forms have grooves and spacers with holes precisely determining the path of the winding and lead wire. (See fig. 2.) Each form is a toroidally shaped cup having a wall thickness of 0.1 in. and one open end for inserting a sample before applying a winding. The cup is designed to allow air circulation. Each wire across either face of the cup makes an 18° angle with the radius except on the tenth and final turn where the leads are separated 0.1 in. The wires along the sides of the form lay perpendicular to the faces. Even though some undesirable stresses may thereby be introduced in the wire, the windings are glued in position with an electrical insulating cement. A toroid of the material to be measured does not touch the winding and is symmetrically spaced within it.

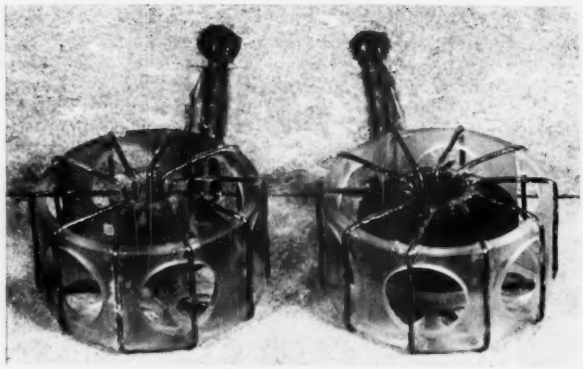

FIGURE 2. *Toroidal coils without and with a sample as they appear in the oven.*
The extra pairs of leads go to thermoelements used to measure temperature.

The type and condition of the wire itself are important considerations. Litz and solid copper wires with insulation were tested. A given piece of litz wire (90 strand No. 24) formed into a winding and subjected to a given temperature change at a given frequency gave erratic values of $(\Delta L/\Delta T)$; each new wire also resulted in a different value. Perhaps a different kind of litz wire would give better results. However, No. 20 solid copper wire proved satisfactory. It was thermally cycled from ~23 to 50 °C before each set of measurements to relieve stresses, which are mostly introduced when making the winding. High temperature stress relieving is not possible. The cycling also relieves a material somewhat from magnetic aftereffect.[3] For several pairs of coils, using No. 20 solid copper wire with insulation, the precision in temperature coefficient of permeability measurements was approximately 5×10^{-6}. The temperature coefficient of inductance of the coils without a sample is about 80×10^{-6}/°C.

2.4. Bridge

A high-frequency Maxwell bridge is used which may have an uncertainty in the magnitude of the impedance of the order of 0.1 percent. The frequency range is of the order of 1 kHz to 2 MHz. The minimum inductance, which can be measured directly, is 2×10^{-9} H; and the minimum resistance is 2×10^{-4} Ω. By using the bridge as an equality indicating device in the manner already discussed, changes of inductance two orders of magnitude smaller than this minimum may be determined. Errors from bridge instability are negligible.

[3] Interestingly, measurements show that any apparent aftereffect phenomena are greater in the materials with bakelite binder than those with Teflon. The former materials need cycling several times while the latter generally once.

FIGURE 3. *Equipment used in making temperature coefficient of permeability measurements.*
On the left, coil leads are shown from the oven to the bridge. On the right and center, standards are shown attached to the bridge (cylindrical objects).

2.5. Standards and Connectors

High precision adjustable NBS standards of capacitance and resistance fitted with NBS connectors are utilized as parallel components compensating for impedance changes in the coil forms being evaluated. (See fig. 3.) These components have well-defined immittances at their NBS terminals. A cube connector (fig. 3) with six NBS terminals is used to make the component and bridge connections of the circuit shown in figure 1. The uncertainty in temperature coefficient of permeability due to the uncertainties in these standards is negligible when compared to the precision of the measurement.

The ranges of the standards and their calibration frequencies are

Range of standards	Calibration frequencies
Capacitance, 50–1100 pF	300 kHz to 1.5 MHz
Resistance, 600–3000 Ω	300 kHz
500–610 Ω	600 kHz and 1 MHz
1000–1110 Ω	1 MHz and 1.5 MHz

2.6. Thermal System

The uncertainty in the oven temperature is ± 0.1 °C. The circulating air is warmed by heating coils and cooled by injecting CO_2. The heater, injector, and circulator are turned off during the short periods of actual data taking. Copper-constantan thermocouples monitor the temperature of the coils and samples.

2.7. Data

The temperature coefficient of permeability data shown in tables 1, 2, 3, and 4 have an estimated uncertainty of approximately 5×10^{-6}/°C. Accuracy is affected by any nonuniformity in the winding. (See tables.) Material 1 data for three frequencies and coil pairs 1 and 2 show excellent agreement. Coil pairs 3 and 4 do likewise, but differ somewhat from coil pairs 1 and 2, presumably because of inadvertent overheating of the sample. Measurements not shown on two different size samples of material 1, using another size form, yielded $(TC)_{\mu'}$ of 73×10^{-6}/°C and 74×10^{-6}/°C at 1 MHz, which indicates a uniform $(TC)_{\mu'}$. The fourth set of material 1 data also indicates no apparent change in properties after the toroidial ID is increased from 0.7 in. to 0.9 in. The purpose in reducing the volume of the sample was to ascertain whether the data were being affected by the proximity of the toroid to the center of the fused silica form. There appears to be no apparent change in $(TC)_{\mu'}$ with the frequency for each material, implying that the self-capacitance change of the coils with temperature is negligible. Data obtained using litz wire, not reported for reasons already discussed, show an effective $(TC)_{\mu'}$ unchanged to 1.5 MHz, where the greatest correction, if any, from the change of self-capacitance would occur. When coils with more uniform properties can be made, the accuracy in temperature coefficient of permeability measurements should improve. Tables 1, 2, 3, and 4 temperature coefficient of permeability, $(TC)_{\mu'}$, for the temperature interval of approximately 23 to 50 °C, low-loss, powdered iron toroids were measured.

TABLE 1. *Powdered iron material 1, Teflon binder, $\mu' = 6.32$*

Sample dimensions: O. D. 1.402 in., I. D. 0.701 in., and H 0.333 in. $(TC)_{\mu'}$

Frequency	Coil pair 1 [a]	Coil pair 2 [a]	Coil pair 3 [b]	Coil pair 4 [c]
300 kHz	$77 \cdot 10^{-6}$/°C	$74 \cdot 10^{-6}$/°C	$69 \cdot 10^{-6}$/°C	$69 \cdot 10^{-6}$/°C
600 kHz	78	74	72	71
1 MHz	79	78	75	74

[a] Obtained without grooves and lead spacers on the form to position precisely the path of the windings and leads.
[b] Sample inadvertently heated at 75 °C for 1 hr between pair 2 and pair 3.
[c] Sample 4 with I. D. increased from 0.7 in. to 0.9 in.: measured after coil pair 3.

TABLE 2. *Powdered iron material 2, carbonyl SF, $\mu' = 8.15$*

Sample dimensions: O. D. 1.300 in., I. D. 0.701 in., and H 0.300 in.

Frequency	$(TC)_{\mu'}$
300 kHz	$36 \cdot 10^{-6}$/°C
600 kHz	41
1 MHz	40

TABLE 3. *Powdered iron material 3, Teflon binder, $\mu' = 8.52$*

Sample dimensions: O. D. 1.316 in., I. D. 0.714 in., and H 0.301 in.

Frequency	$(TC)_{\mu'}$
300 kHz	$177 \cdot 10^{-6}$/°C
600 kHz	177
1 MHz	182

TABLE 4. *Powdered iron material 4, carbonyl E, $\mu' = 9.30$*

Sample dimensions: O. D. 1.250 in., I. D. 0.701 in., and H 0.275 in.

Frequency	$(TC)_{\mu'}$
300 kHz	$67 \cdot 10^{-6}$/°C
600 kHz	72
1 MHz	69

Pertinent Information for Data in Tables 1, 2, 3, and 4

Fused silica form dimensions: O. D. 2.000 in., I. D. 0.480 in., H 1.000 in., and walls 0.100 in. $L_{space} = 7.04 \cdot 10^{-9}$ H.

Winding materials and turns: No. 20 solid copper wire with insulation coating; ten turns.

Data Used: Mean value of inductance changes between states 2 and 1 and between states 2 and 3 without sample and with sample coils. See section 2.1 for a description of the states. Using heating and cooling data, the difference in values of temperature coefficient of permeability, $(TC)_{\mu'}$, is of the order of 1×10^{-6}/°C.

Formula used: Equation (14) of text.

Estimated uncertainty: $\approx 5 \times 10^{-6}$/°C.

The author thanks R. S. Yoshida for making most of the measurements, assisting with instrumentation, winding coils, and performing numerous other tasks; and A. E. Hess and L. E. Huntley for their suggestions pertinent to the NBS standards.

3. References

[1] Dunton, J. A., The temperature coefficient of permeability of carbonyl-iron power cores—its assessment and control, Progress in Powder Metallurgy—1964, Proc. Twentieth Annual Powder Metallurgy Technical Conf. and Magnetic Inductance Core Conf., 244–258.

[2] Dunton, J. A., An equipment for measuring the temperature coefficient of permeability of powder cores, Progress in Powder Metallurgy—1960, Proc. Sixteenth Annual Powder Metallurgy Technical Conf. and Magnetic Inductance Core Conf., 200–209.

[3] Rodrian, R. H., Method of determining temperature coefficient of electronic core materials, Progress in Powder Metallurgy—1954, Proc. Tenth Annual Powder Metallurgy Technical Conf. and Magnetic Inductance Core Conf., II—Electronic Core Session, 78–83.

[4] Rasmussen, A. L., and A. E. Hess, RF permeameter techniques for testing ferrite cores, Elec. Mfg. **61**, No. 5, 86 (May 1958).

[5] Polydoroff, W. J., High-frequency magnetic material, their characteristics and principal application, pp. 100–107 (John Wiley & Sons Inc., New York, N.Y., 1960).

[6] Hoer, C. A., and A. L. Rasmussen, Equations for the radio-frequency magnetic permeameter, J. Res., NBS **67C** (Engr. and Instr.) No. 1, 69–76 (Jan.–Mar. 1963).

[7] Danielson, B. L., and R. D. Harrington, A technique for reducing errors in permeability measurements with coils, Proc IRE **48**, 365–366 (1960).

(Paper 70C1–168)

JOURNAL OF RESEARCH of the National Bureau of Standards—C. Engineering and Instrumentation
Vol. 70C, No. 1, January–March 1966

A Test Apparatus for the Study of Forced Air-Mixing Devices

T. K. Faison, J. C. Davis, and P. R. Achenbach

(October 28, 1965)

The National Bureau of Standards has initiated a study of mixing devices for air streams to improve the techniques for measuring the capacity of air-conditioning, heating, and refrigeration equipment. Better mixers in these test apparatus will reduce the amount of instrumentation required, and increase the accuracy in capacity determinations that are based on enthalpy change of the air passing through the equipment. An apparatus for measuring the effectiveness of mixing devices, a small-scale apparatus for visually observing the mixing process, and some illustrative results are presented. The apparatus for measuring mixer effectiveness generates a stream of moving air of known and reproducible nonuniformity of temperature or humidity, provides for the installation of one or more mixers in a measuring section, and incorporates the means for measuring static pressure, velocity pressure, temperature, and humidity upstream and downstream of the mixer. The flow-visualization apparatus provides a qualitative visual evaluation of the effectiveness of small-scale models of mixers as a basis for selecting the specimens for the more elaborate measurements. Graphic material is included which illustrates the performance of the apparatus and the methods used in determining effectiveness of mixing devices.

Key Words: Air-conditioning capacity, air-mixing devices, forced air-mixing, turbulence, mixer effectiveness, apparatus design, air properties, temperature measurement.

1. Introduction

Professional societies, standards organizations, and manufacturers' associations have published test procedures for measuring the capacity of heating, air-conditioning, and refrigerating equipment in which air is the heat-transfer medium. These standards describe methods for measuring the mass flow rate of air and the unit change in enthalpy of the air stream between selected stations in the air circuit as a means of determining a heating or cooling capacity. Various types of flowmeters have been used for measurement of the mass flow rate of air, and the performance characteristics of some of these have been described in detail in the literature [1].[1] The unit change in enthalpy of a stream of air while passing through a heating or air-conditioning device is usually determined from the dry-bulb temperature only when no change in moisture content of the air has occurred, and from the dry-bulb temperature and wet-bulb temperature or dew point if evaporation or condensation has occurred.

In a typical situation the stream of air entering and leaving a piece of air-conditioning equipment is nonuniform with respect to velocity, dry-bulb temperature, and moisture content in the cross section of both the inlet and outlet openings. Under these conditions the enthalpy of the air stream at the inlet and outlet can be accurately determined only if an accurate average of temperature and moisture content of the air is obtained at each station. If the velocity of the air is uniform at the cross section where the temperature and humidity measurements are made, an arithmetic average of these properties in a suitable number of incremental areas of equal size in the cross section is adequate. However, if the velocity, temperature, and humidity are all nonuniform, appropriate averages of the temperarue and humidity are very difficult to obtain. On the other hand, if the temperature and humidity of the air stream were made uniform at the measurement stations by a suitable mixing process, the velocity pattern at the measurement stations would not be important, and single measurements of temperature and humidity at each station in conjunction with a measurement of mass flow rate would suffice for determining a net change of enthalpy for the entire air stream.

The simplicity of this latter method is attractive, and from time to time has provided the incentive for limited studies of effective means for mixing an air stream to produce uniform temperature and humidity. Various laboratories have experimented with baffles, louvers, and orifices to meet their own needs for air mixing in a specific test apparatus, and the use of such elements is specified in some standard test procedures [2, 3]. Turbulence is one of the main vehicles for the transfer of energy from one segment of a stream to another, and the creation of turbulence is an essential part of the mixing process. The current approach to the study of turbulence is statistical, and is usually carried out experimentally by the use of hot-wire anemometer techniques. The literature describes no comprehensive study of flow processes or turbulence that is directly related to the forced mixing of air streams, and no information has been found comparing the effectiveness of various methods or devices for the mixing of nonhomogeneous air streams in the present context.

The National Bureau of Standards has initiated a study of mixing processes and mixing devices for air streams to improve the measurement techniques in the field of air-conditioning, heating, and refrigeration.

[1] Figures in brackets indicate the literature references at the end of this paper.

This paper is concerned primarily with the design and function of the apparatus constructed for the investigation. The design features of the apparatus are discussed, a description of a scale-model device used in conjunction with the apparatus is given, and an example of some of the results is presented.

2. Design Concept

For experimental evaluation of mixing devices and study of the mixing processes, it was necessary to design an apparatus which could reproduce and control desired conditions in a moving air stream. The criteria for the design of the apparatus were:

(1) To obtain, control, and reproduce the desired velocity and nonuniformity of temperature or humidity conditions in the air stream at a point upstream from the mixer under test.

(2) To provide a section for the installation and support of the mixing devices.

(3) To make accurate measurements of the properties of the air stream at selected positions throughout the system.

2.1. Range of Variables

The apparatus was designed to produce and maintain control of the several variables in the following ranges:

a. Average air velocity, 0 to 2000 ft/min.

b. Nonuniformity of temperature at the inlet to the mixer, 0 to 20 °F.

c. Nonuniformity of relative humidity at the inlet to the mixer, 0 to 50 percent.

d. Installation of one mixer, or two mixers in series, in the mixer section of the apparatus.

e. Three different temperature or humidity patterns at the inlet to the mixer.

The three variations in temperature pattern that can be produced with the present apparatus are illustrated in figure 1. Other patterns of nonuniform temperature or humidity, such as concentric areas at different conditions, could be investigated by modifying the design of the baffles in the preconditioning section of the duct.

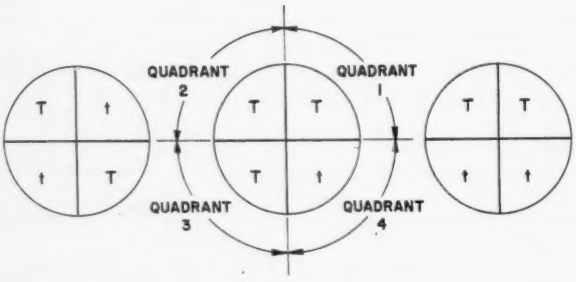

FIGURE 1. *Three possible variations of temperature patterns in the test apparatus.*
T and *t*, represent quadrants at different temperatures.

3. Description of Apparatus

A photographic view and a schematic diagram of the mixing apparatus are shown in figures 2 and 3, respectively. The entire apparatus performed three main functions, as follows:

(1) Preconditioning the air.

(2) Mixing the air stream.

(3) Measurement of air-stream properties at selected stations.

3.1. Preconditioning the Air

The part of the apparatus used for preconditioning the air upstream of the mixer was comprised of an inlet duct and blower and a section of 24- by 24-in. duct containing one elbow, and the necessary heaters, humidity sources, baffles, and dividers to establish a known and reproducible variation in temperature or humidity. To control and maintain the nonuniformity in air-stream properties, the duct was divided into four quadrants of equal size and shape by internal metal partitions, as shown in section A-A of figure 3. A base electric heater of 5-kW capacity and a trimmer electric heater of 500-W capacity were installed in each quadrant for temperature conditioning. A constant-voltage transformer was used in the supply line to the base heaters to correct for fluctuations in line voltage, and a variable transformer was used on each base heater to select a constant level of energy output. The 500-W trimmer heaters were thermostatically controlled in response to a thermocouple sensing element near section A-A in the test duct. For the trimmer heaters and thermocouple control to be effective in minimizing the time variation in temperature at the measuring stations, it was necessary to limit the temperature differential of the air at the inlet blower to ± 0.25 °F.

Water-vapor inlets for humidity variation and control were also located in the conditioning section of the apparatus at section A-A of figure 3. These inlets were arranged so equal or different amounts of water vapor could be supplied to each of the four quadrants of the duct.

The air-flow rate through the test duct was regulated by dampers at the inlet and outlet of the apparatus. By the use of the two dampers it was always possible to maintain a positive pressure in the apparatus, thus preventing leakage of unconditioned air into the system. Additional dampers were used at the entrances of the four quadrants to provide approximately equal volumetric air-flow rates in each quadrant. Mixing baffles were installed in each quadrant of the duct immediately downstream of the elbow, to promote uniformity of temperature and humidity in each quadrant. To avoid as far as practicable premature mixing of the four streams of air before they enter the mixer under test, straightening tubes were placed in the final 18 in. of each quadrant, as shown in section B-B of figure 3. These tubes served to aline the flow as it approached the first measuring station near the outlet of the preconditioning section.

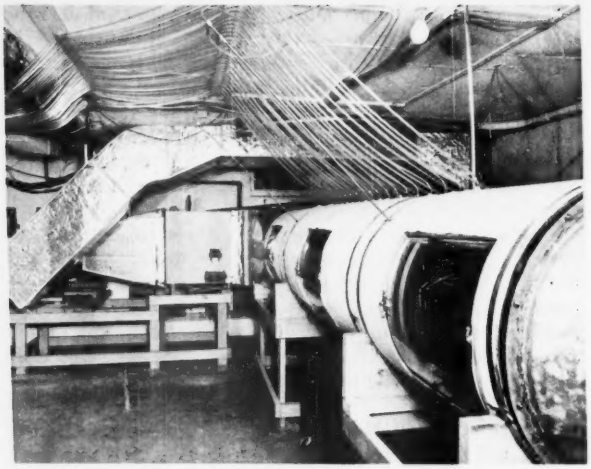

FIGURE 2. *Physical makeup and assembly of test apparatus.*

3.2. Mixing Section

A conversion piece at the discharge end of the preconditioning section changed the cross section of the test duct from square to circular. A circular duct, 24 in. in diameter, was used for housing the mixing devices. The length of the mixing section could be extended to 9½ ft by inserting sections of duct, thus making it possible to study the mixing process for a greater distance downstream from the mixer. The design of the mixing section permitted the installation of two mixing elements in series, and for variation of the distance between them. The mixing section also housed the measuring stations for determing the psychrometric conditions of the air, and the instrumentation for determining the static pressure and velocity pressure of the air upstream and downstream from the mixing device under test. Three removable plastic windows in the side of the mixing section provided access to and observation of the temperature- and pressure-measuring devices and the mixers during the course of the tests.

The mixing section was insulated with formed glass-fiber insulation, 1 in. in thickness, to reduce the heat transfer in this section and to provide a better environment for temperature and humidity measurement.

3.3. Measurements and Instrumentation

Two temperature-measuring stations, each consisting of 24 copper-constantan thermocouples, were used in obtaining temperature profiles upstream and downstream from the mixing device. At each station two thermocouples were located in each of 12 approximately equal areas of the cross section of the duct, as shown in figure 3 at section C-C. For determination of humidity during future studies, 12 of the 24 thermocouples will be converted into wet-bulb thermocouple psychrometers. The thermocouples were made of

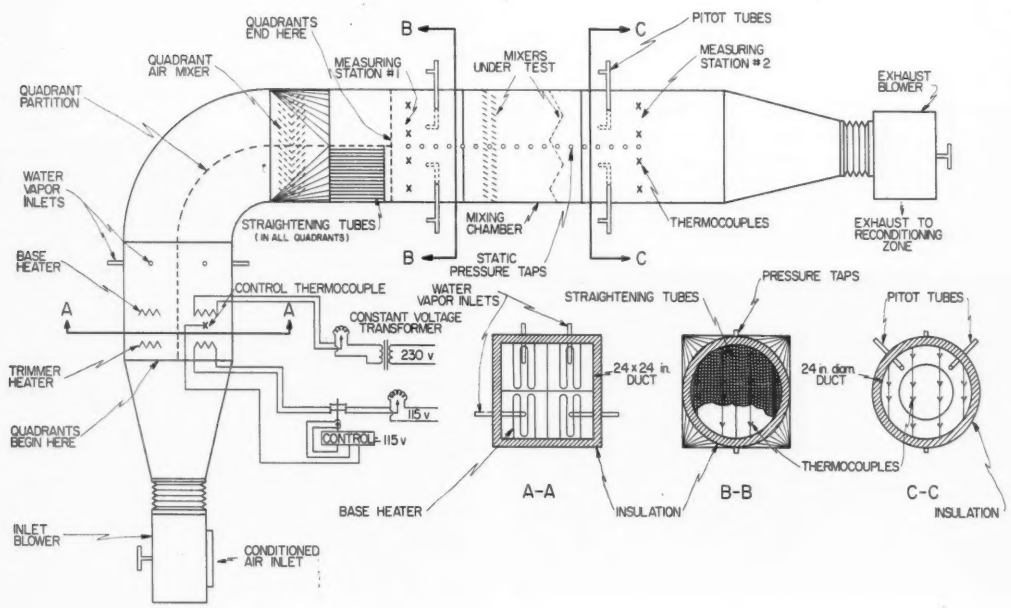

FIGURE 3. *Schematic of apparatus and details showing cross-sectional views.*

30-gage wire calibrated at the National Bureau of Standards. The measuring station located upstream from the mixing device was permanently fixed, and the measurements at this station were made to determine and monitor the degree of nonuniformity in the air stream before mixing occurred. At the downstream measuring station, the nonuniformity of the temperature was measured after passage through the mixer. Since the mixing process for all devices was not the same and the distance for mixing to be accomplished varied with the mixing device, the downstream station was movable so the overall distance required for optimum mixing could be determined.

Each thermocouple was held in a semirigid position by a clamp and a plastic jacket to minimize cold-working of the wire and consequent drift from the original calibration. The lead-lengths of the thermocouples inside the duct were long enough to make conduction errors negligible. The elbow in the preconditioning duct served to shield the thermocouples from the radiant energy of the electric heaters farther upstream, and permitted a greater length of straight duct downstream from the conditioning section in the laboratory space available.

The emfs produced by the thermocouples were measured with a precision manual potentiometer capable of being read directly to the nearest 0.5 μV and estimated to 0.1 μV. The potentiometer was calibrated before use. A temperature-zone box [4] was constructed to permit the use of a common ice bath and an all-copper switching mechinism for sequentially connecting the various thermocouples into the potentiometer circuit, thus eliminating strays emfs from developing in the selector switch. An aluminum plate, 5 in. by 10 in. by 3/8 in., was used in constructing the zone box to provide a mass that would maintain a sufficiently uniform temperature at all junctions secured to it mechanically. This plate was enclosed in a block of polystyrene-foam insulation measuring 9 in. by 14 in. by 4 in.

Two pitot-static tubes were installed on diameters 90° apart at a location just upstream of the mixer under test for making velocity traverses across the section along lines bisecting the four quadrants. Another pair of pitot-static tubes was similarly installed downstream from the mixer. These stations are indicated in figure 3. Static-pressure taps were located at 4-in. intervals along the top of the mixing section between the two temperature-measuring stations to determine static-pressure loss and regain during the mixing process. These pressure taps can be seen in figures 2 and 3. A Hook gage, readable to 0.002-in. vertical water column, was used to indicate differential pressure for the measurement of both velocity and static-pressure distribution.

The access doors in the mixing section permitted periodic comparisons between the permanently installed thermocouples and other calibrated instruments. Comparisons were made between all of the thermocouples at a given station by immersing all of them in water in a thermos bottle. The difference in emf observed between any two thermocouples did not exceed 0.6 μV at either station.

4. Flow Visualization

In the study of new devices for mixing air, a technique employing flow visualization and small-scale models was used for a preliminary evaluation of the devices. Smoke [5], titanium tetrachloride ($TiCl_4$), was used to simulate the portion of an air stream that was at a different level of temperature or humidity from other portions of the stream. By observing the smoke patterns in the air stream before, during, and after it passed through a mixing device in a section of transparent-plastic duct, the effectiveness of a mixer could be estimated. As new devices were designed and built, observation of the smoke patterns gave a quick visual indication of the quality of the mixing process. Flow visualization was used as a tool for selecting the devices which appeared to warrant more intensive investigation in the larger instrumented apparatus.

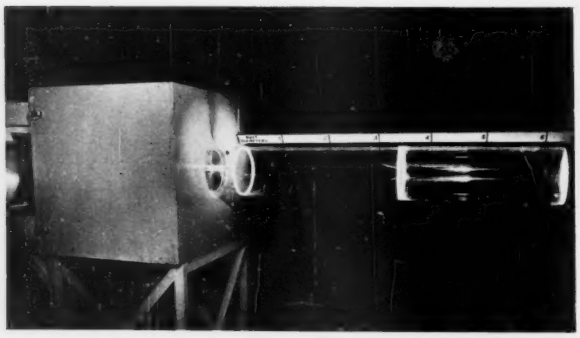

FIGURE 4. *Smoke generator and viewing tube used for flow visualization.*

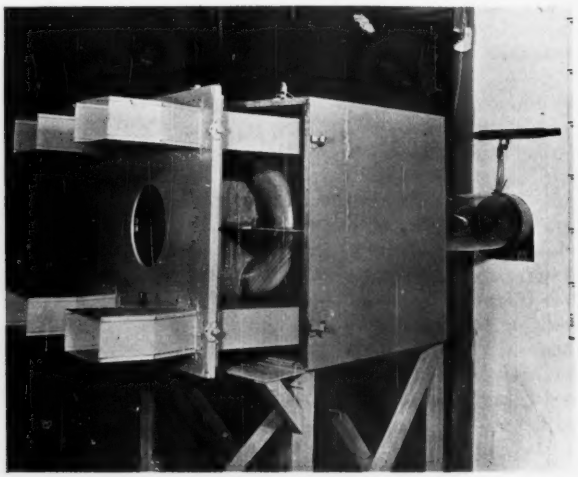

FIGURE 5. *View showing internal detail of smoke generator.*

The small-scale mixers used for flow visualization were made geometrically similar to the full-size devices. The Reynolds numbers in the two apparatus also were made approximately equal, in order to make the comparison more indicative. Figures 4 and 5 show the small-scale apparatus used in the flow-visualization tests.

5. Illustrative Results

Exploratory tests were performed without a mixing device in the air stream to determine the amount of mixing inherent in the nature of the flow. The results of these tests showed that this was very small, as illustrated in figures 6 and 7. Figure 6 shows the temperature pattern at the upstream measuring station, which had a temperature difference between quadrants of about 3 °F, and the resulting pattern at the downstream station. The distance between the stations was three duct diameters. Shown in the figure are temperature values in degrees F at the thermocouple locations in the cross section of the air stream. Also shown is a contour line that represents the 81.0 °F isotherm and defines the boundary between the three warmer quadrants and the remaining cooler quadrant. The figure also shows that little deformation of the 81.0 °F isotherm had occurred between the two measuring stations.

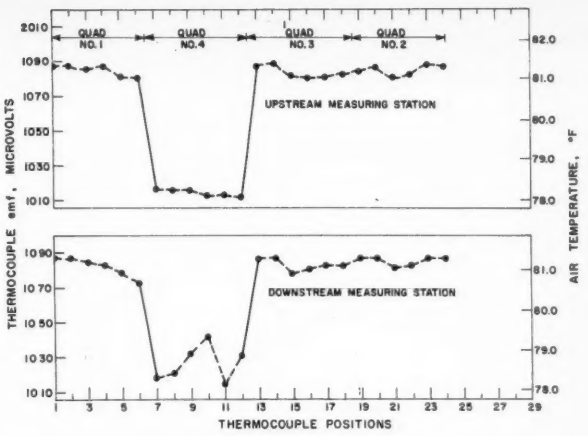

FIGURE 7. *Temperature profiles at upstream and downstream measuring stations without a mixing device in the air stream.*

Figure 7 is another illustration of the temperature profile at the two stations for the same test. Corresponding areas at the upstream and the downstream stations are represented by thermocouple positions 1 through 24, respectively. This illustration again shows that inherent mixing between the two stations was small.

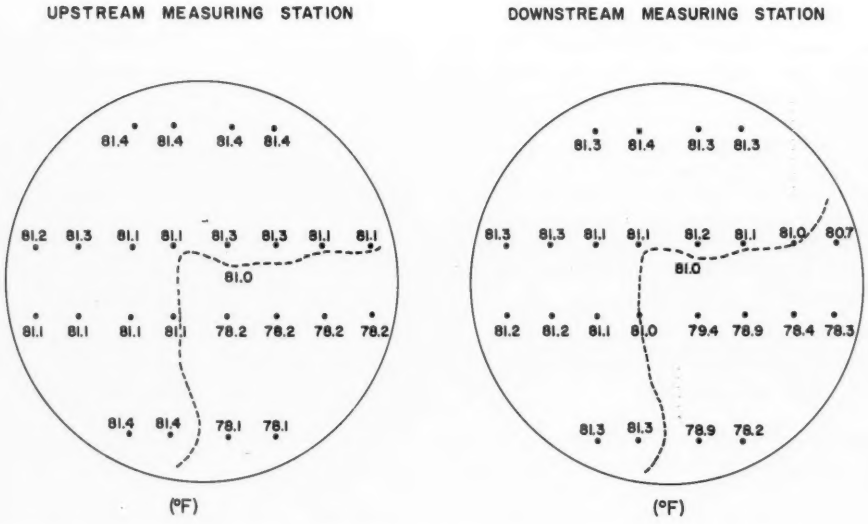

FIGURE 6. *Temperature patterns at upstream and downstream stations without a mixing device in the air stream.*

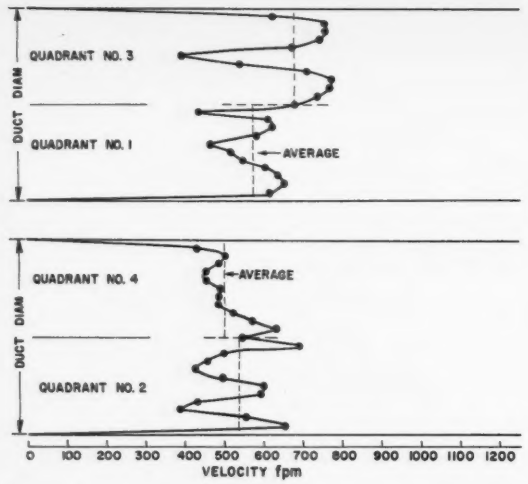

FIGURE 8. *Velocity profile at the upstream measuring station.*

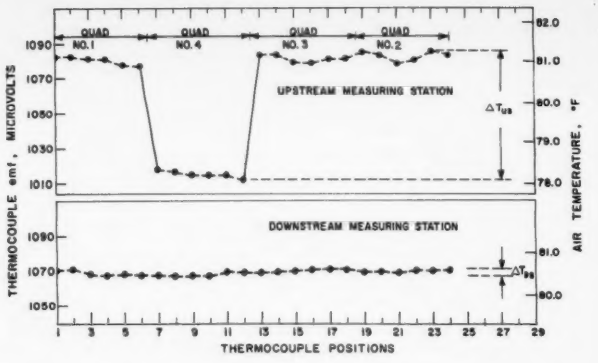

FIGURE 9. *Graphs illustrating mixer effectiveness and showing the temperature profiles before and after mixing.*

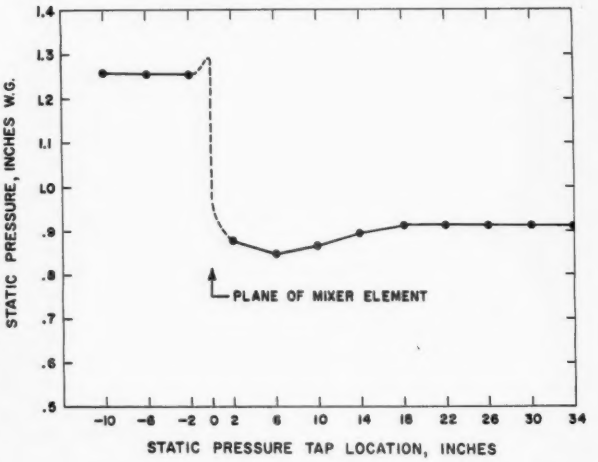

FIGURE 10. *Static pressure profile of a louvered type mixer.*

Figure 8 shows the velocity profile at the upstream measuring station. Measurements were made to show the uniformity of flow at the plane prior to entering the mixing section. The two velocity profiles shown in figure 8 were obtained by setting the two pitot-static tubes in sequence at various radial positions on lines bisecting the quadrants and calculating the velocity for each position using the mean differential pressures given by each tube along with the density of the air. The tubes were alined with the axis of the duct, and it was assumed for the present purpose that the stream was sufficiently alined and its turbulence was sufficiently low to permit neglecting the effects of misalinement and turbulence. The quadrants were not differentially heated for these tests. The inability to get uniformity of velocity and equality of flow in all four quadrants undoubtedly caused some inherent mixing during the test with no mixing device in the air stream. However, the uniformity was sufficient for achieving the desired temperature conditions.

A method was developed for evaluating the effectiveness of different devices or variations in mixer design. The mixing effectiveness was defined as the ratio of the change in the air-temperature variation between the upstream and downstream measuring stations to the temperature variation at the upstream station, expressed as a percent.

$$\text{Percent effectiveness} = \frac{\text{Max } \Delta T \text{ upstream} - \text{Max } \Delta T \text{ downstream}}{\text{Max } \Delta T \text{ upstream}} \times 100.$$

Figure 9 illustrates the results obtained on a pair of metal-louvered mixing elements spaced 22 in. apart, and the method for determining mixing effectiveness. In this illustration, as in figure 7, the air in quadrants one, two, and three of the test duct was heated about 3 °F warmer than that in the fourth quadrant. The observed temperatures at thermocouple positions upstream of the mixers and those at corresponding points 38 in. downstream of the second element are plotted in figure 9. The maximum variation in emf generated by the 24 upstream thermocouples was about 74 μV, whereas the maximum variation downstream was about 4 μV, corresponding to an effectiveness of 94.6 percent.

A test at a given set of conditions was comprised of steady-state operation for 1 hr with all thermocouples being read and recorded at 15-min intervals. The conditions were considered to be steady when the variation in emf produced by each thermocouple was 6 μV or less during the 1-hr period.

Figure 10 shows a static-pressure profile along the top of the duct from a point 10 in. upstream of a mixing device to a point 34 in. downstream of the device in increments of 4 in. The static pressure is actually the pressure relative to that of the room in which the equipment was located. This illustrates the sharp pressure drop at the plane of the mixer accompanied by a small regain of static pressure which reached a

maximum about 18 in. downstream of the mixer. Tests of several mixers have indicated that mixing is approximately complete at the plane where maximum static-pressure regain was first observed. Thus, the pressure profile offers a simple method for determining the approximate location of final mixer effectiveness.

Tentative plans for future study of mixing devices will include investigation of the following parameters of design and application.

(a) Magnitude and pattern of upstream temperature and humidity variation.

(b) Use of more than one mixer in series.

(c) Relation of mixing effectiveness to the distance between elements and the distance to the plane of downstream measurement.

(d) Variation of air velocity.

(e) Effectiveness of orifices, baffles, turning vanes, screens, and other configurations as mixers.

In addition to the items mentioned above, a hot-wire anemometer will be used to investigate the turbulence and determine, for example, the intensity and integral scale of the turbulence and its energy spectrum. An attempt will be made to correlate such quantities with the mixing effectiveness determined from temperature, humidity, and velocity measurements.

Since one immediate use of air-mixing devices is their application to apparatus for measuring capacity of heating or cooling equipment, the usefulness of a given design will be related to its mixing effectiveness, the space required to attain maximum mixing, and the static pressure loss through the device. As various devices are investigated, a function or figure of merit will be sought for comparing the overall usefulness of different designs. The information furnished through the study should provide for better and easier measurement of stream conditions in moving air. Effective mixing of air streams will have application in fields other than air conditioning, such as the sampling of flue gases for analysis, air filter testing, fluid mechanics investigations, and other processes where homogeneity would improve accuracy of measurement or be desired for other reasons.

6. References

[1] Fluid meters: their theory and application, 5th ed., Am. Soc. Mech. Eng. (1959).

[2] Methods of testing for rating unitary heat pump equipment, ASHRAE Standard 39.61, Am. Soc. Htg. Refr. and Air-Cond. Eng. (1961).

[3] Institute of Boiler and Radiator Manufacturers Testing and Rating Code for Low Pressure Cast Iron Heating Boilers, 7th ed. (1964).

[4] Temperature: Its Measurement and Control, Thermoelectric Thermometry **1**, 202 (Reinhold Publ. Co., 1941).

[5] R. L. Maltby and R. F. A. Keating, Flow visualization in low speed wind tunnels, Current Brit. Practice Tech. Note AERO 2715, Royal Aircraft Establishment (Aug. 1960).

(Paper 70C1–169)

JOURNAL OF RESEARCH of the National Bureau of Standards—C. Engineering and Instrumentation
Vol. 70C, No. 1, January–February 1966

Publications of the National Bureau of Standards*

Selected Abstracts

Photopolarographic behavior of inorganic depolarizers, R. A. Durst and J. K. Taylor, *J. Res. NBS* **69A** (*Phys. and Chem.*), *No. 6, 517–522 (Nov.–Dec. 1965), 75 cents.*
Nickel(II), cobalt(II), and uranium(VI) were studied polarographically to determine the effect of uv-visible irradiation on their reduction characteristics. Photoeffects were observed in all cases. Two mechanisms are proposed for the nickel photokinetic prewave, and the complex photo-effects observed with cobalt and uranium are described. Proposals are made for further studies to clarify and elucidate the photochemical reactions and to apply this technique in the study of the activated states of ions prior to reduction.

Isotherms determined by the National Bureau of Standards acoustical thermometer in the liquid helium temperature range, G. Cataland and H. Plumb, *J. Res. NBS* **69A** (*Phys. and Chem.*), *No. 6, 531–534 (Nov.–Dec. 1965), 75 cents.*
Isotherms of the speed of sound in helium-4 gas as a function of pressure have been measured. Five of the isotherms in the liquid helium-4 temperature range have been analyzed, and the results are discussed. The acoustically determined values of temperature are consistently higher than the values of temperature associated with the liquid helium-4 vapor pressure scale (T_{58}). The deviations are 0.006 °K at 2.323 °K, 0.007 °K at 2.807 °K, 0.008 °K at 3.211 °K, 0.010 °K at 4.212 °K and 0.012 °K at 5.024 °K.

Correlation of large longitudinal deformations with different strain histories, L. J. Zapas and T. Craft, *J. Res. NBS* **69A** (*Phys. and Chem.*), No. 6, 541–546 *(Nov.–Dec. 1965), 75 cents.*
It is shown that the BKZ incompressible elastic fluid theory is in excellent agreement with experimental results obtained in simple extension. From single step stress-relaxation data, the stress-strain response for a number of other simple extension histories are calculated from the theory and are compared with experiments.

Electrode potentials in fused systems X. Measurement of cation concentration in molten salts using glass membrane electrodes, K. H. Stern and S. E. Meador, *J. Res. NBS* **69A** (*Phys. and Chem.*), *No. 6, 553–556 (Nov.–Dec. 1965), 75 cents.*
A potentiometric method utilizing glass membrane reference electrodes in a concentration cell for the measurement of melt composition is presented. Relevant data for the AgCl-NaCl, AgBr-NaBr, and Ag_2SO_4 systems are given. Using cells of the type

$$M_1|M_1A(a_R),\ M_2A(a'_R)|\text{glass}|M_1A(a_2),\ M_2A(a'_2)|M_1$$

where the a's are activities, the unknown mole fraction X_2 can be calculated from the equation

$$\log\left(\frac{X_2}{1-X_2}\right)=\frac{E}{2.303(RT/F)t'}-\log\left(\frac{1-X_R}{X_R}\right)$$

where t' is a concentration-independent constant of the system and X_R is the concentration of M_1A in the reference electrode. The method is capable of measuring X_2 in molten salt with an accuracy of better than 5 percent over a concentration range of 10^4. Application of the method to cations other than silver is discussed.

Thermodynamic and related properties of parahydrogen from the triple point to 100 °K at pressures to 340 atmospheres, H. M. Roder, L. A. Weber, and R. D. Goodwin, *NBS Mono. 94 (Aug. 10, 1965), 75 cents.*
Experimental programs on parahydrogen at this laboratory have provided pressure-density-temperature relations and heat capacities at temperatures from 15 to 100 °K and at pressures from 2 to 350 atm. The two types of data have been correlated to yield a consistent set of functions. The properties tabulated for selected isobars and isochores are temperature, volume or pressure, the isotherm derivative $(\partial P/\partial\rho)_T$, the isochore derivative $(\partial P/\partial T)_\rho$, internal energy, enthalpy, entropy, the specific heats at constant volume and at constant pressure, and the velocity of sound. Also presented are the derived Joule-Thomson inversion curve and some comparisons with normal hydrogen near 100 °K.

Standard Reference Materials: Methods for the chemical analysis of white cast iron standards, J. I. Shultz, *NBS Misc. Publ. 260–6 (July 16, 1965), 45 cents.*
The procedures described in this publication are those used at the National Bureau of Standards in the analysis of white cast iron standard reference materials for the ten (10) major elements; namely, carbon, manganese, phosphorus, sulfur, silicon, copper, nickel, chromium, vanadium, and molybdenum.
Carbon and sulfur are determined by combustion; manganese, chromium and vanadium by titrimetry; phosphorus, copper, and molybdenum by photometry; and silicon and nickel by gravimetry. These procedures, which are slight modifications of well-established and previously published methods, were selected for their accuracy and dependability.

Guide to instrumentation literature, J. F. Smith and W. G. Brombacher, *NBS Misc. Publ. 271 (July 7, 1965), $1.25. Supersedes NBS Circ. 567.*
This compilation is a source list of instrumentation literature, with a subject index and an index of personal and corporate authors.

Interrelations between cement and concrete properties, Part 1. Materials, techniques, water requirements and trace elements, R. L. Blaine, H. T. Arni, B. E. Foster, et. al., *NBS Bldg. Sci. Series 2, Pt. 1 (Aug. 20, 1965), 35 cents.*
The studies of the interrelations between cement and concrete properties are presented in a series of related articles. This first section presents the type classification of the cements and the areas from which they were procured together with the tests performed on the cements and concretes. Also presented are the methods employed in the statistical treatment of the data and a discussion of the significance of the various statistical techniques employed in the following sections dealing with specific aspects of the interrelations between cement and concrete properties.

Accuracy in measurements and calibrations, 1965, ed. W. A. Wildhack, R. C. Powell, and H. L. Mason, *NBS Tech. Note 262 (June 15, 1965), $1.00.*
NBS estimates of uncertainties associated with physical measurements, and with some NBS calibration services, are shown by 66 provisional "accuracy charts." Each chart is accompanied by a facing page giving a brief statement of the state of the art and tentative plans for NBS work in areas where improvement is needed.

Electrochemical analysis: Studies of acids, bases, and salts by EMF conductance, optical and kinetic methods July 1964 to June 1965, Ed. R. G. Bates, *NBS Tech. Note 271 (Sept. 6, 1965), 60 cents.*
This survey of the activities of the Electrochemical Analysis Section, Analytical Chemistry Division, covers the period July 1964 to June 1965. An attempt is made to summarize a year's progress on the technical projects of the Section in such a way as to stress the program and capabilities of the organizational unit as a whole. Consequently, a description of facilities and equipment is presented first and is followed by brief summaries of the several lines of work currently under way. Emphasis is given to the reasons why each study was undertaken. The main areas of investigation include the study of acidity and solvent effects in water, deuterium oxide, and water-methanol solvents by emf methods; the development of reference indicator bases for nonaqueous media and reference

794-732 O-66—3

materials for dielectric measurements; measurement of the thermodynamic properties of mixed salt solutions; and investigation of special problems in trace analysis by conductometric and kinetic methods. The survey concludes with lists of the members of the Section staff, publications and manuscripts produced during the year, and talks given by the staff.

Solubility of solids in dense gases, J. M. Prausnitz, *NBS Tech. Note 316 (July 1965), 35 cents.*
The thermodynamics of solid-dense gas equilibria is discussed, and two techniques are described for calculating the solubility of a solid component in a gas at high pressure. The first one is based on the recent empirical equation of state of Redlich which, in turn, is derived from Pitzer's generalized tables of fluid-phase volumetric properties. The second one is based on the Hildebrand-Scatchard theory of solutions. Both methods give good semiquantitative results but cannot accurately predict solubilities from pure-component data alone.

Grading of abrasive grain for grinding, *CS271–65 (Apr. 12, 1965). Supersedes SPR R118–50.*
This Standard sets forth the grit size designations, the size limits and the sieves used in determining them, as well as the test procedure which is used by industry in classifying abrasive grain by its dimensions. A uniform means of indicating compliance with the Standard is also given.

Constancy of a modified Weston standard cell over long periods, W. C. Bosburgh and R. G. Bates, *J. Electrochem. Soc.* **111,** *No. 8, 997–998 (Aug. 1964).*
Observations on the e.m.f. of five modified saturated Weston cells have been made over a period of 26 years. The modifications in design were as follows: (a) the electrolyte of the cell was saturated with $CdSO_4$, $Na_2SO_4 \cdot 2H_2O$ as well as with $CdSO_4 \cdot 8/3H_2O$ (with excess of both salts), and (b) enough bismuth was added to the cadmium amalgam to make a three-phase amalgam. The temperature coefficient of e.m.f. is about one-quarter that of the Weston normal cell at 25 °C. The average change in e.m.f. over a period of 26 years was less than 0.03 mv.

High-precision coulometric titrations with special reference to the determination of uranium, J. K. Taylor and G. Marinenko, *Proc. Conf. High-Precision Analysis of Substances of Interest to Nuclear Energy, Jan. 18–22, 1965, pp. 147–161 (Bureau Central des Mesures Nuclaires, Brussels, Belgium, 1965).*
Investigations at the National Bureau of Standards have established constant-current coulometry as an analytical technique of the highest reliability. Experimental conditions required for precise coulometric analyses are reviewed. A detailed description is given of the method developed for the precise determination of uranium in metal and its compounds.

High pressure single crystal studies of ice VI, S. Block, C. E. Weir, and G. J. Piermarini, *Science* **148,** *947 (1965).*
The cell constants of ice VI have been determined to be $a = 8.38$Å, $b = 6.17$Å, $c = 8.9$Å from single crystal x-ray diffraction at room temperature and approximately 9 kb. The space group is either $P_{**}a$ or monoclinic pseudoorthorhombic with $\beta = 90°$. The data were taken with a diamond pressure cell modified for use with a precession camera. The crystals of ice VI were grown in the pressure cell using distilled H_2O and a metal gasket.

High temperature microwave spectroscopy: AlF and AlCl, D. R. Lide, *J. Chem. Phys.* **42,** *No. 3, 1013–1018 (Feb. 1965).*
A technique is described for making vacuum tight seals between sapphire windows and impervious ceramic materials. Seals employing this technique have been made and tested at temperatures up to 1125 °C which is several hundred degrees below the expected service limit of the seal based on physical properties of materials.

Method of obtaining a range of current densities with a resistive cathode, M. Brenner and A. Brenner, *Plating* **56,** *No. 6, 527–530 (June 1965).*
A device for obtaining a range of current densities on a single cathode in electrodeposition is described. It consists of a nickel-chromium tape, about 300 cm long, wound to form a helix with about 40 turns. The electrical resistance of the tape results in a large decrease in the current density at which metal is deposited from the top of the helix, where current enters, to the bottom. The nature of the coating deposited over a range of current density is readily ascertained by visual inspection of the cathode.

National Standard Reference Data Program, E. L. Brady and S. A. Rossmassler, *D. C. Libraries* **35,** *No. 4, 57–61 (Oct. 1964).*
In June 1963 the National Bureau of Standards was assigned the responsibility by the President's Office of Science and Technology of administering a government-wide program to promote and coordinate systematic data compilation and evaluation activities in all fields of the physical sciences. This government-wide program has been called the National Standard Reference Data System. The background of this program and its implementation within the National Bureau of Standards are described briefly.

Photo-oxidation of asphalts in the presence of ozone, J. R. Wright and P. G. Campbell, *ACS Div. of Petroleum Chem. Preprints* **9,** *No. 3, 161 (Aug. 1964).*
The effects of oxone on the photo-oxidation of coating-grade asphalts were compared to those of air and of oxygen under a variety of radiant energy conditions. Oxidative changes were measured by infrared spectroscopy and by the time to film failure as denoted by cracking.
Surfaces of non-catalyzed asphalts were oxidized when treated with ozone in total darkness, room light, solar radiation, and the radiant energies of the carbon and xenon arcs. No oxidation was detected when the asphalts were exposed to room light in oxygen alone. A $FeCl_3$-catalyzed asphalt was not oxidized by ozone in total darkness. Photo-oxidation rates of all asphalts increased as exposures were made to carbon-arc radiation in air, in oxygen, and in ozone-enriched oxygen. Each asphalt exhibited a different oxidative response to solar, xenon-arc, and carbon-arc radiant energy sources.

Precise assay of copper using small samples, T. J. Murphy and J. K. Taylor, *Anal. Chem.* **37,** *No. 7, 929–931 (June 1965).*
A method has been developed for the precise assay of copper metal and solutions using small samples. The method is based on the electrodeposition of the copper and the colorimetric determination of residual copper in the electrolyte. It has been shown that samples of 0.10 to 0.25 g of copper can be assayed with a standard deviation of about 0.007 percent.

Pyrolytic technique, G. M. Brauer, *J. Polymer Sci., Pt. C, No. 8, 3–26 (1965).*
Pyrolytic techniques, especially those used in conjunction with gas chromatography, are a very useful tool for elucidating the structure of macromolecules. These methods have not only proven a powerful tool in the qualitative characterization of the "gross structure", but have also found an increasing number of applications for the quantitative analysis of copolymeric systems. Recent studies indicating that the shape of the pyrogram is influenced by structural characteristics such as the degree of branching or crosslinking, stereoregularity and the presence of block or grafts in copolymeric systems opens up new avenues for pyrolytic techniques in studies of the ultimate arrangement of monomeric units within the polymer chain.

A comparison of atomic frequency standards, R. E. Beehler and R. C. Mockler, *Book, Progress in Radio Science 1960–1963, Vol. I. Radio Standards and Measurements, pp. 20–26 (Elsevier Publ. Co., Amsterdam, The Netherlands, 1965).*
Two laboratory cesium beam frequency standards were intercompared and evaluated as primary standards over a three-year period. Experimental variations of parameters affecting the measured frequency and theoretical studies of the dependence of frequency on radiation field intensity and the presence of other signals gave what we consider convincing evidence of an accuracy of 1×10^{-11}. X^2 tests demonstrated a gaussian distribution of data. Manual and servo measurements of frequency over a period of one year agreed within $\pm 2 \times 10^{-12}$. The frequency difference between the machines has not changed more than $\pm 2 \times 10^{-12}$ in the three year period. The best precision so far attained is 1 to 2×10^{-13}. A third larger cesium beam machine is now in operation and under test. The smallest of the three machines was converted for a

thallium beam. The precision of the thallium measurements is about the same as that for cesium. The thallium beam is still being evaluated as a primary frequency standard. In past years ammonia masers have undergone considerable testing in the NBS laboratories and found to be resettable to within $\pm 3 \times 10^{-11}$ for $N^{14}H_3$. A somewhat improved value was attained for $N^{15}H_3$. Because of the extreme care required to control the parameters affecting the maser frequency, these devices are not considered by us to be competitors to the atomic beam devices.

A DC–RF substitution error in dual element bolometer mounts, G. F. Engen, *IEEE Trans. Instr. Meas.* **IM-13,** *No. 2 & 3, 58–64 (June–Sept. 1964).*
Most of the coaxial type bolometer mounts in current use employ a pair of bolometer elements which are connected in series for the dc or audio-frequency bias powers, and in parallel at radio or microwave frequencies. A number of practical advantages accrue from such a mode of operation.
In the frequency range where these techniques are most often employed, the dc-rf substitution error is generally believed to be negligible. It is quite possible, however, for this to be true of the elements individually, and yet fail to be true of a pair of these elements as used in a typical coaxial mount. If only the *sum* of the resistances of the two elements is maintained at a constant value, and if because of imperfect symmetry the resistance division between the two elements changes with the application of rf power, an error is introduced which is given by the equation: $\epsilon = [(1/\gamma_b) - (1/\gamma_a)]\Delta r$, where γ_a and γ_b are the "ohms per milliwatt" coefficients of the two bolometer elements, and Δr the shift in resistance division. An experimental study indicates that, in the existing state of the art, this error may be ignored in many applications, but is large enough to be important in others.

A mechanistic model for the limits of auditory perception, E. L. R. Corliss, *Proc. Symp. Models for the Perception of Speech and Visual Form, Boston, Mass., Nov. 11–14, 1964 (Air Force Research Center, Cambridge, Mass., 1964).*
From a number of apparently diverse experiments on human hearing it has proved possible to construct a simple model describing the limits of auditory perception for normal and impaired ears. The model has been applied to interpret the perception of distorted speech by persons with normal and impaired hearing. Two mechanisms are required: One element emits unit responses whose number is proportional to the amplitude of a sound. It is followed by a selector mechanism, analogous to a resonant circuit, that integrates the responses. Correspondingly, just two parameters are involved: the threshold of hearing and the "Q" of the selector mechanism. The theory of the selector mechanism is based upon a recently published study of the limits of performance of a system capable of storing oscillatory energy reversibly, but the remainder of the theoretical description makes use of ordinary communication theory.

A multistub coaxial line tuner, W. E. Little and E. Niesen, *IEEE Trans. Microwave Theory Tech.* **MTT-12,** *No. 5, 570–571 (Sept. 1964).*
This paper presents the description of a Multi-Stub Coaxial Line Tuner designed specifically for reflectometer work. Results obtained from a tuner designed to tune out a 2 to 1 VSWR from 1 to 4 Gc are also given.

A survey of research on frozen food transport refrigeration, P. R. Achenbach, *ASHRAE J.* **6,** *No. 11, 29–36 (Nov. 1964).*
Recent and current research programs on frozen food transport refrigeration at the National Bureau of Standards, the U.S. Department of Agriculture, the National Research Council of Canada and elsewhere are discussed. These programs cover testing and rating methods for refrigerated vehicles and refrigerating units, air circulation in refrigerated vehicles and cooling by non-mechanical means. Some of the continuing needs for investigation are identified as well as areas where two or more industry, professional, or business groups in the refrigerated transport field should cooperate for optimum solutions to common technical problems.

A two-channel nulling method for measuring attenuation constants of short sections of waveguide and the losses in waveguide joints, R. W. Beatty, *Proc. IEEE* **53,** *No. 6, 642–643 (June 1965).*
A two-channel nulling method is described to measure the attenuation constants of short sections of waveguide and the losses in waveguide joints.
The method is especially convenient because only stock items of commercially available equipment are used.
The waveguide section under test in one channel is arranged so that the microwave signal traverses it once, is reflected and traverses it again before it is combined with a signal from the other channel. The other channel contains a variable attenuator and phase shifter which are adjusted for balance between the two channels as indicated by a detector null.
A measurement is made by obtaining two balances, one before, and one after insertion of the test section of waveguide. Ideally, one divides the change in the attenuation by 2 and then by the length of the test section of waveguide to determine the attenuation constant. However, serious errors can occur unless the procedures described in the paper are used.
A simple extension of the method permits the measurement of losses in waveguide joints. It is easily possible to obtain an accuracy of ± 0.002 dB in these measurements.

Advances in electrical instrumentation, F. L. Hermach, *Ind. Res. pp. 60–66 (June 1965).*
Recent advances in the measurement of electrical quantities at low frequencies (up through 30 kHz) are discussed in terms of the improvements in a few key components which made many of these advances possible.

An automatic method for obtaining data in the Weissfloch-Feenberg node-shift technique, R. W. Beatty, *Proc. IEEE* **53,** *No. 1, 79–80 (Jan. 1965).*
A method is described to automatically obtain data in the well-known Weissfloch-Feenberg node shift technique. This technique is used for investigation of discontinuities in coaxial lines and has more general application in the measurement of parameters of 2-ports.
The method uses mechanical coupling of the probe to the sliding short-circuit, as in Tischer's semi-automatic method, but permits automatic readout of the nodal shift curve on a recorder.
The probe is initially and purposely displaced from the nodal position so that subsequent relative displacements between them due to nodal shifts cause changes in the probe output which is fed to a recorder.
Calibration of the probe output in terms of relative displacement is described and precautions to be observed during the measurement are mentioned.

Breakdown characteristics of semi-conductor materials, H. A. Schafft, *Electro-Technol.* **75,** *No. 6, 77–82 (June 1965).*
Second breakdown is a mode of operation of the transistor that should be avoided because it will cause circuit malfunction and can damage the transistor. Its existence is a serious problem to the transistor industry not only in the fabrication of the transistor but also in the definition of operations that fully utilize the transistor's capabilities. An outline of the characteristics of second breakdown is given and used to provide an understanding of the variety of approaches that the transistor industry has used to specify conditions of transistor operation free of second breakdown. These approaches are reviewed and discussed with the aim of maximizing their usefulness.

Code for electricity metering, revised, F. K. Harris, *Mag. Std.* **36,** *No. 5, 143–145 (May 1965).*
A revision of the Code for Electricity Metering is announced. The history of the code is briefly reviewed, its economic and quasi-legal importance are cited, and the important areas of revision are discussed.

Comparison of single-point and two-point loading for determining the strength of flat glass, J. J. Kerper and T. G. Scuderi, *Proc. Am. Soc. Testing Materials* **64,** *1037–1043 (1964).*
The strength of annealed glass was determined by testing in flexure with areas of different sizes subjected to uniform stress. The results showed that as the area subjected to uniform stress increased the strength decreased. Fracture origins for mid-point loading tended to cluster about the point of maximum stress while fracture origins in the two point loading tests were distributed rather uni-

794-732 O-66—4

formly throughout the area of uniform stress. Specimens that failed from fractures that originated on the surface tended to be stronger than those specimens that failed from fractures that originated on the edge of the specimen.

Composites in construction, A. A. Bates, *Stanton Walker Lecture Series on the Materials Sciences, Nov. 20, 1963, Lecture No. 1, p. 15 (University of Maryland, College Park, Md., 1964).*
The Stanton Walker Lecture deals with relationship between the aggregates and the ready-mix concrete industries and the general array on building and construction industries which use concrete. The principal theme revolves around the placement and exercise of responsibility in these highly complex and disjointed industries. The main current trend in buildings industries is toward industrialization as distinct from the traditional handicraft operations. The technologic and the ethical results of industrialization are suggested. The lecture was given at the University of Maryland under auspices of a Foundation set up by the National Sand and Gravel Association and the National Ready Mixed Concrete Association. This is the first of an annual series of Stanton Walker Lectures endowed for the purpose of honoring Mr. Walker, an individual who has had a profound effect on the industries involved. By agreement in the original Foundation Charter, the University of Maryland has publication rights to the Stanton Walker Lectures.

Computer control of precision instrument inventory, S. N. Alexander and P. E. Doule, *Research/Development pp. 38–43 (May 1965).*
A system consisting of four elements (organization, procedures, information files, and computer programs), is described to illustrate a possible method of computer control of precision instrument inventory and use. An integrated management information system is postulated, part of which is a modern supply system including the equipment management subsystem suggested by this article. The cost effectiveness of a proposed subsystem can be estimated after detailed analysis of a few typical organizations.

Design of static elastomeric seals for cryogenic temperatures, D. H. Weitzel, P. R. Ludtke, and R. F. Robbins, *Proc. Conf. Design of Leak-tight Separable Fluid Containers* **2,** *139–165 (NASA, Huntsville, Ala., Mar. 1964).*
The use of elastomeric O-rings for static seals which are cooled to cryogenic temperatures is discussed. Experiments developing principles to be followed and materials to be used in the design of this type of seal are reviewed. Several designs which incorporate the advantages of spring loading and pressure actuation are suggested. It is conclusively shown that elastomers should not be overlooked when considering the problem of leak tight fluid connectors for service at cryogenic temperatures.

Effect of surface texture on diffuse spectral reflectance, Part A. Diffuse spectral reflectance of metal surfaces, H. J. Keegan, J. C. Schleter, and V. R. Weidner, *(Symp. Measurement of Thermal Radiation of Solids, San Francisco, Calif., Mar. 4–6, 1964). NASA SP–55, Session II, Paper 17, pp. 165–169 (1965).*
In an attempt to correlate the effect of surface finish (texture) on the diffuse spectral directional reflectance of metals, measurements were made over the wavelength range 0.26 to 2.1 microns for samples of sintered beryllium, steel gage blocks, machine lapped steels with various degrees of abrasives, polished and sandblasted aluminum, platinum, and a chemically polished beryllium block. Surface texture measurements were made on some of the same surfaces by interferometry and are described in Part B.

Effects of connectors and adapters on accurate attenuation measurements at microwave frequencies, R. W. Beatty, *IEEE Trans. Instr. Meas.* **IM–13,** *No. 4, 272–284 (Dec. 1964).*
A source of error in microwave attenuation measurements, not previously evaluated is treated in an original analysis.
The error is caused by effects of deviations of connectors or adapters from standard specifications.
For example, if the coaxial connector at the insertion point in an attenuation measuring system deviates from standard specifications, the measured attenuation of a coaxial pad inserted in this system will differ from the measured attenuation of the same pad when inserted in a system having a standard connector at the insertion point.
In the analysis, an attenuator installed in a system is represented by three cascaded 2-ports, the central one representing the core or kernel of the attenuator, and the others representing connector pairs.
Three general cases are considered, the waveguide component under test has (1) either sexless or mating connectors, (2) non-mating connectors of the same type and sex, or (3) non-mating connectors of different types.
The results indicate that significant errors are possible with present connectors, such as the type N, but that these types of errors become negligible when "high precision" connectors are used. The analysis permits one to tell how good a connector must be for a specific attenuator application.

Fire endurance of small gypsum slabs, J. V. Ryan, *(Proc. American Society for Testing Materials Annual Meeting on Moisture Influence on Material Behavior During Fire Test, Chicago, Ill., June 1964), Am. Soc. Testing Materials Spec. Tech. Publ. No. 385, pp. 96–111 (May 1965).*
A study was undertaken to obtain increased knowledge of the relationship between moisture content of gypsum plaster and its fire endurance. Specimens 2 ft square were prepared in nominal thicknesses of 3 in., 1½ in., ¾ in., and ⅜ in. They were conditioned in air at 73 °F and 50 percent relative humidity for periods ranging from 1 to 259 days. Each specimen was exposed to fire controlled to produce the furnace time-temperature curve defined in ASTM E–119. The fire endurance was taken as the elapsed time to a limiting temperature rise on the unexposed surface.
The relationships between fire endurance and each of several factors—age, thickness, weight loss, and moisture content—are presented. It is shown that endurance did not change significantly during the initial aging period, despite appreciable change in moisture content. The initial period was followed by an intermediate period of aging marked by more significant changes in endurance. Finally there was an extended period of small changes in endurance. It was shown that endurance was affected by fairly small changes in the moisture content of gypsum plaster as equilibrium was approached.

Flexural behavior of prestressed split-beam composite concrete sections, J. O. Bryson, L. F. Skoda, and D. Watstein, *J. Prestressed Concrete Inst.* **10,** *No. 3, 77–91 (June 1965).*
An investigation of the general flexural characteristics of prestressed composite concrete beams is described. The composite beams were made by separately forming the tensile and compressive sections of the beams. The tensile section was cast first and prestressed, and the compressive section was formed with plain concrete bonded to the prestressed element. These composite beams are referred to as "Prestressed Split-Beams."
Three sets of split beams with interfaces at different levels were tested in duplicate and the results compared with those from two sets of duplicate conventionally prestressed beams. The results of the tests indicate that the structural characteristics of the split beams failing in flexure are essentially the same as those of conventionally prestressed beams.
Since the prestressing is confined to the tensile portion in the split beams while the compressive portion is stress free, this design concept affords significant savings in the amount of prestressing steel as compared with a conventionally prestressed beam.

Fracture topography, I Wolock and S. B. Newman, *Book, Fracture Processes in Polymer Solids, Phenomena and Theory, ed. B. Rosen, ch. IIC, pp. 235–290 (Interscience Publ. Inc., New York, N.Y., 1964).*
This chapter is a survey of work in the field of fracture topography of polymers. It is largely descriptive and covers related phenomena such as crazing.

Further analysis of the modulated subcarrier technique of attenuation measurement, W. E. Little, *IEEE Trans. Instr. Meas.* **IM–13,** *No. 2 & 3, 71–76 (June–Sept. 1964).*
The modulated subcarrier technique of attenuation measurement offers an accurate and convenient means of calibrating rotary vane attenuators. The technique also has the possibility of being extended to other types of attenuation measurement. This paper gives a more detailed analysis of the technique than has been given.

It consists of an analysis of the output of the microwave detector, assuming it is completely linear; an error analysis of the technique; and a comparison of the technique with the 30 mc i-f substitution technique of attenuation measurement.

Measuring impedance through an adapter without introducing additional error, R. W. Beatty, *Proc. IEEE* **53,** *No. 6, 656–657 (June 1965).*
In making impedance measurements through an adapter or transition section, one usually needs either to evaluate the characteristics of the adapter or to tune out its reflection. It is usually assumed that the adapter or transition is lossless. Such an evaluation or tuning generally introduces additional errors, and the error due to the presence of unwanted losses is difficult to evaluate.
Use of the tuned reflectometer in such a situation can make evaluation of the adapter unnecessary, and no assumption of losslessness is required. The source of error mentioned above is thus avoided. It is required that the reflectometer output be a section of waveguide fitted with a connector which mates with the 1-port under test. Also provision must be made for sliding loads in this waveguide section in order to tune the reflectometer. However no change in the normal tuning or measuring procedure is required.

Method and equipment for measuring thermal emittance of ceramic oxides from 1200 ° to 1800 °K, H. E. Clark and D. G. Moore (*Symp. Thermal Radiation of Solids, San Francisco, Calif., Mar. 4–5, 1964), NASA SP–55, Session III, Paper 26, pp. 241–257 (1965).*
A description is given of the rotating cylinder equipment developed by the National Bureau of Standards for measuring the total normal emittance and normal spectral emittance from 1 to 15μ of nonmetals as well as metals over the temperature range 1200 to 1800 °K. Preliminary data are presented for eleven different ceramic oxide specimens at 1200 °K and for platinum at 1400 °K. A comparison is made between these data and emittance values obtained by measuring room temperature spectral reflectance from 0.26 to 2.10μ for six of the eleven ceramic oxides. Possible sources of error are discussed.

Microwave discharge cavities operating at 2450 MHz, F. C. Fehsenfeld, K. M. Evenson, and H. P. Broida, *Rev. Sci. Instr.* **36,** *295–298 (Mar. 1965).*
Five simple microwave cavities for producing discharges in gases were tested in He and H_2 at pressures from one micron to one atmosphere. Three of the cavities are commonly used, and two have been recently designed. One of the newly designed cavities offered a considerable improvement over early models with respect to compactness, ease of attachment to the system, and efficiency.

New mode of operation of a phase sensitive detector, Y. Beers, *Rev. Sci. Instr.* **36,** *696–700 (May 1965).*
The P.S. detector plays an important role in the instrumentation for spectroscopy and radio astronomy and in atomic frequency standards. Usually the phase sensitive detector is preceded by a narrow band-pass amplifier centered on the reference frequency or one of its harmonics. Such a procedure discards useful information contained in the other harmonics. It is suggested that the narrow-band amplifier be replaced by a wide-band one and that the reference waveform be shaped to be identical with that of the desired signal. First order calculations show that this method gives slightly better sensitivity than the conventional one. Also, discrimination against coherent signals of other waveforms can be obtained. If a differentiating circuit is inserted into either the input or the reference circuit, the detector output is an odd function of the phase angle. Therefore, this arrangement can be used as a sensor for a servo system used to lock the phase of the reference oscillator to the signal.

Preliminary studies directed toward determination of spectra absorption coefficients of homogeneous materials in the infrared at elevated temperatures, W. B. Fussell and R. Stair, *(Symp. Measurement of thermal radiation of solids, San Francisco, Calif., Mar. 4–6, 1964), NASA SP–55, Session III, Paper 29, pp. 287–292 (1965).*
A double-oven, single-beam, infrared spectrophotometer system has been used successfully at the National Bureau of Standards to measure the normal spectral radiance ratio and absorption coefficient of infrared optical materials from 2.5 to 15 microns at temperatures from 600 to 1300 °K. The basic principle of the system is the comparison of the spectral radiance of a sample of material with the radiance of a blackbody, at the same temperature and wavelength. Measurement of the spectral radiance ratio spectra of several samples of the same material having different thicknesses allows both the spectral absorption coefficient and surface reflectance to be computed. The major components of the system are: (1) a recording infrared spectrophotometer, (2) "blackbody" and "sample" ovens, mounted adjacent to each other on a movable carriage, which heat the blackbody and sample to the desired temperature, (3) a spherical and a plane mirror which direct the radiant flux from the ovens into the spectrophotometer, (4) two Pt-10 percent Rh thermocouples—one for each oven—to indicate the temperature at a point inside the oven cavity, (5) a hollow cylindrical blackbody with a calculated emissivity of better than 0.9995, (6) a Pt-plated sample holder, and a radiation shield to reduce as much as possible background radiation from the sample oven. It is shown mathematically that a sample optical thickness of 1/2 allows the absorption coefficient to be computed most accurately, if the surface reflectance is known.

Project FIST: Fault isolation by semi-automatic techniques, G. Shapiro, G. J. Rogers, O. B. Laug, and P. M. Fulcomer, Jr., *IEEE Spectrum, pp. 98–111 (Aug. 1964); pp. 130–144 (Sept. 1964).*
The method of Fault Isolation by Semi-automatic Techniques developed at the National Bureau of Standards, to which the acronym FIST has been applied, creates a new field of metrology which permits the measurement of the dynamic performance of electronic circuits by unskilled personnel under field operating conditions. It is a diagnostic tool for rapidly isolating faults in modularized, non-computer type electronic equipment without removing the modules from the prime equipment.
The system consists of test points and associated circuitry which are built into the prime equipment, and a small, hand-carried, general-purpose test instrument. The test points are located on an easily accessible test panel and are arranged in an order which permits rapid checking of the modules in a logical sequence.
Fault isolation is accomplished by testing the dynamic performance of each module with a test instrument which is basically a device for comparing the peak-to-peak amplitudes of two periodic voltage waveforms. Since many circuit properties other than voltage must be measured, transformation networks are provided to convert the characteristic being measured to a periodic voltage which is within the range of the test instrument.
The tests are usually made while the module under test is performing its normal function with the normal inputs to the module providing the stimuli for the tests. When this is not possible, a stimulus generator is used to furnish the necessary signal or signals. One of the more complex stimulus generators is described. Finally, a prototype test instrument capable of simultaneously testing four characteristics of the module or of its stimuli is described in detail.

Recent developments in using elastomers for static cryogenic seals, P. R. Ludtke, *Proc. Seventh National Society Aerospace Materials Process Engineers Symp., pp. 25–1–25–14 (Western Periodicals, Los Angeles, Calif., 1964).*
It has been found that certain elastomeric O-rings are capable of reliable cryogenic seals in spite of their brittle nature at cryogenic temperatures. Fluid non-compatibility, vibration sensitivity and the high compressive forces required for sealing have limited the applications of this type seal. New improved flange designs require only moderate bolt loading. The minimum amount of force necessary to maintain a seal to 76K has recently been measured for the better compounds.
Leakage past a compressed O-ring is due to minute leak paths forming at the elastomer-flange interface during cooldown. This interface "unseating" has been attributed to radial differential contraction. Polytetrafluoroethylene, aluminum, lead, gold and indium films have been tested as interface "lubricants" to prevent these leak passages from forming. Of these materials indium performs best as an interface film. An elastomer-indium sandwich seal has evolved which requires only 35 percent of the force required for a plain elastomer O-ring and is relatively insensitive to vibrations and shock. A modified seal of this design could also protect the compressed elastomer from noncompatible fluids, except liquid oxygen. Indium is LOX sensitive.

Sensitivity indices for Hall generators, S. Rubin, *Solid State Design Mag.* **5,** *No. 12, 38–39 (Dec. 1964).*
The Hall generator is usually characterized as a product-sensitive device, but product sensitivity (the ratio of the Hall voltage to the product of control current and magnetic induction) is unsatisfactory as a figure of merit for many applications. For this reason, two additional sensitivity indices, one a function of magnetic induction, and the other a function of control current are proposed, defined, and illustrated by example.

Some factors affecting the sensitivity and spectral response of thermoelectric (radiometric) detectors, R. Stair, W. E. Schneider, W. R. Waters, and J. K. Jackson, *Appl. Opt.* **4,** *No. 6, 703–710 (June 1965).*
A number of thermal detectors (thermopiles) has been studied for variations in sensitivity which exist over their surfaces and also for variations of sensitivity with wavelength. These variations differ depending upon whether the thermoelectric output is measured with dc instrumentation, with conventional ac instrumentation, or with ac synchronous-rectifier instrumentation. In general, lower responses for the longer wavelengths are observed when commercial thermopiles are compared with a new cavity "blackbody" detector—and the difference may be greater when measured with ac synchronous-rectifier instrumentation. When the output of a detector is measured through the use of a conventional tuned ac amplifier, variation in sensitivity of as much as 5 to 1 has been found for different areas of the surface. When a phase-sensitive amplifier is employed, first set for maximum response with the entire thermopile irradiated, even larger variations in sensitivity may be observed.

Standard test for determining alkali resistance of porcelain enamels, M. D. Burdick, *Proc. Porcelain Enamel Inst. Forum* **26,** *227–236 (Oct. 14–16, 1964).*
A detailed procedure for a standard test for determining the alkali resistance of porcelain enamels is presented. Modifications of the present PEI alkali test equipment are suggested to increase its capacity and reliability and to reduce its cost. The variables in alkali testing requiring consideration and control are discussed together with their effect on obtaining reproducible test results. The selection of various procedural steps was made after a statistical evaluation of relative merit.

Standarization of definitions for Hall effect devices, S. Rubin, *Proc. Rotating and Static Precision Components Symp., Apr. 1964, pp. 344–460 (Bureau Naval Weapons, Washington, D.C., 1964).*
When an electric and a magnetic field interact in any noninsulating medium, the galvanomagnetic effects occur. These two effects, the Hall effect and magnetoresistance, are defined. A Hall plate and a Hall generator are defined, and described. The relation of the Hall electric field and magnetoresistance to the Hall plate characteristics and to each other are described. Examples of Hall generator application are given. The work in process on the standarization of terminology and measuring methods for Hall generators is described and a list of the terms now defined is given. Specific terms are defined in detail. The need for and advantage occurring from the use of standard terms is noted.

Weather resistance of porcelain enamels exposed for seven years at various sites, M. A. Rushmer and M. D. Burdick, *Proc. Porcelain Enamel Inst. Forum* **26,** *214–226 (Oct. 14–16, 1964).*
An exposure test of porcelain enamels at seven representative sites in the continental United States was initiated by the National Bureau of Standards and the Porcelain Enamel Institute in 1956. After seven years all specimens were returned to Washington and the changes in gloss and color determined. These changes were found to correlate with the acid resistance ratings of the enamels. Comparison with the relative humidity at the respective sites showed that the largest gloss and color changes occurred at the sites with the highest average relative humidities. The *p*H of particulate matter collected at the sites also was found to correlate with site severity.

Weight checking of aerosols, S. Hasko, *Mod. Packaging Mag.* **38,** *No. 11, 141 (July 1965).*
Weights and measures officials, representatives of the aerosol industry, and others have expressed an urgent need for a solution to the problems that relate to the determination of net contents of aerosol packaged products. Checking procedures were developed in cooperation with the Chemical Specialties Manufacturers Association and statistically evaluated for two of the four broad categories (or over 80%) of aerosol products on the market. Procedures on the remaining two categories are in the development and evaluation process.

Analogies between theories of antenna arrays and passive networks, M. T. Ma., *IEEE Intern. Conv. Record* **13,** *Pt. 5, 150–154 (Mar. 1965).*
This paper demonstrates the analogy between two different fields, antenna arrays and passive networks, which are generally not known to each other. Successful application, either directly or with modification, of various known techniques for synthesizing a passive network when an impulse response is specified, to the synthesis of linear antenna arrays with amplitude excitations, phase distributions and element spacings as the controlling parameters when a desired radiation pattern is given, is presented with many interesting examples. Providing the antenna array theorists with information known to circuit theorists and vice-versa, this paper should prove to be helpful to both groups in extending their interest.

Relation between normal trichromatic vision and dichromatic vision representing a reduced form of normal vision, D. B. Judd, *Acta Chromatica* **1,** *No. 3, 89–92 (Oct. 1964).*
In 1860 Maxwell substracted the tristimulus values of a color set by a dichromatic observer from the tristimulus values of the same color set by an observer with normal color vision, and stated that the three differences specified "that color, the lack of sensation of which forms a defect of the dichromatic eye." Nuberg and Yustova, in 1955, gave a vectorial proof of this relation, and in the present paper an analytical proof is given.

A system for accurate D-C and A-C voltage measurements, F. L. Hermach, J. E. Griffin, and E. S. Williams, *IEEE Intern. Conv. Record* **13,** *Pt. 11, 172–182 (Mar. 1965).*
A system for calibrating and using a group of d-c and a-c standards has been developed at NBS to meet increasing needs for greater accuracy in the measurement of d-c and rms audio-frequency voltages. This consists of: a) a group of saturated standard cells; b) a six-dial universal ratio set (URS), with a control box so that it may be used as an accurate potentiometer; c) a simplified volt box of the Silsbee type and a convenient method for calibrating it with the URS; d) a new differential-thermocouple ac-dc comparator and e) an inductive voltage-divider for low a-c voltage measurements and for calibrating the URS.
With the system of intercomparisons the sustained accuracy in use depends only on the standard cells, the very stable inductive divider, and the ac-dc difference of the comparator. As a result, it is believed that an accuracy of 20 ppm can be obtained for d-c voltage measurements from 0.5 to 1000 volts, and 40 ppm of rated voltage of the range in use for rms voltages from 1 to 500 volts at frequencies between 20 and 20,000 Hz, in terms of the d-c volt and the ac-dc transfer standards maintained at NBS.

An international comparison of inductive voltage divider calibrations at 400 and 1000 hertz, W. C. Sze, A. F. Dunn, and T. L. Zapf, *IEEE Intern. Conv. Record* **13,** *Pt. 11, 126–135 (Mar. 1965).*
The establishment and maintenance of the highest possible order of accuracy for the measurements of voltage ratio and phase angle are responsibilities of the national laboratories. This paper reports the results of an international comparison of a seven-decade inductive voltage divider by the U.S. National Bureau of Standards and the National Research Council of Canada. The calibration techniques used in each laboratory are discussed in detail, and the results of calibration at 400 and 1000 Hz are compared. The accuracies of measurements are within 0.1 ppm of input for voltage ratio and 1/(setting of dials) ½ microradians for phase angle.

APPA-TAPPI reference material program. III. A discussion of lambda variance and its application to TAPPI standard T 414 m-49 for internal tearing resistance of paper, T. W. Lashof, *TAPPI* **47,** *No. 8, 445 (Aug. 1964).*
The causes, statistical aspects, and practical significance of the "lambda variance" are discussed. It is shown that the new-type tearing strength instrument with cutaway to prevent rubbing of the

specimen as a significantly larger lambda variance than does the older-type instrument. The cause is unknown, although several possibilities have been eliminated. The design of the new-type instrument is theoretically more desirable because of the absence of rubbing; consequently, the new-type instrument has been accepted as the standard, despite the limitation on standardization resulting from higher lambda variance.

Microwave calibration techniques at the National Bureau of Standards, R. E. Larson, (*Proc. Intern. Measurements Conf.*), *Acta Imeko* **3,** *383–393 (1964).*
The measurement systems to be discussed have been developed for regularly scheduled microwave calibration services in the U.S. National Bureau of Standards' Boulder Laboratories, and the stated accuracy data and limitations apply to their application as such. Calibration systems in the microwave region have been developed for the measurement of low-level c-w power, reflection coefficient magnitude, frequency, attenuation, and noise power. The operating frequency for the calibration systems, all utilizing rectangular waveguide, ranges from 2.6 Gc for all quantities to as high as 90 Gc for the calibration of cavity wavemeters. The present status in the development of this large number of microwave calibration systems is reviewed briefly. An error analysis considering both systematic and random errors is given briefly for each of the quantities measured, and the resulting overall accuracy reported for the calibration of interlaboratory standards is stated.

National Bureau of Standards gas thermometer. III. Constant volume valve, R. L. Anderson and L. A. Guildner, *Rev. Sci. Instr.* **36,** *No. 5, 615–616 (May 1965).*
Special valves have been constructed to meet the constant volume requirements of a gas thermometry program. With a total volume inside the valve block less than 20 mm^3, and that which is a part of the gas thermometer about 3 mm^3, no change in excess of 0.005 mm^3 is expected. This is achieved by extending the valve stem past the seat through a seal on the opposite side, so that the volume of stem pulled into the gas chamber is equal to the volume withdrawn when the valve is opened.

Simultaneous dielectric constant and volume measurements on liquids at high pressures, N. L. Brown, *Proc. Electrical Insulation Conf., Cleveland, Ohio, Oct. 1964, Natl. Acad. Sci.-Natl. Res. Council Publ. 1238, pp. 36–40 (1965).*
A combined dilatometer and dielectric cell is described which can be used at pressures from atmospheric to 2000 kgf/cm^2 and at temperatures from room to about −150 °C. Techniques for measuring the volume of the liquid and its dielectric constant and loss are also described.

Planning for better measurement accuracy, R. D. Huntoon and W. A. Wildhack, *ISA J.* **12,** *No. 1, 57–60 (Jan. 1965).*
The NBS Institute for Basic Standards attempts to promote accuracy at all levels of measurement: by providing accurate calibrations at the highest level, by developing and publishing methods of precision measurements for general use, by offering general consultation, by cooperation with technical societies, by arranging specialized conferences, and by sponsorship of the National Conference of Standards Laboratories. While it has no legal power to require industry to use its services, IBS cooperates closely with industry and other Government agencies through advisory and consultative committees, to determine developing needs for increased accuracy and measurement services. Since the space, defense, and atomic energy industries are primary generators of high-accuracy measurement and calibration needs, these industries, together with IBS and other Government agencies, face common problems, not only in forecasting critical needs, but also in funding R and D for standards, both in government and industrial laboratories.

Uncertainties associated with proving ring calibration error, T. E. Hockersmith and H. H. Ku, *ISA J.* **12,** *No. 6, 73–77 (June 1965).*
A method of error analysis is presented using data obtained from dead-weight calibration of various capacity proving rings. A breakdown of the errors into components by statistical methods and their combination into a final uncertainty statement is discussed in detail. Graphical representations are used in several places to help in the exposition.
Extension of the analysis and method of handling calibration data for multiple proving ring setups is discussed in an effort to show that the same general method of analysis should be adequate.

Annual observatory report from the National Bureau of Standards, C. E. Moore, *Astron. J.* **69,** *No. 9, 696–698 (Nov. 1964).*
This report, submitted annually to the Astronomical Journal, stresses the research carried on at the NBS, that is of astrophysical interest.

Beam loading in linear accelerators, J. E. Leiss, *IEEE Trans. Nuclear Sci.* **NS–12,** *No. 3, 566–579 (June 1965).*
The interaction of the bunched particle beam in a linear accelerator with the waveguide structure produces several effects which go under the general name of beam-loading. These effects include reduction, redistribution, and phase shift of the rf field in the waveguide, changes in the tuning of the waveguide structure, excitation of other waveguide modes, and various transient phenomena.
A discussion of the various effects and methods for their calculation will be presented.

Calibration of Schlieren systems, J. R. Meyer-Arendt and E. P. Shettle, *J. Appl. Opt. Letter* **4,** *No. 6, 757 (June 1965).*
Brief description of a schlieren calibration system that is derived from the Ronchi test for measuring focal lengths.

Chromatography on glass of controlled pore size, W. Haller, *Nature* **206,** *693–696 (1965).*
A new type of chromatographic column, composed of controlled-pore size glass was investigated for separation efficiency, packing characteristics, hydraulic behavior and chemical resistance. The study covered columns from 170 to 1700 Å average pore diameter. Excellent separation behavior was found, exceeding the range presently available with cross-linked gels. All columns regardless of the pore sizes were found to be completely rigid, resulting in reproducible characteristics and an extremely low flow resistance which was not affected by flow velocity or age of column. Columns can be heat-sterilized and cleaned with hot nitric acid for removal of organic contaminants. The method suggests itself for the separation of cell components, virus particles and macromolecular substances, particularly in large scale or sterile operations where speed, reproducibility and reprocessing of contaminated bed-material is of benefit. Easily controlled and measured pore size and narrow pore size distribution further suggest the use of the technique for size determination and diagnostic procedures on unknown particulate and macromolecular material.

Correction of optical distance measurements for the fluctuating atmospheric index of refraction, P. L. Bender and J. C. Owens, *J. Geophys. Res.* **70,** *No. 10, 2461–2462 (May 15, 1965).*
A direct optical method is proposed for geodetic distance measurements. It is argued that a measurement of the difference in optical path length for blue and red light permits the correction for the fluctuating atmospheric index of refraction to be made considerably more accurately than before. It appears to be possible, using this method, to measure distances of the order of ten kilometers roughly an order of magnitude more accurately than by present optical methods.

Critical examination of birational energy-transfer theory, F. H. Mies, *J. Chem. Phys.* **42,** *No. 8, 2709–2720 (Apr. 15, 1965).*
An accurate He-H_2 interaction potential is used to test the validity of the potential that has been employed in energy transfer theory. It is found that a model based on the assumption of additive exponential potentials acting between atomic centers does not reproduce the forces, matrix elements or transition probabilities derived from the exact potential. The cross-section for vibrational excitation is critically dependent on the details of the intermolecular potential; it is particularly sensitive to small differences in the diagonal matrix elements of the interaction potential. The discrepancies that are found for the relatively simple He-H_2 system suggest that the predictions of the model potential for more complicated systems are based on pure speculation and are of only qualitative value.

High voltage Laue x-ray photography of large single crystals, B. Paretzkin and H. S. Peiser, *Science* **146,** *260 (1964).*
The perfection of relatively large single crystals can be tested by Laue-type transmission X-ray diffraction pictures using much higher voltages for X-ray generation than is conventional in diffraction experiments. Applications are described to orientation spread of subcrystal units and to the study of loss of primary extinction due to occluded chemical impurities. An advantage of this method is its possible application to crystals inside polycrystalline or galss containers.

Higher-order skewnesses in a turbulent field, F. N. Frenkiel and P. S. Klebanoff, *Compt. Rend.* **260,** *6026–6029 (1965).*
Experimental measurements of certain statistical characteristics of wind-tunnel grid turbulence are determined using high-speed computing techniques and compared with the results derived from a non-Gaussian probability density distribution for the turbulent velocities.

Measurements of the viscosity of parahydrogen, D. E. Diller, *J. Chem. Phys.* **42,** *No. 6, 2089–2100 (Mar. 1965).*
The coefficient of shear viscosity, η, of parahydrogen has been measured by the torsional crystal method at temperatures from 14 to 100 degrees K and at pressures up to 345 atmospheres. Twenty compressed fluid isotherms emcompass the density range 0.003–0.087 g./cm³ and include the critical region. The precision and accuracy of the measurements is about 0.5 percent. The temperature-dependence of η changes sign at a density approximately twice the critical density. The viscosity at the critical point is estimated to be $35.5 \pm 0.5 \times 10^{-6}$ g./cm-sec. The viscosity of saturated liquid normal hydrogen is up to 5 percent greater than that of parahydrogen at the same temperature. Data of this report have been represented within experimental error by an empirical equation of the form

$$\eta = \eta_0(T) + A(\rho) \exp B(\rho)/T$$

where $\eta_0(T)$ is the viscosity in the low density limit and $A(\rho)$ and $B(\rho)$ are density-dependent coefficients.

Potential distribution in a rectangular semiconductor bar for use with four-point probe measurements, M. J. Reber, *Solid State Electron.* **7,** *No. 7, 525–529 (July 1964).*
The electric potential distribution is given for an arbitrary placement of current contacts on one side of a rectangular bar of semiconductor material having finite dimensions and two conducting ends. A factor is derived which can be used in conjunction with a four-point probe to correct the measured conductivity of such a bar for the effects of its dimensions and plated ends. This factor is of utility in the correlation of conductivity measurements made on a single specimen by means of two- and four-point probes.

Some considerations relative to an atomic definition for the unit of time, R. C. Mockler and J. M. Richardson, *Proc. Consultative Committee for the Definition of the Second of the International Committee of Weights and Measures, Paris, France, Apr. 1961, pp. 58–65 (Dec. 1964).*
The presently attained accuracy of Cs beam frequency standards is established by several examples. Independent estimates of relative accuracy based on the quantitative uncertainty in various experimental factors and the comparison of frequency between two independent machines gives $\pm 1 \times 10^{-11}$ (one standard deviation) for each of two standards. The daily frequency difference between these two standards has remained fixed and within this accuracy for 3 years in spite of great modification to each. Intercontinental comparison of six diverse Cs standards by VLF radio gives long term (18 month) agreement to $\pm 1 \times 10^{-10}$ for laboratory type standards. Radio comparison of two Cs controlled time scales over 1½ years gives agreement to $\pm 1 \times 10^{-11}$ on the average for this period. Major limitations to accuracy arise from uncertainty in the C field and from phase differences between the separated oscillatory fields exciting the atomic transitions. Both of these individual limitations have recently been reduced well below the 1×10^{-11} figure, allowing some promise of future improvement in overall accuracy. Preliminary results on a Tl beam give $\nu_0(\text{Tl}) = 21{,}310{,}833{,}946.5 \pm 0.4$ c/s, a relative accuracy of $\pm 2 \times 10^{-11}$. This relative accuracy is a preliminary estimate (one standard deviation) for a single machine. Tl standards promise future accuracy beyond this, but presently lack lengthy and widespread study. A similar statement applies to hydrogen masers. Time scales continuously controlled by atomic standards for several years have been constructed. It is shown that atomic frequency and time standards now accurate to at least $\pm 1 \times 10^{-10}$ are both needed and available. Future progress is likely both to allow and to require refinement of any presently recommended atomic definition.

Fading on microwave line-of-sight paths, H. T. Dougherty, *Proc. 3d Tropospheric Refraction Effects Meeting* **1,** *125–135 (Nov. 1964).*
The sources of fading on microwave line of sight propagation paths are described. The results of a preliminary analysis of 7 months of signal recordings for the MISTRAM I data link paths are presented.

Ionospheric effects observed around the time of the Alaskan earthquake of March 28, 1964, K. Davies and D. M. Baker, *J. Geophys. Res.* **70,** *No. 9, 2251–2253 (May 1, 1965).*
Some observations are reported on the spectra of ionospherically reflected radio signals about the time of the Alaskan earthquake of March 28, 1964. These observations consisted of vertical soundings of 4 and 5 Mc/s and oblique signals from WWVH-10 Mc/s recorded at Boulder, Colorado. Attention is drawn to some peculiar features on the records which may be associated with the earthquake.

Ionospheric propagation on high frequencies, K. Davies, *4U11TU Calling* **2,** *112–113 (1965).*
This is a short invited contribution to the International Amateur Club of the International Telecommunications Union in Geneva, Switzerland. It deals with frequency selection using (1) predicted ionospheric data and (2) auxiliary ionosondes.

Noise tests of an airborne microwave refractometer system, M. C. Thompson, Jr., and W. B. Grant, *Rev. Sci. Instr.* **36,** *No. 6, 758–759 (June 1965).*
An airborne microwave refractometer system was tested to determine its noise spectrum and the distribution of this noise within the system. Samples of atmospheric turbulence spectra are shown from about 600 ft to 6000 ft above ground (about 6000 ft to 11,000 ft above m.s.l.). Total noise in a 0.03–15 c/s pass-band is found to be about 0.04 N-units rms and to be approximately "white".

Radiation efficiencies of half-wave dipole antennas, R. G. FitzGerrell, *IEEE Trans. Ant. Prop.* **AP-13,** *326–327 (Mar. 1964).*
The radiation efficiencies of copper, silver, and aluminum half-wave dipole antennas in free space are calculated. The data is presented graphically with the efficiency shown as a function of d/λ and frequency.

Electrical properties, A. J. Curtis, *Book, Crystalline Olefin Polymers, ed.* R. A. V. Raff, **2,** *105–130 (Interscience Publ. Inc., New York, N.Y., 1964).*
In this section emphasis is on the dielectric properties with brief discussions of breakdown and volume resistivity. The relationship between molecular structure and dielectric properties is emphasized particularly, since only slight experimental data on certain lower members of this series of polymers are as yet available. The effects of various modifications, oxidative degradation, plasticizers and high energy irradiation on the electrical properties are also discussed.

Receiver noise factor, E. Hildner, *Proc. Intern. Telemetry Conf., Washington, D.C., May 16–20, 1964, pp. 326–333 (May 1965).*
The Institute of Radio Engineers' definition of receiver noise factor is reviewed. The definition's implications are explored. CW- and dispersed-signal source measurement techniques are discussed and the mathematical base for each method is displayed. The quantities which must be measured in each method are pointed out with their respective advantages and disadvantages. It is concluded that the dispersed-signal source measurement technique is simpler than the CW-signal source techniques considered in this paper, although less supplementary information, viz bandwidth, is obtained.

High pressure x-ray diffraction studies, G. J. Piermarini, *Proc. 13th Chemical Engineering Conf., Montreal, Canada, Oct. 19–23, 1963, pp. 182–185 (Chemical Institute of Canada, 1963).*
A device containing an opposed diamond-anvil pressure cell and capable of obtaining x-ray diffraction powder patterns photographically of materials subjected to pressures of up to 70 kilobars or more is described. Experimental results obtained with this apparatus are presented which serve to illustrate its range of application, and its usefulness as a crystallographic tool in high-pressure research.

High temperature measurements and standards: 1000–3000 °C, R. F. Walker, (*Proc. Intern. Symp. High Temperature Technology, International Union of Pure and Applied Chem.,*

Asilomar, Pacific Grove, Calif., Sept. 1963), Book, High Temperature Technology. Suppl. to Pure and Applied Chem., p. 7 (Butterworths Inc., Washington, D.C., 1964).
Current interest in high temperature technology places increasing demands and responsibilities on those concerned with high temperature measurements and standards. The general philosophy behind the current activity to advance the measurement science is discussed and illustrated with reference to the current progress that is being made, primarily at the National Bureau of Standards. The discussion is limited to problems which are encountered with condensed phases in the 1000–3000 °C temperature range. Examples of the experimental program in the areas of temperature measurement and the physical and chemical properties of substances are given. Associated with the experimental program is an increasing effort to systemize and rationalize the compilation of reference data and to formulate standards and codes of practice. The interest of various national and international bodies in the promulgation of the needs and stimulation of the activities are also discussed.

Oxidation of asphalt in the presence of ozone, J. R. Wright and P. G. Campbell, *Am. Chem. Soc. Div. Petroleum Chem. Preprint* **9,** *No. 2, B99 (Apr. 1964).*
The effects of ozone on the oxidation of an asphalt flux and on the photo-oxidation of a commercial coating-grade asphalt were investigated under a variety of experimental conditions. Oxidative changes were measured by infrared spectroscopy and by increased softening points of the asphalts.
In oxidation of the flux, ozone-enrichment of air reduced the time required to reach a given softening point to one-half that needed for air alone. Ozone-enriched oxygen reduced this time to one-fifth that needed for air. Reaction temperatures did not exceed 158 °C, approximately one-half those used in commercial air-oxidation; gas flow rates were about one-fourth the commercial rate. Coating-grade asphalts produced under these mild conditions were more stable to photo-oxidation than was a commercial asphalt from the same flux.
Asphalt surfaces were oxidized when treated with ozone in total darkness, in room light, and in the radiant energy of a carbon arc. No oxidation was detected when asphalt was exposed to oxygen in room light. Photo-oxidation rates of asphalt films increased approximately three-fold when the films were exposed to carbon-arc radiation in ozone-enriched oxygen as compared to exposure in air.

Radiochemical determination of uranium of low activity, L. A. Currie, G. M. France, III, and P. A. Mullen, *Health Phys.* **10,** *751–755 (1964).*
A systematic investigation of uranium analysis was undertaken down to levels as low as one-tenth of the respective maximum permissible concentrations in water and in urine. Two new procedures were developed, having improved recoveries and reproducibilities 0.96 ± 0.04 and 0.87 ± 0.06, based upon six and seven samples, respectively. (The indicated values are the arithmetic mean and computed standard deviation of a single determination.) The new procedures require only 25 ml samples and considerably less time than one generally accepted procedure. The recovery of one of the new procedures showed no significant change when uranium concentration varied by about a factor of 10^6.

Radiolytic stress relaxation of an ethylene-propylene copolymer, H. Yu and L. A. Wall, *J. Phys. Chem.* **69,** *2072–2078 (June 1965).*
The kinetics of network chain scission, induced by γ-rays, has been studied by stress relaxation at a constant elongation in vacuum and in air. The rate of chain scission of 1:1 ethylene-propylene copolymer was found to be independent of initial network chain density, and the initial rates were roughly the same in air and in vacuum. Parameters for crosslinking, induced by γ-rays, were obtained by sol extraction and by measurement of elastic properties of the resulting networks. G-values for scission and crosslinking and gel dose, obtained by stress relaxation and elastic properties and by sol extraction, were found to be in an agreement with each other.

Sampling of leather for physical and chemical examination, J. Mandel and J. R. Kanagy, *Book, The Chemistry and Technology of Leather* **4,** *Ch. 59, 223–242 (Reinhold Publ. Corp., New York, N.Y., 1965).*
A presentation of some general principles of sampling, with application to the sampling of leather.
The topics discussed in this chapter include:
1. General statistical principles of sampling: effect of sample size and of lot size;
2. Formulas for the determination of sample size;
3. The selection of a sampling location on a leather side;
4. Tables of the variability of physical and chemical tests between locations and between hides;
5. Acceptance sampling;
6. A survey of the literature.

Stress relaxation of γ-irradianted fluorocarbon elastomers, T. Yoshida, R. E. Florin, and L. A. Wall, *J. Polymer Sci.* **A3,** *No. 5, 1685–1712 (May 1965).*
Polyvinylidene fluoride, polytrifluoroethylene, and two rubbery copolymers with vinylidene fluoride were crosslinked by gamma irradiation in vacuum. Radiation-induced chain scissions in the copolymers were studied by observing the relaxation of stress at constant extension during further irradiation at 27 °C, at 0.31 to 2.7 megaroentgens per hour, in nitrogen and in air. From gel content, swelling and elasticity, the values of G_c (crosslinking) and G_d (scission) were respectively, CF_2CFH, $G_c = 2.2$ and $G_d = 0.4$: CF_2CH_2, 2.0 and 0.3: $CF_2CH_2 + C_3F_6$, 3.4 and 1.3; $CF_2CH_2 + CF_2CFCl$, 1.8 and 1.4. The G_d values from stress relaxation were variable; the lowest were: for $CF_2CH_2 + C_3F_6$, 4.6 in nitrogen and 8.4 in air; for $CF_2CH_2 + CF_2CFCl$, 1.9 in nitrogen and 3.6 in air.

The determination of beta-emitting radionuclides in aqueous formamide solutions, A. Schwebel, *Proc. Bioassay and Analytical Chemistry Meeting, Argonne Natl. Lab., Argonne, Ill., Oct. 1962, ANL Publ. 6637, p. 29 (1962).*
A method is described for the radioassay of β or β–γ emitting nuclides in an aqueous formamide solution placed in a windowless flow counter.

The half-life of carbon-14; comments on the mass-spectrometric method, E. E. Hughes and W. B. Mann, *(Proc. Radio-Carbon Dating Conf., Cambridge, 1962), Intern. J. Appl. Radiation Isotopes* **15,** *97–100 (1964).*
An assessment has been made of the mass-spectrometer results in the recent NBS determination of the half-life of carbon-14.
Evidence is presented to show that the uncertainties due to effusive separation and the dependence of the sensitivity constant on the isotopic abundance of carbon-14 are well within the 0.8 percent uncertainty already assigned to these sources.

The role of carbon dioxide in the bone char process, F. G. Carpenter, V. R. Deitz, and D. Larry, *Proc. 1963 Sugar Industry Technologist* **22,** *No. 2, 27–45 (Chemistry Inst. New York, N.Y., May 1963).*
A study has been made of the flux of carbon dioxide into and out of bone char during the bone char process. The primary measurements were adsorption isotherms of carbon dioxide at various temperatures and after specified pre-treatments. The outgassing behavior and rates of adsorption were observed. The immersion of bone char with adsorbed carbon dioxide in water was also studied. Of the two major components of bone char, the basic calcium phosphate (B.C.P.) adsorbed more carbon dioxide per unit area than did the carbonaceous component. Behavior similar to bone char was found for bone ash and hydroxylapatite; the carbonaceous residue was found similar to coconut charcoal. The calculated isosteric heats of adsorption for different adsorbents were in the same sequence as the corresponding adsorption isotherms expressed per unit surface area. The wetting of the char by water displaces some of the adsorbed carbon dioxide and the resulting carbonic acid shows chemical reactivity with the B.C.P. support and thus in turn with the sugar liquor. The pickup of carbon dioxide by revivified char shows a unique behavior in regard to *p*H.

Theoretical electromotive forces for cells containing a single solid or molten fluoride, bromide, or iodide, W. J. Hamer, M. S. Malmberg, and B. Rubin, *J. Electro. Chem. Soc.* **112,** *No. 7, 750–755 (July 1965).*
Theoretical electromotive forces have been calculated for reversible

cells of the type: metal |metallic halide| halogen for fluorides, bromides, and iodides from 25 to 1500 °C using available thermodynamic data. The data for each halide type are arranged in electromotive force series and compared with the respective series in aqueous solutions.

Weathering: theoretical and practical aspects of asphalt, J. R. Wright, *Book, Bituminous Materials: Asphalts, Tars, and Pitches, Ed. A. J. Hoiberg, Vol.* **2,** *Asphalts, pt. 1 , chapt. 8, 249–306 (John Wiley & Sons, Inc., New York, N.Y., 1965).*
The technical literature relating to the durability of asphalt upon exposure to weather was reviewed and discussed on the basis of the main destructive factors. These were: oxygen, light, heat, water, atmospheric oxidants, and mechanical stress. Both steam-refined and air-blown asphalts were included. Asphalt weathering test methods employed in accelerated weathering were evaluated with respect to the technical significance of test results. Natural weathering results were compared to accelerated weathering results whenever possible. A general correlation appeared to exist, but no direct time ratio of accelerated weathering exposure to outdoor exposure could be established. Rapid methods for predicting asphalt durability included the Oliensis Spot Test, solubility parameter, paraffinics content, asphaltene content, filtration time, and carbonyl index. The need for the development of scientifically sound, quantitative test methods was emphasized as the basis for product quality specifications.

X-ray study of isothermal thickening of lamellae in bulk polyethylene at the crystallization temperature, J. D. Hoffman and J. J. Weeks, *J. Chem. Phys. Note* **42,** *No. 2, 4301–4302 (June 15, 1965).*
Low-angle x-ray measurements have been made on bulk polyethylene at 128 °C as a function of time. The results show that the chain-folded lamellae slowly thicken in accord with deductions made previously from melting point data.

A liquid-medium step-function pressure calibrator, R. O. Smith, *J. Basic. Eng. Series D,* **86,** *No. 4, 723–727 (Dec. 1964).*
Some characteristics of a step-function pressure calibrator of the type devised by D. P. Johnson and J. L. Cross of NBS have been investigated. Theoretical prediction of the wave generation appears to be impracticable. It has been found possible, by empirically determined adjustments, to produce monotonic step-functions having 95 percent rise times in about 10 milliseconds suitable for calibration of transducers. Calibration accuracies are around 5 percent to 7 percent. The monotonic step-function pressure is also useful in evaluating creep or hysteresis in high frequency transducers which previously could not be inspected for that characteristic.

Automatic optical design, O. N. Stavroudis, *Book, Advances in Computers, ed. F. L. Alt and M. Rubinoff,* **IV,** *227–255 (Academic Press Inc., New York, N.Y., 1964).*
Various approaches to the application of high speed digital computers to the design of optical systems are presented in some detail. Some background in the form of a brief description of conventional methods of lens design is provided.

Clinical evaluation of complete dentures made of 11 different types of denture base materials, J. B. Woelfel, G. C. Paffenbarger, and W. T. Sweeney, *J. Am. Dental Assoc.* **70,** *No. 7, 1170–1188 (May 1965).*
Subjective clinical observations and objective laboratory measurements of 63 dentures from three to six years old showed a gradual decrease in serviceability with time without significant dimensional changes or warpage of the dentures. The relative effectiveness of a properly made denture depends upon how well the tissues of the wearer tolerate the stresses imposed in use. The findings demonstrate that subjective observations with proper discipline can furnish reliable and valid information in the clinical evaluation of dentures.

Comments on the paper "A liquid-medium step-function pressure calibrator", by R. O. Smith, J. L. Cross, *Trans. Am. Soc. Mech. Eng. Series D,* **86,** *729 (1964).*
The observed limitations of the step-function pressure generator have been functional. These comments show that some theoretical limitations might be reached by improved design and construction.

Comments on three papers on fire tests, J. V. Ryan, *ASTM Fire Test Symp., Oct. 1, 1962, Am. Soc. Testing Material Spec. Tech. Publ. No. 344, 52 (Oct. 1963).*
The author comments on points of interest in the following three papers:
1. Fire endurance tests of wall and partition assemblies, R. W. Bletzacker, Ohio State University.
2. Fire test of floor and ceiling assemblies, J. A. Bono, Underwriters Laboratories, Inc.
3. The fire marshal's viewpoint of fire tests, R. E. Carlson, California State Fire Marshal Office.

Digitizing pictorial information with a precision optical scanner, R. T. Moore, M. C. Stark, and L. Cahn, *Photogrammetric Eng.* **XXX,** *No. 6, 923 (Nov. 1964).*
An electromechanical scanner has been developed at the National Bureau of Standards which dissects a nine-inch square aerial photograph into 2.98 million picture elements and assigns one of eight numbers representing possible gray scale values to each element. The numerical representation of a stereo-photo pair is recorded on magnetic tape for subsequent processing in a high-speed electronic computer. A variety of matching techniques is being developed to facilitate recognition of conjugate points and permit the calculation of information necessary for a three-dimensional representation of the terrain.

Dimensional changes of dental amalgam associated with strain release in the silver alloy particles, G. Dickson and R. M. Waterstrat, *J. Dental Res.* **44,** *No. 3, 620 (May–June 1965).*
Most mechanisms proposed to explain the dimensional changes of dental amalgam are based on phase changes during the setting period. An experiment was made to determine the magnitude of dimensional change which might be associated with strain release rather than a phase change. To obtain a strained specimen and eliminate any effects from phase changes, particles of a commercial alloy for dental amalgam were compressed at a pressure not greater than 965×10^6 N/m² (140,000 psi) in a steel mold. On heating the specimen through temperature intervals between room temperature and 200 °C a growth of approximately 10 microns per cm was observed. The results suggested that dimensional changes associated with strain release in the silver alloy particles should not be ignored in explaining the expansion of dental amalgam during setting.

Effect of surface texture on diffuse spectral reflectance, Part B. Surface texture measurement of metal surfaces, D. B. Spangenberg, A. G. Strang, and J. L. Chamberlin, *(Symp. Measurement of Thermal Radiation of Solids, San Francisco, Calif., Mar. 4–6, 1964), NASA Spec. Publ. SP–55, Session II, Paper 17, pp. 169–177 (1965).*
Twenty-two specimens of varying degrees of surface texture, consisting of six specially prepared sintered beryllium samples, ten specially prepared tool steel samples and six commercially finished steel samples, were measured. The techniques of measurement and the experiment data obtained are presented.
These specimens were used by other investigators in an attempt to correlate the effect of surface texture on diffuse spectral reflectance. This experiment is discussed in the first part of this paper ("Diffuse Spectral Reflectance of Metal Surfaces" by H. J. Keegan, J. C. Schleter and V. R. Weidner).

Fracture topography of brittle polymers, S. B. Newman, *Polymer Engr. Sci.* **5,** *No. 3, 159–165 (July 1965).*
Fracture surfaces record the kinetics of failure at two levels in the structure of polymeric solids. The first is evidenced by the formation of geometric markings resulting from the interaction of the primary fracture front with secondary fractures developing radially just ahead of the primary fracture. These markings are often visible to the unaided eye and have minimal dimensions in the micron range. The second fracture phenomenon appears to involve the orientation of molecular chains or bundles. Such orientation manifests itself in the interference-color producing film found on the fracture surfaces of poly(methylmethacrylate) and polystyrene. It is also apparent in the free or adherent film found on the surfaces of large fractured crazes. Some evidence is presented for the existence in these films of chain bundles 30 A or less in diameter. Similar mechanisms are apparently operating in the production of "craze matter" and of fracture surface films.

Gold in dentistry, W. T. Sweeney and C. L. Burns, *American Society for Metals Monograph on Gold. Recovery, Properties and Applications, ch. 13, pp. 227–235 (D. Van Nostrand Co., Inc., Princeton, N.J., 1964).*
This is a resume of the use of gold in dentistry to be included in monograph on Gold. It was prepared at the request of the editor, Dr. E. M. Wise. The data are chiefly from similar articles in the Metals Handbook. This chapter contains no data not already published.

Guide to dental materials, 1964–1965, G. C. Paffenbarger, J. W. Stanford, and W. T. Sweeney, *Am. Dental Assoc. 2d ed., 159 pages (Chicago, Ill., 1964).*
The sixth edition of this booklet covers all changes made in the *Guide to Dental Materials* since the fifth edition published in January, 1962. Also included are changes in the List of Certified Dental Materials and the bibliography of dental research at the National Bureau of Standards since the fifth edition.

Interferometer test of the 26-inch refractor at Leander McCormick Observatory, J. B. Saunders, *Astron. J.* **69,** *No.6, 449 (Aug. 1964).*
An eyepiece interferometer has been developed that permits the measurement of aberrations in large telescope objectives. This interferometer permits the measurement of the shape of the wave front produced by an objective with light from a star. The test has been applied to the 26 inch refractor at the Leander McCormick observatory. The results show that this lens approximates the Rayleigh tolerance of one quarter wave. Photographs of the interference fringes and graphical representations of the aberrated wave fronts are shown.

Measurement of very-high pressures, E. C. Lloyd and A. A. Giardini, *Acta Imeko* **2,** *305 (1964).*
The state-of-the-art in measurement of pressures above a few kilobars is summarized in a graph of accuracy of measurement versus pressures over the pressure range of interest for each of a number of present and possible future techniques. Problems involved in the measurement of high pressures in solid pressure media are discussed. Construction, performance and characteristics of several devices for measurement of high pressures to 100 kilobars are described. These devices utilize (1) a deadweight loaded piston-and-cylinder configuration for pressures to 30 kilobars; (2) a multiple-event calibration cell utilizing polymorphic transitions of bismuth, challium, and barium; (3) a modification of Bridgman's manganin wire gage for use in solid systems; (4) an ionic pressure sensor; and (5) an inductive pressure sensor. The last two devices constitute novel continuous-reading cells of high sensitivity.

Programmed maneuver-spectrum fatigue test of aircraft beam specimens, L. Mordfin and N. Halsey, *Am. Soc. Testing Mater. Spec. Tech. Publ.* **338,** *251–272 (1963).*
Constant- and variable-amplitude fatigue tests were conducted on 7075–T6 aluminum alloy built-up beam specimens in bending to study certain aspects of spectrum fatigue. It was found that existing cumulative fatigue damage theories were inadequate for the dual purpose of predicting spectrum fatigue life and evaluating the effects of individual load levels in a spectrum. However, the observed spectrum fatigue properties were consistent with the measured effects of preloading, overloading and underloading.
Preloading was beneficial when the preload was considerably greater than the subsequent fatigue loads, and when the preload was applied in the same direction as the fatigue loads. When the preload and the fatigue loads had opposite signs a reduction in fatigue life resulted. These effects were magnified by the periodic application of overloads.
The periodic application of repeated low loads during a fatigue test was ineffectual when these underloads were applied in the same direction as the fatigue loads. When the underloads and the fatigue loads had opposite signs serious reductions in life resulted.
The fatigue properties of the beam specimens were notably similar to those of certain full scale aircraft structures, and rather insensitive to variations in testing technique and material.
A pneumatic testing machine and an automatic programmer which were developed for this investigation are described.

Some physical characteristics of agar impression materials, M. Ohashi, G. C. Paffenbarger, and J. W. Stanford, *J. Nihon Univ. Sch. Dent.* **7,** *No. 1, 1–11 (Mar. 1965).*
The newly revised American Dental Association Specification No. 11 for Dental Hydrocolloidal Impression Material—Agar Type did not exclude the agar impression materials on the current List of Certified Dental Materials as established by the American Dental Association. Therefore, these materials comply with both the old and the revised specifications which define materials having a wide range of flexibility. The authors recommend that serious consideration be given to the use of agar impression materials, especially in indirect methods.

Summary of symposium on methods of metallographic specimen preparation, L. L. Wyman, *Am. Soc. Testing Mater. Spec. Tech. Publ.* **285,** *130 (May 1961).*
The basic mechanism of mechanical specimen preparation has remained unchanged for decades, but certain refinements have enhanced the art; the most noticeable changes being in the greater effort to minimize surface distortion and artifacts. This is manifest in the general tendency toward the use of "hard" cloths, accurately graded and sharply cutting abrasives, and slower wheel speeds. The widespread use of diamond powders particularly emphasizes this tendency. Appreciable attention is also given to the pH of polishing media to prevent undesirable etching effects.
Recent approaches are represented by improved equipment for automatic polishing and for electrolytic polishing. There is an increase in the use of polish-etch techniques, and now chemical polishing has been added to the non-mechanical methods of preparation.

The cement and concrete reference laboratory inspection service for concrete testing laboratories, J. R. Dise, *Concrete Construc.* **9,** *No. 8, 234 (Aug. 1964).*
The historical development and work of the Cement and Concrete Reference Laboratory are described together with the benefits which may accrue from the inspection of concrete testing laboratories.

The liquefaction of hydrogen. 3B–2. Large scale hydrogen liquefaction facilities, P. C. Vander Arend and D. B. Chelton, *Book, Technology and Uses of Liquid Hydrogen, ch. 3, pp. 79–105 (Pergamon Press Inc., New York, N.Y., 1964).*
The basic principles of hydrogen liquefaction are discussed on the basis of both the First and Second Law of Thermodynamics. The minimum work of liquefaction for parahydrogen is determined for several cyclic processes. In addition, the influence of process variables on the minimum work of liquefaction is discussed in detail. General considerations are given for large scale commercial production of liquid hydrogen. Schematic process arrangements are discussed. A detail description of an existing large scale production facility is given.

What is needed next in the simulation of the arterial street? M. C. Stark, *Proc. Highway Conf. Progress Related to the Future of Surveillance, Simulation and Control, Washington, D.C., Sept. 14–15, 1964, p. 144 (Bureau of Public Roads, Washington, D.C., 1964).*
An element-by-element computer simulation of the volume and movement of traffic on a nine-block section of 13th Street, NW., in Washington, D.C., has been completed and is reviewed. A computer program causes the cars to behave in what seems to be a realistic manner. The cars stop at red lights, they yield the right-of-way at stop signs, they maneuver into correct positions for turns, they have different desired speeds, they accelerate and decelerate, they shift lanes to overtake slower cars, they form queues, they do most of the definable things that cars can be expected to do in city traffic.
So far, reasonableness is the only criterion for judging the performance. Validation is strongly indicated as the next step. Scores of input parameters can readily be changed until the simulation performance meets rigorous statistical tests.
Validation is the necessary keystone after which further research effort should go into: (1) generalization of the model for applicability to other locations, (2) validation sensitivity tests to determine to what extent the time and distance units may be lengthened without destroying validation and (3) modification of the program to reduce

computer time requirements. These are the research tasks needed to produce a valuable tool for traffic engineers and transportation planners.

Address encoding—A study of the double-binary keyboard as a link in the machine—sorting of mail, J. R. Cornog, J. F. Hockman, and J. C. Craig (*Proc. Winter Annual Meeting, American Society of Mechanical Engineers, Philadelphia, Pa., Nov. 17–22, 1963*), *ASME Publ. 63–WA–338 (1964).*
In its search for the fastest and consequently least expensive means for an operator to communicate with the computer in a letter-sized mail sorting machine complex, the Office of Research and Engineering of the U.S. Post Office authorized the development and testing of a double-binary or "chord" type keyboard. Twenty-eight people, many of them manual letter sorters, learned to operate the keyboard and to use an extraction code for shortening envelope addresses for computer input. The keyboard, the training program and equipment, the address encoding task, and the results of 36 weeks of practice are described.

The current status of graphic storage techniques: their potential application to library mechanization, S. N. Alexander (*Proc. Conf. Library Automation, Airlie Foundation, Warrenton, Va., May 26–30, 1963*), *Book, Libraries and Automation, ed. B. E. Markuson, pp. 111–140 (Library of Congress, Washington, D.C., 1964).*
This paper is presented in the form of a state-of-the-art precis that has the following sequence: First, a brief history of microform and related facsimile recording systems is given. Next, the nature of the intellectual task associated with designing an effective system is considered. These topics are followed by a discussion of facsimile storage and retrieval systems in terms both of their utility characteristics of replication methods and media related to microform systems. The implications of this technology for the library environment are then examined, and finally conclusions that may be inferred regarding the direction that further technological development might take are presented. A set of systems descriptions specifying their individual characteristics and a selected list of references are appended to provide each reader with access to such additional detail as may be of interest.

Accurate length measurement of meter bar with helium-neon laser, K. D. Mielenz, H. D. Cook, K. E. Gillilland, and R. B. Stephens, *Science Letter* **146,** *No. 3652, 1672–1673 (Dec. 1964).*
A helium-neon gas laser has been successfully used in conjunction with an automatic fringe-counting interferometer to measure the length of a meter bar. The agreement obtained was 7 parts in 100 million with respect to the assigned length of the bar.

Direct quantitative analysis of microstructures by a digital computer, G. A. Moore, *Am. Soc. Metals Tech. Report No. 16.3 (1964); (condensed version), Book, Computer Applications in Metallurgical Engineering, pp. 111 (Am. Soc. Metals, Metals Park, Ohio, 1964).*
Accurate quantitative data, pertinent to the structure of solid materials at the microsize level, are now obtained directly by a digital computer, which can directly accept a micrographic print as the information input. In a program on the National Bureau of Standards SEAC Computer, a "master" routine accepts a list of single word commands in English language format and compiles the operational orders needed to carry out the requested work.
Twenty-eight basic commands provide for picture input, output and relocation; for Boolean operations between two pictures and logical modifications of any image; and for statistical measurements of an image and of individual objects therein. Basic algorithms are shown for some essential operations. Applications to statistical and morphological problems in quantitative metallography are illustrated.

Metrology as related to microminiaturization processes, T. R. Young, *Proc. Microminiaturization Congress, New York, N.Y., Mar. 10–13, 1962 (American Watchmakers Inst., New York, N.Y., Mar. 1963).*
A talk presented to the American Watchmakers Institute's Microminiaturization Congress provides a brief survey of the development of line and end standard systems of measurement. Limits to accuracy for each case are discussed and the significance of these limits to microminiaturization processes is shown. Advantages of the recent soption of the wavelength standard of length are indicated.

The definition of alginate impression materials by a specication, M. Ohashi, G. C. Paffenbarger, and J. W. Stanford, *J. Nihon Univ. School Dent.* **7,** *No. 1, 12–28 (Mar. 1965).*
The formulation of a specification for dental alginate impression materials, which will characterize them adequately, is described and much of the experimental data obtained during the development is presented.

The statistical construction of a single standard from several available standards, E. L. Crow, *IEEE Trans. Instr. Meas.* **IM–13,** *No. 4, 180–185 (Dec. 1964).*
In the case of physical quantities for which no international standards exist, such as microwave power and microwave noise, it may be desirable to establish an international standard by combination of the data from several laboratory standards. Even if there is an international standard, it conceivably might be replaced by a new composite standard, for example the mean of several laboratory atomic time standards. A weighted mean may be preferable.
It is noted that the best combination of observations for estimating a theoretical mean or median value depends on the theoretical frequency distribution from which the observations are drawn. Since the theoretical distribution for observations from different laboratories would in general be unknown, two weighted means are suggested which are reasonably good for many distributions, allowing for wild observations particularly, and in which the weight of each observation depends only on its order when the observations are ordered in size. The efficiencies of these and other estimates are evaluated for each of four distributions.

Experimental fires in enclosures, D. Gross and A. F. Robertson, *Proc. 10th Symp. (Intern.) Combustion, Cambridge, England, Aug. 1964, pp. 931–942 (1965).*
Results are presented of experimental measurements of the mass rates of burning, temperatures and gas compositions in model enclosures of three sizes. Interest was confined to the fully developed period of burning in which the burning rate of a combustible fiberboard crib was limited by the size and shape of the ventilation opening. The burning rate was found to be generally proprotional to $A\sqrt{h}$ (A = area, h = height of window opening), but a characteristic transition region was found for each enclosure which resulted in a pronounced shift in the data line. Burning rate data were correlated in terms of the ventilation parameter $A\sqrt{h}$ and the exposed surface area of the sticks comprising the crib.
The overall process involved in enclosure fires appears to be a combined gravity-controlled fluid dynamic regime and a radiation-controlled thermal regime. The dimensionless Froude group is the criterion for similarity in a gravity-(buoyancy-) controlled regime, and from the limited agreement found among the data for the two larger enclosures, this group appears to include the essential parameters in the scaling of burning rates of fires in geometrically similar enclosures.

Gas mixtures and pressures for optimum output power of RF excited helium-neon gas lasers at 632.8 nm, K. D. Mielenz and K. F. Nefflen, *Appl. Opt. Letter* **4,** *565 (May 1965).*
Two laser discharge tubes, of 50 cm length and 3 and 5 mm inside diameter, respectively, were filled with three different mixtures of helium and neon at varying total pressures. The gas fillings for which the two tubes yielded optimal lasing action under rf-excitation in a 60 cm confocal cavity at 632.8 nm were a 7 : 1 gas mixture at 2.3 Torr for the 3 mm tube, and a 9 : 1 mixture at 2.0 Torr for the 5 mm tube. The 3 mm tube was found to be superior in peak output power and ease of adjustment of the laser.

Impurity controlled properties of ionic solids, A. D. Franklin (*Proc. Symp. Physics and Chemistry of Ceramics, Pennsylvania State Univ., University Park, Pa., May 28–30, 1963*), *Book, Physics and Chemistry of Ceramics, pp. 77–109 (Gordon and Breach, New York, N.Y., 1963).*
The influence of trace amounts of impurities on the physical properties of ionic solids is reviewed. The properties are classified according to the way in which the impurities influence them, as directly or indirectly influenced. The directly influenced properties are in turn subdivided into additive localized, additive non-localized, domain, and scattering effects. Data drawn from the literature is used to illustrate these impurity effects. An extended discussion is given for paramagnetic resonance, dielectric and anelastic relaxation, the photographic effect, dislocation pinning, thermal conductivity, and impurity-induced dislocation climb.

Introduction, Book, Technology and Uses of Liquid Hydrogen, R. B. Scott, *pp. 1–8 (Pergamon Press Ltd., London, England, 1964).*
This is an introduction to a book on liquid hydrogen, edited by Denton and Nicholls of AERE, Harwell, England, and R. B. Scott. The chapters, 11 in all, are authored by various authorities from Europe and U.S.A. From the title, it will be noted that the material is principally of an applied nature, and includes little basic physics or theory.

Nuclear magnetic resonance in bulk nickel samples, L. H. Bennett, *Phil. Mag.* **12,** *No. 115, 213–215 (July 1965).*
Nuclear magnetic resonance (NMR) experiments in bulk metals suffer from a small effective filling factor due to the small penetration depth of the rf field. We have found that the NMR signal in bulk Ni metal, however, is extraordinarily intense.

Volume relaxations in amorphous polymers, R. S. Marvin and J. E. McKinney, *Book, Physical Acoustics, ed. W. P. Mason, IIB, ch. 9, 165–229 (Academic Press Inc., New York, N.Y., 1965).*
Volume relaxations in amorphous polymers are treated along with the effect of static hydrostatic stress on time dependent molecular motion. The relationship between a linear viscoelastic constitutive equation and a general phenomenological equation is discussed, and the linear equation related to molecular mechanisms through a free volume concept. Experimental techniques and results involving dilatation are reviewed, and information from such measurements on amorphous polymers summarized and evaluated. These data indicate that the simple free volume concept is applicable in some cases. In general, polymers for which the primary molecular motions seem to involve large segments of the polymer molecule agree closely with the predictions of the combined phenomenological and molecular theories available. Other types of motion, which are not specifically considered in most current theories, appear to give rise to more complicated behavior.

Adhesive bonding of various materials to hard tooth tissues. I. Method of determining bond strength, R. L. Bowen, *J. Dental Res.* **44,** *No. 4, 690–695 (July–Aug. 1965).*
A tensile adhesion test was developed to compare the degrees of bonding of various materials to hard tooth tissues such as dentin and enamel.
The analysis of variance by means of two-way tables eliminated from the error the systematic differences between dentin specimens. The experimental error proved to be sufficiently small to make the apparatus suitable for discriminating between treatments to be described in subsequent parts of this series.

Determining moisture in solid materials by reaction with calcium carbide, S. Dahl, *Mater. Res. Std.* **5,** *No. 9, 446–453 (Sept. 1965).*
The moisture was determined by reaction with CaC_2 and volumetric measurement of the acetylene produced. The sample-CaC_2 mixture was heated to liberate the water from the sample. An apparatus is described in which a run of six determinations can be made in about 40 minutes. Volatile substances, other than water, which impair accuracy in drying methods, do not interfere in the CaC_2 method products gaseous at room temperature are not formed. An experimental error of the order of 2% was obtained in applications to samples of leathers, papers, and grains. The method probably is applicable to solids generally, but can not be used with liquids.

Dissociation constant of acetic acid in deuterium oxide from 5° to 50°. Reference points for a pD scale, R. Gray, R. G. Bates, and R. A. Robinson, *J. Phys. Chem.* **69,** *No. 8, 2750–2753 (1965).*
Electromotive force measurements of a cell without liquid junction have been used to determine the dissociation constant of acetic acid in deuterium oxide from 5 to 50°. The enthalpy, entropy, and heat capacity changes on dissociation of acetic acid have been calculated. Values of $-\log (a_{D^+}\gamma_{Cl^-})$ and the conventional pa_D values for the equimolal (0.05 *m*) acetic acid-sodium acetate buffer solutions have been determined. These provide a second fixed point for standardizing the pD scale, supplementing data for the equimolal mixture of KD_2PO_4 and Na_2DPO_4 established in an earlier investigation.

Focused-beam electron bombardment evaporator, D. H. Blackburn and W. Haller, *Rev. Sci. Instr.* **36,** *No. 7, 901–903 (July 1965).*
A simple focused-beam electron bombardment evaporator was developed for the controlled vaporization of carbon and other refractory materials. An electrically-isolated cylindrical shield reflects and focuses the electron beam, allowing a large anode to cathode distance. This avoids interference by gas conductance, resulting in a more efficient and stable bombardment process. A performance comparison is made between the described evaporator and a conventional carbon-arc evaporator.

The effect of environment on the fatigue strengths of four selected alloys, T. R. Shives and J. A. Bennett, *NASA Contractor Report CR–267, 2–22 (Aug. 1965).*
Rotating beam fatigue tests of unnotched specimens of AISI 4340 steel, free-cutting brass, titanium alloy Ti–4–Al–4Mn, and magnesium alloy AZ61A showed that the fatigue strength was lower in a moist environment than in a dry one. A coating of dodecyl alcohol was found to have a beneficial effect on the fatigue strength of the steel and magnesium alloy specimens, but did not completely eliminate the effect of humidity. The effect of environment on crack propagation was investigated with notched specimens of the magnesium alloy. An interesting tarnishing effect was observed on the fatigue portion of magnesium fracture surfaces.

The temporal dimensional stability of surface-hardened steels, M. R. Meyerson, *Metal Treating* **15,** *No. 6, 5 (Dec. 1964–Jan. 1965).*
Procedures are described for heat treating and surface hardening a variety of steels to produce a high degree of temporal dimensional stability. A minimum surface hardness of Rockwell C 65 was obtained with each treatment. Specimens surface hardened by nitriding had an additional advantage over other types in that stability and hardness were retained after exposure to mildly elevated temperatures.

A method for measuring polarization in the vacuum ultraviolet, K. Rabinovitch, L. R. Canfield, and R. P. Madden, *Appl. Opt.* **4,** *No. 8, 1005–1010 (Aug. 1965).*
A simple experimental method for determining the degree of plane polarization of a far ultraviolet monochromator was developed and tested. This determination requires only a measurement of the reflectance at 45° angle of incidence with two or more orientations of the reflector about the optic axis. This procedure works at all wavelengths without requiring a detailed knowledge of the optical constants of the reflector material. The degree of plane polarization has been determined for a 1/2-meter Seya-Namioka monochromator. The polarization has been found to depend strongly on wavelength and on both the grating and the grating overcoating.

Historical background of image formation, L. Marton, *Lab. Invest.* **14,** *No. 6, Pt. I, 739 (1965).*
Review of historical background on image formation on the electron microscope between the years 1930–1950.

Investigation of the anomaly in the response of silicon semiconductor radiation detectors at low temperatures, W. R. Dodge, S. R. Domen, A. T. Hirshfeld, and D. D. Hoppes, *IEEE Trans. Nuclear Sci.* **NS–12,** 295 (Feb. 1965).
Investigation of the response anomaly in silicon semiconductor radiation detectors cooled to temperatures below 40 °K has been continued. Experiments with surface barrier detectors show that the mean temperature at which normally ionized impurity atoms accept electrons (as deduced from dE/dx measurement of the depletion depth) is a slowly varying function of the impurity concentration. This behavior is expected from the dependence of the Fermi level on the temperature, impurity concentration and ionization energy. Below the narrow temperature interval in which the majority of the impurity atoms accept electrons and hence become electrically neutral, particles which produce low ionization densities (beta particles) produce pulse heights with room temperature magnitudes, while particles with high ionization densities (alpha particles) produce pulse heights which are lower than those characteristic of room temperature operation and which depend on the detector bias voltage. The results of experiments conducted to investigate polarization effects in lithium-drifted semiconductor radiation detectors are described.

The annealing of vacancies in dilute alloys, R. E. Howard and A. B. Lidiard, *Phil. Mag.* **11**, *No. 114, 1179–1187 (June 1965).* The annealing of vacancies in dilute alloy is analysed using a more general phenomenological model than that employed in previous discussions. Specific results are presented also for an f.c.c. alloy in which the impurities and vacancies interact only at short range. It is shown that the effective vacancy diffusion coefficient contains another term additional to those obtained by Damask and Dienes using their rate equation model. This additional term is associated with jumps of vacancies from positions where they are free to positions where they are in interaction with impurity atoms. In the special case of an f.c.c. alloy with only nearest neighbor impurity-vacancy interactions the additional term does not alter the qualitative predictions of the Damask and Dienes model about the dependence of vacancy flux, j_v, upon these interactions; but one expects this term to become increasingly important as the range of interaction increases. The associated impurity flux, j_b, however, may not be correctly given in their model. Only for strongly bound impurity-vacancy pairs with high vacancy jump rates, is j_b in the same sense as j_v. For weakly bound pairs it is in the opposite sense. The rate equation model always predicts that both j_b and j_v are towards vacancy sinks.

Other NBS Publications

J. Res. NBS 69A (Phys. and Chem.), No. 6 (Nov.–Dec. 1965), 75 cents.

Arc measurement of some argon transition probabilities. C. H. Popenoe and J. B. Shumaker, Jr.
Theoretical interpretation of the third spectrum of gold (Au III). Y. Shadmi.
Photopolarographic behavior of inorganic depolarizers. R. A. Durst and J. K. Taylor. (See above abstracts).
Spectral structure of critical opalescence: binary mixture. R. D. Mountain.
Irregularities in the NBS (1955) provisional temperature scale. H. M. Roder.
Isotherms determined by the National Bureau of Standards acoustical thermometer in the liquid helium temperature range. G. Cataland and H. Plumb. (See above abstracts).
Synthesis of D-glucose-3-^{14}C and related compounds. H. L. Frush, L. T. Sniegoski, N. B. Holt, and H. S. Isbell.
Correlation of large longitudinal deformations with different strain histories. L. J. Zapas and T. Craft. (See above abstracts).
Crystallography of tetracalcium phosphate. W. E. Brown. and E. F. Epstein.
Electrode potentials in fused systems XII. Measurement of cation concentration in molten salts using glass membrane electrodes. K. H. Stern and S. E. Meador. (See above abstracts).

J. Res. NBS 69B (Math. and Math. Phys.), No. 4 (Oct.–Dec. 1965), 75 cents.

Table of Dedekind sums. R. D. Shipp.
Lattice points in a sphere. M. Bleicher and M. I. Knopp.
Error analysis of phase-integral methods. I. General theory for simple turning points. F. W. J. Olver.
Error analysis of phase-integral methods. II. Application to wave-penetration problems. F. W. J. Olver.
A random walk model of chain polymer adsorption at a surface. II. Correlation between neighboring steps. Robert J. Rubin.
Groups of unimodular circulants. Richard H. Austing.
A generalization of a result of Newman on multipliers of difference sets. R. L. McFarland.
The bridge tournament problem and calibration designs for comparing pairs of objects. R. C. Bose and J. M. Cameron.
The condition of certain matrices. L. F. Shampine.
Some number-theoretic calculations. K. E. Kloss.

Radio Sci. J. Res. NBS/USNC–URSI, 69D, No. 12 (December 1965), $1.00.

Symposium on Planetary Atmospheres and Surfaces, May 1965:
I Session: Jupiter, as observed at long radio waves.
II Session: Jupiter, as observed at short radio waves.
III Session: Passive radio observations of Venus, Saturn, Mercury, Mars, and Uranus.
IV Session: Passive radio observations of the Moon.
V Session: Radar observations of the planets.
VI Session: Radar observations of the Moon.
Index to volume 69D, January to December 1965.

Hydraulic research in the United States 1965, ed. H. K. Middleton, NBS Misc. Publ. 270 (July 22, 1965), $1.25.
Grading of abrasive grain for grinding, CS271–65 (April 12, 1965). Supersedes SPR R118–50.
Quarterly radio noise data March, April, May, 1964, W. Q. Crichlow, R. T. Disney, and M. A. Jenkins, NBS Tech. Note 18–22 (Aug. 2, 1965), 50 cents.
Analysis and purification section: Summary of activities July 1964 to June 1965, ed. J. K. Taylor, NBS Tech. Note 273 (Oct. 1, 1965), 50 cents.
A numerical representation of CCIR report 322 high frequency (3–30 Mc/s) atmospheric radio noise data, K. L. Lucas and J. D. Harper, Jr., NBS Tech. Note 318 (Aug. 5, 1965), 55 cents.
Acid bases in analytical chemistry, I. M. Kolthoff, S. Bruckenstein, and R. G. Bates, Interscience Reprint from Kolthoff-Elving "Treatise on Analytical Chemistry", pt. I. sec. B, ch. 10, pp 361–542 (Interscience Publ. Inc., New York, N.Y., 1965).
Acids and bases in alcohol-water solvents, R. G. Bates, Chem. Chem. Ind. (Japan) **18**, 680–685 (May 1965).
Configuration interaction calculation of H_3 and H_2, C. Edmiston and M. Krauss, J. Chem. Phys. **42**, No. 4, 1119 (Feb. 1965).
Crystal structure of gamma-dicalcium silicate, D. K. Smith, A. Majumdar, and F. Ordway, Acta. Cryst. **18**, 787 (Apr. 1965).
Designation of ligand positions in coordination complexes, R. F. Pasternack and P. M. McDonnell, Inorg. Chem. **4**, No. 4, 600–602 (Apr. 1965).
Determination of reducing end-groups by reactions with C^{14}-labeled cyanide, H. S. Isbell, Book, Methods in Carbohydrate Chemistry, ed. R. L. Whistler, **5**, 249–250 (Academic Press Inc., New York, N.Y., 1965).
Direct observation of the decomposition of multiply charged ions into singly charged fragments, K. E. McCulloh, T. E. Sharp, and H. M. Rosenstock, J. Chem. Phys. **42**, No. 10, 3501–3509 (May 1965).
Electron impact studies of aromatic hydrocarbons. III. Anzulene and naphthalene, R. J. Van Brunt and M. E. Wacks, J. Chem. Phys. **41**, No. 10, 3195–3199 (Nov. 15, 1965).
Electron paramagnetic resonance and primarily 3d wavefunctions of the tetrachlorocuprate ion, M. Sharnoff, J. Chem. Phys. **42**, No. 10, 3383–3395 (1965).
Electron paramagnetic resonance spectra of zinc-doped copper acetate monohydrate, G. F. Kokoszka, H. C. Allen, Jr., and G. Gordon, J. Chem. Phys. **42**, No. 10, 3693–3697 (May 15, 1965).
Electron paramagnetic resonance spectrum of bis-8-hydroxyquinolate copper (II) dihydrate, G. F. Kokozska, H. C. Allen, Jr., and G. Gordon, J. Chem. Phys. **42**, No. 10, 3730–3731 (May 15, 1965).
Extinction coefficients of triplet ↔ triplet transitions in aromatic compounds, R. A. Keller and S. G. Hadley, J. Chem. Phys. **42**, No. 7, 2382 (Apr. 1965).
Franck-Condon factors for polyatomic molecules, T. E. Sharp and H. M. Rosenstock, J. Chem. Phys. **41**, No. 11, 3453 (Dec. 1, 1964).
Improved measurement of the electric dipole moment of the hydroxyl radical, F. X. Powell and D. R. Lide, J. Chem. Phys. **42**, No. 12, 4201–4202 (June 1965).
Infrared emission spectrum of HBr excited in an electric discharge. Determination of molecular constants, T. C. James and R. J. Thibault, J. Chem. Phys. **42**, No. 4, 1450–1457 (Feb. 1965).
Interaction of carbon dioxide with carbon adsorbents below 400 °C, V. R. Deitz, F. G. Carpenter, and R. G. Arnold, Carbon **1**, 245 (1964).
Isotopic fractionation of uranium related to roll features in sandstone, Power River Basin, Wyoming and Colorado Plateau, J. N. Rosholt, A. P. Butler, E. L. Garner, and W. R. Shields, Econ. Geol. **60**, No. 2, 199–213 (Mar.–Apr. 1965).
Mass spectrometric study of photoionization. III. Methane and methane-d_4, V. H. Dibeler, M. Krauss, R. M. Reese, and F. N. Harllee, J. Chem. Phys. **42**, No. 11, 3791–3796 (June 1965).

Negative surface ionization of complex molecules, J. T. Herron, H. M. Rosenstock, and W. R. Shields, Nature **206,** No. 4984, 611 (May 1965).

Non-equilibrium chemical excitation and chemical pumping of lasers, K. E. Shuler, T. Carrington, and J. C. Light, Appl. Opt. Suppl. **2,** pp. 81–104 (1965).

Phase equilibria studies in mixed systems of rare earth and other oxides, R. S. Roth, Book, Progress in Science and Technology of the Rare Earths, ed. L. Ewring, **1,** 167–202 (Pergamon Press Inc., New York, N.Y., 1964).

Photolysis of ethane at the argon resonance lines 1067 and 1048 A, A. H. Laufer and J. R. McNesby, J. Chem. Phys. **42,** No. 9, 3329–3330 (May 1, 1965).

Pressure-induced trapping phenomenon in silver iodide, H. C. Duecker and E. R. Lippincott, Science **146,** 1295–1297 (1964).

Radiochemical methods of analysis (Report on Salzburg Conference), W. W. Meinke, Science **147,** No. 3654, 182–183 (Jan. 1965).

Recommended materials and practices for use with cryogenic propellants, A. F. Schmidt, AIR **839,** 29 pages (SAE Inc., New York, N.Y., Jan. 1965).

Rotational constants of excited vibrational states of $^{14}N_2$ ^{16}O, W. J. Lafferty and D. R. Lide, J. Mol. Spectry. **14,** No. 4, 407–408 (Dec. 1964).

Second order effects in the phosphorescene of benzophenone crystals at 77 °K, R. A. Keller, J. Chem. Phys. **42,** No. 11, 4050–4051 (June 1965).

Spectrophotometric determination of the rate of dissociation of tetrafluorohydrazine behind a shock wave, L. M. Brown and B. Darwent, J. Chem. Phys. **42,** No. 6, 2158–2165 (Mar. 15, 1965).

Standardization of plastics in the U.S., G. M. Kline, Courrier de la Normalisation No. 182, pp. 280–282 (Mar.–Apr. 1965); Mod. Plastics **42,** No. 9, 176 (May 1965).

Substoichiometric radiometric analysis: Determination of trace amounts of cobalt, A. R. Landgrebe, L. T. McLendon, and J. R. DeVoe, Book, Radiochemical Methods of Analysis, II, 321–333 (Intern. Atomic Energy Agency, Vienna, Austria, 1965).

The consitution of $CuFe_5O_8$, C. F. Jefferson, J. Appl. Phys. **36,** No. 3, 1165–1166 (Mar. 1965).

The gas-phase photolysis of cyclohexane in the far ultra-violet: Modes of decomposition of the neutral excited cyclohexane molecule and reactions of the parent cyclohexane ion, R. D. Doepker and P. Ausloos, J. Chem. Phys. **42,** No. 11, 3746 (June 1, 1965).

The place of radiochemical methods of analysis: Today and tomorrow, W. W. Meinke, (Proc. Intern. Atomic Energy Agency Symp. Radiochemical Methods of Analysis, Salzburg, Austria, Oct. 19–23, 1964), Book, Radiochemical Methods of Analysis **I,** 13–19 (Intern. Atomic Energy Agency, Vienna, Austria, 1965).

The vibrational assignment of sulfuryl fluoride, D. R. Lide, D. E. Mann, and J. J. Comeford, Spectrochim. Acta. **21,** 497 (1965).

Vacuum-ultraviolet photolysis of ethane at high temperature, R. F. Hampson, Jr., and J. R. McNesby, J. Chem. Phys. **42,** No. 6, 2200–2208 (Mar. 15, 1965).

An unimodulated twin channel microwave attenuation measurement system, D. H. Russell, ISA Trans. **4,** 162–169 (Apr. 1965).

Color filter nomograph, C. S. McCamy, Am. Cinematographer **46,** No. 5, 314–315 (May 1965).

Comments of surface characterization of real metals, D. P. DeWitt, (Symp. Thermal Radiation of Solids, San Francisco, Calif., Mar. 4–5, 1964), NASA SP–55, Session II, Paper 12, 141–144 (1965).

Correlation and prediction of thermal conductivity of metals through the application of the principle of corresponding states, A. Cezairliyan and Y. S. Touloukian, Proc. Advances in Thermophysical Properties at Extreme Temperatures and Pressures, Purdue Univ., Lafayette, Ind. Mar., 1965, pp. 301–313 (American Society of Mechanical Engineers, New York, N.Y., 1965).

Current programs in the U.S. Department of Commerce for advancing state science and technology, W. C. Bandy (Proc. 11th Annual Meeting, Denver, Colo., Oct. 19–20, 1964), Mid-Continent Research and Development Council Report, pp. 70–76 (1965).

Experimental fires in enclosures, A. F. Robertson, 10th Symp. (Intern.) on Combustion, Cambridge, England, Aug. 1964, pp. 931–942 (1965).

Flow field in a swirl chamber, D. H. Tsai, AIAA J. Tech. Notes **2,** No. 8, 1504–1505 (Aug. 1964).

High temperature seal of sapphire windows to ceramics, G. A. Hornbeck, Rev. Sci. Instr. **36,** No. 6, p. 845 (June 1965).

Importance of surface films, J. C. Richmond (Symp. Thermal Radiation of Solids, San Francisco, Calif., Mar. 4–5, 1964), NASA SP–55, Session II, Paper 15, pp. 157–158 (1965).

International intercomparison of standards and microwave power measurements, G. F. Engen (Proc. 3d Intern. Measurement Conference, Stockholm, Sweden, 1964), Acta Imeko **1,** 337–346 (1964).

Microwave and high frequency calibration of the National Bureau of Standards (Parts I–IV), R. E. Larson, IEEE Trans. Microwave Theory Tech. Part I, **MTT–12,** No. 4, 480–482 (July 1964); Part II, **MTT–12,** No. 5, 572–576 (Sept. 1964); Part III, **MTT–12,** No. 6, 623–624 (Nov. 1964); Part IV, **MTT–13,** No. 1, 138–139 (Jan. 1965).

On the optimum frequency deviation in an FM system over a scatter-propagation path, H. Akima, Proc. IEEE **53,** No. 2, 182–183 (Feb. 1965).

Progress report on aerosol packaged products, H. F. Wollin and S. Hasko, Aerosol Age Mag. **9,** No. 9, 20 (Sept. 1964).

Project FIST: fault isolation by semiautomatic techniques, G. J. Rogers, Design Disclosure Workbook (Packaging), U.S. Naval Applied Science Laboratory, Brooklyn, N.Y., Draft 5 (June 1965).

Project FIST: fault isolation by semiautomatic techniques, G. Shapiro, G. J. Rogers, O. B. Laug, and P. M. Fulcomer, Jr., IEEE Spectrum, pp. 98–111 (Aug. 1964); pp. 130–144 (Sept. 1964).

Radio standards and measurements, microwaves, a progress review from 1960, R. W. Beatty, Book, Progress in Radio Science, 1960–1963. Vol. **I.** Radio Standards and Measurements, pp. 78–81 (Elsevier Publ. Co., Amsterdam, The Netherlands, 1965).

Standard—still a continuing project, H. L. Mason, Control Eng. **12,** No. 1, 74 (Jan. 1965).

The evolution of control system standards, H. L. Mason, 1965 Joint Automatic Control Conf., June 22–25, 1965, Session VII, Paper 1, pp. 76–78 (Renssalaer Polytechnic Inst., Troy, N.Y., 1965).

The rapid selector as currently used for information search and replica copy retrieval, T. C. Bagg, (Proc. 26th Annual Meeting of the American Documentation Institute, Chicago, Ill., Oct. 1963), Automation and Scientific Commun. Pt. 2, 227–228 (Oct. 1963).

Waveguide noise-tube mount for use in an interlaboratory noise standard, C. K. S. Miller, W. C. Daywitt, and E. Campbell, Acta. Imeko 3, 371–382 (1964).

A new differential operator of the pure wave type, J. E. Lagnese, J. Different. Eq. **1,** No. 2, 171–187 (Apr. 1965).

Aggregation in matrix models of resource flows, D. Rosenblatt, Am. Stat. **19,** No. 3, 36–39 (June 1965).

An application of the inverse Z-transform theory to the synthesis of linear antenna arrays, M. T. Ma, IEEE Trans. Ant. Prop. **AP–12,** No. 6, 798–799 (Nov. 1964).

Application of Bernstein polynominals and interpolation theory to linear array synthesis, M. T. Ma, IEEE Trans. Ant. Prop. **AP–12,** 668–677 (Nov. 1964).

Mechanical translation: U.S.—Japan Joint Conference, F. L. Alt, Science **147,** No. 3665, 1599–1600 (Mar. 1965).

Some unorthodox predictions, F. L. Alt, Computers and Automation **XIV,** No. 1, pp. 11 (Jan. 1965).

The standardization of programming languages, Proc. 19th Association for Computing Machinery Conf., Philadelphia, Pa., pp. B2–1 (Aug. 1964).

Training a computer to assign descriptors to documents, M. E. Stevens and G. H. Urban, Proc. Spring AFIP Joint Computer Conf., Washington, D.C., April 1964, pp. 563–575 (1964).

Use of general purpose coding systems for statical calculations, J. M. Cameron and J. Hilsenrath, Proc. IBM Scientific Computing Symp. Statistics, Thomas J. Watson Research Center, Yorktown Heights, N.Y., Oct. 21–23, 1963, pp. 281–299 (IBM, White Plains, N.Y., 1965).

You can always tell a computer but you can't tell it much, J. H. Wegstein, Proc. ARO Working Group on Computers, Harry Diamond Laboratories, Washington, D.C., Feb. 4–5, 1964, pp. 129–151 (Feb. 1965).

Comments on Zener diodes as voltage standards, W. G. Eicke, Jr., Comite Consultatif D'Electricite 10^e Session, May 2–3, 1963, pp. 27–30 (Gauthier-Villars, Paris, France, 1963).

Construction and behavior of a transportable ten picofarad capacitor, R. D. Cutkosky and L. H. Lee, Comite Consultatif D'Electricite 10^e Session, May 2–3, 1963, pp. 44–48 (Gauthier-Villars, Paris, France, 1963).

Electronic g factor of rubidium, R. L. Driscoll, Phys. Rev. **136,** No. 1A, A54–A57 (Oct. 5, 1964).

Spacetime coordinate systems, G. E. Hudson, Proc. Intern. Conf.

Chronometry, pp. 197–221 (Lausanne, Switzerland, June 1964).

Standards, sources, and detectors in radiation measurements, R. Stair and W. E. Schneider, (Symp. Measurement of Thermal Radiation of Solids, San Francisco, Calif., Mar. 4–6, 1964), NASA SP–55, Session III, Paper 24, pp. 217–231 (1965).

The value of the Faraday, W. J. Hamer and D. N. Craig, J. Electrochem. Soc. **111,** No. 12, 1434 (Dec. 1964).

A dumbbell model for dielectric dispersion in paraffin-like solids, M. G. Broadhurst, Proc. Electrical Insulation Conf., Cleveland, Ohio, Oct. 1964, Natl. Acad. Sci.-Natl. Res. Council Publ. 1238, pp. 129–132 (1965).

A method for determination of the tropospheric temperature structure from ground-based measurement of oxygen emission, E. R. Westwater, Proc. 3d Remote Sensing of the Invironment, Infrared Phys. Lab., Inst. Sci. Tech., Univ. Michigan, Ann Arbor, Mich., Feb. 1965, pp. 245–256 (Mar. 1965).

A possible mechanism for light absorption by interstellar grains, E. E. Ferguson and H. P. Broida, Astrophys. J. **141,** No. 2, 807–809 (Feb. 15, 1965).

A test of analytical expressions for the thermal emittance of shallow cylindrical cavities, F. J. Kelley and D. G. Moore, (Symp. Thermal Radiation of Solids, San Francisco, Calif., Mar. 4–5, 1964), NASA SP–55, Session I, Paper 10, pp. 117–121 (1965); Appl. Opt. **4,** No. 1, 40–41 (1965).

A theoretical study of the Martian and Cytherian ionospheres, R. B. Norton, Natl. Aeron. Space Admin. NASA Tech. Note D–2333 (July 1964).

Albert Einstein, as I remember him, C. Eisenhart, J. Wash. Acad. Sci. **54,** 325–328 (Nov. 1964).

An experimental study of the backscattering of 5.3 meV alpha particles from platinum and monel metal, D. H. Walker, Intern. J. Appl. Radiation Isotopes **16,** 183–189 (1965).

Characteristics of soil and vegetated surfaces to reflected and emitted radiation, D. M. Gates, Proc. 3d Symp. Remote Sensing Environment, Infrared Phys. Lab., Inst. Sci. Tech., Univ. Michigan, Ann Arbor, Mich., Feb. 1965, pp. 573–600 (Mar. 1965).

Compound-atom states for two-electron systems, T. F. O'Malley and S. Geltman, Phys. Rev. **137,** No. 5A, A1344–A1352 (Mar. 1, 1965).

Condensation of tungsten on tungsten in atomic detail: Monte Carlo and statistical calculations vs. experiment, R. D. Young and D. C. Schubert, J. Chem. Phys. **42,** No. 11, 3943–3950 (June 1965).

Condensation of tungsten on tungsten in atomic detail: Observation with the field ion microscopy, P. Gurney, Jr., F. Hutchinson, and R. D. Young, J. Chem. Phys. **42,** No. 11, 3939–3943 (June 1965).

Continuum states of H^- and the free-free absorption coefficient, S. Geltman, Astrophys. J. **141,** No. 2, 376–394 (Feb. 12, 1965).

Correlated walk and diffusion equations in a driving force, J. R. Manning, Phys. Rev. 139, No. 1A, A126–A135 (July 5, 1965).

Coupling of particle-hole states and two particle-two hole states: damping, M. Danos and W. Greiner, Book, Physique Nucleaire, ed. P. Gugenberger, II, 615–616 (Editions du Centre National de la Recherche Scientific, Paris, France, 1964).

Crystal growth and thermal etching of argon, G. L. Pollack and E. N. Farabaugh, J. Appl. Phys. **36,** 513 (1965).

Damping of the giant resonance in heavy nuclei, M. Danos and W. Greiner, Phys. Rev. **138,** No. 4B, B876–B891 (May 1965).

Dissociative recombination in helium afterglows, E. E. Ferguson, F. C. Fehsenfeld, and A. L. Schmeltekopf, Phys. Rev. **138A,** A381–A385 (Apr. 1965).

Dynamic collective theory of odd-A nuclei, M. Danos, W. Greiner, and C. B. Kohr, Phys. Rev. **138,** No. 5B, B1055–B1066 (June 1965).

Electron accelerators for food processing, H. W. Koch and E. H. Eisenhower, Proc. Intern Conf. Radiation Preservation of Foods, Boston, Mass., Sept. 27–30, 1964, Natl. Acad. Sci.-Natl. Res. Council Publ. 1273, pp. 149–180 (1965).

Electron spin resonance of Mo^{5+} in rutile, T. T. Chang, Phys. Rev. **136,** No. 5A, A1413–A1416 (Nov. 30, 1964).

Empirical relations for energy levels of atoms and ions, A. E. Goertz, J. Opt. Soc. Am. **55,** 742–743 (June 1965).

Energy levels of Pr^{3+} in the vapor state, J. Sugar, Phys. Rev. Letters **14,** No. 18, 731–732 (May 3, 1965).

Energy levels of polarons in a magnetic field, D. M. Larsen, Phys. Rev. 135, No. 2A, A419–A426 (July 1964).

Energy of the formation of the anion Frenkel pair in calcium fluoride, A. D. Franklin, J. Phys. Chem. Solids **26,** 933–934 (1965).

Etch pits in chromic oxide, W. S. Brower, Jr., and E. N. Farabaugh, J. Appl. Phys. **36,** No. 4, 1489–1490 (Apr. 1965).

Excitation of molecular rotation by slow electrons, K. Takayanagi and S. Geltman, Physics Letters **13,** No. 2, 135–137 (Nov. 15, 1964); Phys. Rev. 138, No. 4A, A1003–A1010 (May 17, 1965).

Expertise or experiments, C. Eisenhart, Science **146,** No. 3647, 997–998 (Nov. 20, 1964).

4fnl configurations of doubly ionized cerium (Ce III), N. Spector, J. Opt. Soc. Am. **55,** No. 5, 492–501 (May 1965).

Γ_0 selection rules in Su(12) $\bar{p}p$ annihilation, H. Harari, H. J. Lipkin, and S. Meshkov, Phys. Rev. Letters **20,** No. 14, 845–847 (May 17, 1965).

Generalized master equation for quantum mechanical systems to all orders in the density, J. Weinstock, Phys. Rev. **136,** 2d series, No. 4A, A879–A888 (Nov. 1964).

High energy X-ray photon albedo, J. S. Pruitt, Nuclear Instr. Methods 27, 23 (1964).

Hyperfine structure of Hg^{193*}, Hg^{195*} by Zeeman level crossings, W. W. Smith, Phys. Rev. **137,** No. 2, 580–591 (Jan. 1965).

Interaction potential between He and H_2, M. Krauss and F. H. Mies, J. Chem. Phys. **42,** No. 8, 2703–2708 (Apr. 15, 1965).

International comparison of atomic frequency standards via VLF radio signals, A. H. Morgan, B. E. Blair, and E. L. Crow, Book, Progress in Radio Science, Vol. I. Radio Standards and Measurement, p. 40 (Elsevier Publ. Co., Amsterdam, The Netherlands, 1965).

Isotopic determination of the vibrational numbering for the $B^3\Pi_{0^+_u}$, R. L. Brown and T. C. James, J. Chem. Phys. **42,** No. 1, 33–35 (Jan. 1965).

Laser double-quantum photodetachment of I^-, J. L. Hall, E. J. Robinson, and L. M. Branscomb, Phys. Rev. Letters **14,** No. 25, 1013–1016 (June 21, 1965).

Loop prominences and coronal condensations. I. Non-thermal velocities within loop prominences, J. T. Jefferies and F. Q. Orrall, Astrophys. J. **141,** No. 2, 505–518 (Feb. 15, 1965).

Loop prominences and coronal condensations. II. The sources of mass and energy and a model of the loop prominence mechanism, J. T. Jefferies and F. Q. Orrall, Astrophys. J. **141,** No. 2, 519–525 (Feb. 15, 1965).

Low-Z dye systems for ionizing radiation measurement, W. L. McLaughlin and L. Chalkley, J. Photo. Sci. Engr. **9,** No. 3, 159–166 (May–June 1965).

Master equations and Markov processes, I. Oppenheim and K. E. Shuler, Phys. Rev. **138,** No. 4B, B1007–B1011 (May 24, 1965).

Matrix-isolation study of the reaction of F atoms with CO. Infrared and ultraviolet spectra of the free radical FCO, D. E. Milligan, M. E. Jacox, A. B. Bass, J. J. Comeford, and D. E. Mann, J. Chem. Phys. **42,** No. 9, 3187–3195 (May 1965).

Microscopic-astrophysics and the development of astrophysical-laboratories, R. N. Thomas, Bull. Assoc. Devel. Intern. Observatoire de Nice, No. 1, pp. 7–16 (1964).

Microscopic fluctuations and diffusion coefficients of a non-equilibrium plasma in a magnetic field, J. Weinstock, Phys. Fluids **8,** No. 3, 479–481 (Mar. 1965).

Mobilities and reaction rates of ions in helium, E. C. Beaty and P. L. Patterson, Phys. Rev. **137,** No. 2A, A346–A357 (Jan. 1965).

Multipole matrix elements of the translation operator, M. Danos and L. C. Maximon, J. Math. Phys. **6,** 766 (1965).

New odd levels of neutral erbium (Er I), N. Spector, J. Opt. Soc. Am. **55,** No. 5, 576–577 (May 1965).

New Rydberg series in molecular oxygen near 500° A, K. Codling and R. P. Madden, J. Chem. Phys. **42,** No. 11, 3935–3938 (June 1965).

Non-equilibrium thermodynamics of canonically invariant relaxation processes, H. C. Andersen, I. Oppenheim, K. E. Schuler, and G. H. Weiss, J. Chem. Phys. **41,** No. 10, 3012–3019 (Nov. 1964).

Non-equilibrium thermodynamics of creep in polycrystals, R. E. Nettleton, Physica **20,** 1989–2002 (1964).

Note on the theory of cavity ionization chambers, L. V. Spencer, Radiation Res. **25,** No. 2, 352–358 (June 1965).

Nuclear magnetic resonance in $RbMnF_3$, R. E. Payne, R. A. Forman, and A. H. Kahn, J. Chem. Phys. **42,** No. 11, 3806–3808 (June 1965).

Nucleate boiling of hydrogen, D. E. Drayer, Ind. Eng. Chem. Fundamentals **4,** No. 2, 167–171 (May 1965).

Observations of carbon monoxide and oxygen on tantalum with the field emission microscope, R. Klein, J. Chem. Phys. **41,** No. 2, 571 (July 1964).

Observations of dislocation sources in stainless steel, A. W. Ruff, Jr., and H. G. F. Wilsdorf, Acta Met. **13,** No. 6, 694–695 (1965).

On the identification of energy levels of negative ions, U. Fano and J. W. Cooper, Phys. Rev. **138,** No. 2A, A400–A402 (Apr. 1965).

On the nature of plasma resonance, W. M. Leavens, Physics Letters **15,** No. 4, 310–311 (Apr. 1965).

Optical constants of iron in the visible region, H. T. Yolken and J. Kruger, J. Opt. Soc. Am **55,** No. 7, 842–844 (July 1965).

Optical depolarization and scintillation measurements over a terrestrial path, J. R. Meyer-Arendt, Proc. 3d Tropospheric Refraction Effects Meeting **1,** 115–123 (Nov. 1964).

Optical detection of microwave transitions between excited electronic state of CN and the identification of the transitions involved, K. M. Evenson, J. L. Dunn, and H. P. Broida, Phys. Rev. **136,** No. 6A, A1566–A1571 (Dec. 14, 1965).

Optical radar using a corner reflector on the moon, C. O. Alley, P. L. Bender, R. H. Dicke, J. E. Faller, P. Franken, H. H. Plotkin, and D. T. Wilkinson, J. Geophys. Res. **70,** No. 9, 2267–2269 (May 1, 1965).

Optimization of the Czerny-Turner spectrometer, A. B. Shafer, L. R. Megill, and L. A. Droppleman, J. Opt. Soc. Am. **54,** No. 7, 879–887 (July 1964).

Photonuclear reactions, E. Hayward, Book, Nuclear Structure and Electromagnetic Transitions, ed. N. MacDonald, p. 141 (Oliver and Boyd, Edinburgh and London, England, 1965).

Possible implications of the observed profile of (λ 6374) FeX, C. Pecker-Wimel and R. N. Thomas, Astrophys. J. **141,** No. 2, 834–836 (Feb. 15, 1965).

Rearrangement kinetics of the liquid-liquid immiscible microphases in alkali borosilicate melts, W. Haller, J. Chem. Phys. **42,** 686–693 (1965).

Report of subcommittee D-atomic spectra, C. E. Moore, J. Opt. Soc. Am. Tech. Notes **55,** No. 6, 745 (1965).

Report of the acoustics research survey committee, R. K. Cook and G. W. Wood, J. Acoust. Soc. Am. **37,** No. 2, 392–395 (Feb. 1965).

Shell model treatment of nuclear reactions, M. Danos and W. Greiner, Phys. Rev. **138,** No. 1B, B93–B103 (Apr. 1965).

Shift of the R(0) and P(1) infrared lines of HCl perturbed by noble gases, A. Ben-Reuven, J. Chem. Phys. **42,** No. 6, 2037–2042 (Mar. 15, 1965).

Some measured rates for oxygen and nitrogen ion-molecule reactions of atmospheric importance, including $O^+ + N_2 \rightarrow NO^+ + N$, F. C. Fehsenfeld, A. L. Schmeltekopf, and E. E. Ferguson, Planetary Space Sci. **13,** 219–223 (Mar. 1965).

Spin-orbit coupling constant of nitric oxide. Determination from fundamental satellite band origins, T. C. James and R. J. Thibault, J. Chem. Phys. **41,** No. 9, 2806–2813 (Nov. 1964).

Surface ionization of niobium, M. D. Scheer and J. Fine, J. Chem. Phys. **42,** 3645 (1965).

Tables of dielectric constants, dipole moments and dielectric relaxation times, F. I. Mopsik, 1963 Dig. Lit. Dielectrics Publ. 1230, **27,** 23–55 (1964).

Tables of thermodynamic properties of air in chemical equilibrium including second virial corrections from 1500 °K to 15,000 °K, J. Hilsenrath and M. Klein, Arnold Eng. Develop. Center, Air Force Systems Command, AEDC–TR–65–58 (Arnold Air Force Station, Tenn., Mar. 1965).

The effect of moisture on surface flammability of coated and uncoated cellulosic materials, T. G. Lee, J. L. Loftus, and D. Gross, Am. Soc. Testing Materials Spec. Tech. Publ. **385,** 112–123 (May 1965).

Total photonuclear cross sections for low atomic number elements, J. M. Wyckoff, H. W. Koch, B. Ziegler, and R. Uhlig, Phys. Rev. **137,** No. 3B, B576–B594 (Feb. 1965).

Wave mode modification in liquid helium with clamped normal fluid, G. L. Pollack and J. R. Pellam, Proc. 9th Intern. Conf. Low Temperature Physics, Columbus, Ohio, Sept. 1964, p. 166 (Plenum Press Inc., New York, N.Y., 1965).

Width of the microwave lines of oxygen and their relationship to the thermal noise emission spectrum of the atmosphere, R. L. Abbott, Proc. 3d Symp. Remote Sensing of the Environment, Infrared Phys. Lab., Inst. Sci. Tech. Univ., Michigan, Ann Arbor, Mich., Feb. 1965, pp. 257–269 (Mar. 1965).

Widths of transmission Kikuchi lines in silicon and diamond, H. A. Fowler and L. Marton, J. Appl. Phys. **36,** No. 6, 1986–1995 (June 1965).

W-spin analysis of weak decays in U(12), D. Horn, M. Kugler, H. J. Lipkin, S. Meshkov, J. C. Carter, and J. J. Coyne, Phys. Rev. Letters **14,** No. 17, 717–719 (Apr. 1965).

W-spin and B-spin subgroups of SU(12), H. J. Lipkin and S. Meshkov, Phys. Rev. Letters **16,** No. 14, 670–672 (Apr. 1965).

A comparison of mountain slope and radiosonde observations, C. A. Sampson, Mo. Weather Rev. **93,** No. 5, 327–330 (May 1965).

A study of auroral absorption events at the South Pole: I. Characteristics of the events, J. K. Hargreaves, H. J. A. Chivers, and J. D. Petlock, J. Geophys. Rev. **69,** No. 23, 5001–5007 (Dec. 1964).

Attenuation of radio waves in the troposphere, B. R. Bean, Book, Advances in Radio Research 1, 121–155 (Academic Press Inc., New York, N.Y.. 1964).

ESD Maui, Hawaii, measurements, M. C. Thompson, Jr., Proc. 3d Tropospheric Refraction Effects Meeting **1,** 89–93 (Nov. 1964).

Formation of an electron depleted region in the ionosphere by chemical releases, J. W. Wright, D. Golomb, N. W. Rosenberg, and J. A. Barnes, (Proc. 4th Intern. Space Science Symp., Warsaw, Poland, June 4–10, 1963), Space Res. **IV,** 389–398 (North-Holland Publ. Co., Amsterdam, The Netherlands, 1964).

Ionosphere explorer I satellite: first observations from the fixed-frequency topside sounder, W. Calvert, R. W. Knecht, and T. E. VanZandt, Science **146,** No. 3642, 391–395 (Oct. 16, 1964).

Prediction of ionospheric characteristics at CRPL for sky-wave radio propagation at high frequencies, K. Davies, Telecommun. J. **31,** No. 12, 339–350 (Dec. 1964).

Radio astronomy observations with the $8.4 \times 10^4 m^2$ 50 Mc/s antenna of the Jicamarca radar in Peru, W. K. Klemperer and G. R. Ochs, Astron. J. **70,** No. 1327, 141–142 (Mar. 1964).

The contribution of non-thermal electrons to auroral absorption of radio waves, G. C. Reid, J. Geophys. Res. **69,** No. 15, 3296–3298 (Aug. 1964).

The daytime equatorial *F*-layer, R. B. Norton and T. E. VanZandt, J. Atmospheric and Terrest. Phys. **26,** 1047–1054 (1964).

The distribution of electrons in the lower and middle ionosphere, R. W. Knecht, Book, Progress in Radio Science 1960–1963, Vol. **III.** The Ionosphere, pp. 14–45 (Elsevier Publ. Co., Amsterdam, The Netherlands, 1965).

The light of the night sky: astronomical interplanetary and geophysical, F. E. Roach, Space Sci. Rev. **3,** 512–540 (Nov. 1964).

Characteristics of insoluble protein of tooth and bone—I, Fluorescence of some acidic hydrolytic fragments, S. A. Mancewicz and K. C. Hoerman, Arch. Oral. Biol. **9,** 535–544 (Oct. 1964).

Energy loss straggling of protons and mesons: tabulation of the Vavilov distribution, S. M. Seltzer, and M. J. Berger, Natl. Acad. Sci.-Natl. Res. Council Publ. 1133. Studies in the Penetration of Charged Particles in Matter, ch. 9, pp. 187–203 (1964).

Emission spectrum of CF, T. L. Porter, D. E. Mann, and N. Acquista, J. Mol. Spectry. **16,** 228 (June 1965).

H_2-transfer reactions in the gas-phase radiolysis of hydrocarbons, P. Ausloos and S. G. Lias, J. Chem. Phys. **43,** No. 1, 127–135 (July 1, 1965).

Osmotic and activity coefficients of tris (hydroxymethyl) aminomethane and its hydrochloride in aqueous solution at 25 °C, R. A. Robinson and V. E. Bower, J. Chem. Engr. Data **10,** No. 3, 246–247 (1965).

Oxygen atoms reaction with condensed olefins, R. Klein and M. D. Scheer, Science **144,** 1214 (1964).

Present status of project HAYSTAQ, E. C. Marden and H. R. Koller, (Proc. 3rd Annual Meeting Comm. Intern. Cooperation and Information Retrieval Among Examining Patent Offices, Vienna, Austria, Sept. 17–26, 1963), Book, Information Retrieval Among Examining Patent Offices, ed. H. Pfeffer, p. 163 (Spartan Books, Inc., Baltimore, Md., 1964).

Radiolytic stress relaxation of an ethylene-propylene copolymer, H. Yu and L. A. Wall, J. Phys. Chem. **69,** 2072–2078 (June 1965).

Reaction of deuterated polystyrenes with hydrogen and deuterium atoms, L. A. Wall and R. B. Ingalls, J. Chem. Phys. **41,** No. 4, 1112–1120 (Aug. 1964).

Some electrochemical aspects of germanium dissolution. Simultaneous chemical and electrochemical oxidation, W. E. Reid, Jr., J. Phys. Chem. **69,** No. 7, 2269–2277 (July 1965).

The heats of solution and oxidation of sulfur dioxide, W. H. Johnson and S. Sunner, Acta Chem. Scand. **17,** 1917–1924 (1963).

The kinetics of positive ion desorption from polycrystalline tungsten and rhenium, M. D. Scheer and J. Fine (Proc. Intern. Symp. Condensation and Evaporation of Solids, Dayton, Ohio, Sept. 12–14, 1962), Book, Condensation and Evaporation of Solids, ed. E. Rut-

ner, P. Goldfinger, and J. P. Huth, Paper 20, p. 327 (Gordon and Breach, New York, N.Y., 1963).

The molecular symmetry of iodopentaborane, L. H. Hall, J. Am. Chem. Soc. Commun. to Editor **86,** No. 21, 4729 (Nov. 5, 1964).

The structure of carbon subdioxide, W. J. Lafferty and A. G. Maki, Chemistry **37,** No. 7, 19 (July 1964).

Thermodynamics of solid carbon dioxide solubility liquid solvents at low temperatures, A. L. Myers and J. M. Prausnitz, Ind. Engr. Chem. **4,** No. 2, 209–212 (May 1965).

Thermogravimetric study of some new transition metal-schiff base coordination polymers, E. Horowitz, M. Tryon, and R. G. Christensen, J. Appl. Polymer Sci. **9,** 2321–2336 (1965).

Are our neighbors from abroad aware of standards and what standards can do for them? A. T. McPherson, Proc. 13th Annual Meeting Standard Engineering Society, New York, N.Y., Sept. 3, 1964, pp. 11A1–11A2 (1965).

Discussion of paper 63-39 I, "The measurement of short duration impulse voltages," by F. C. Creed and M. M. C. Collins. H. N. Cones, IEEE Trans. Commun. Electron. **EC-69,** 629 (Nov. 1963).

Intense resonance line sources for photochemical work in the vacuum ultraviolet region, H. Okabe, J. Opt. Soc. Am. **54,** 478 (Apr. 1964).

Letter to the Editor of Industrial Research in answer to letters regarding "Synthesis of Food", A. T. McPherson, Ind. Res. Feedback Col. **4,** No. 5, 15–16 (May 1962).

Spectral distribution of typical daylight as a function of correlated color temperature (condensed version), D. B. Judd, Illum. Eng. **60,** No. 4, 272–278 (Apr. 1965).

The Institute for Applied Technology, D. A. Schon, Engineer **V,** No. 2, 3 (Summer 1964).

The liquefaction of hydrogen. 3A. Basic principles, P. C. Vander Arend and D. B. Chelton, Book, Technology and Uses of Liquid Hydrogen, ch. 3, pp. 38–55 (Pergamon Press, Inc., New York, N.Y., 1964).

The work of NOMAD–1, W. Hakkarinen, Proc. Buoy Technology Symp., Washington, D.C., Mar. 24–25, 1964, p. 443 (Marine Technology Society, 1964).

What's new in control standards, H. L. Mason, Control Eng. **11,** No. 6, 85–87 (June 1964).

Approximations to the distribution of quadratic forms, M. M. Siddiqui, Ann. Math. Stat. **36,** No. 2, 677–682 (Apr. 1965).

Estimation for a one-parameter exponential model, J. A. Speckman and R. G. Cornell, J. Amer. Stat. Assoc. **60,** 560–572 (1965).

How people influence experimental results, J. R. Cornog, Proc. Social Statistics Section Convention, American Statistical Association, Cleveland, Ohio, pp. 119–122 (1964).

Inequalities for permanents and permanental minors, R. A. Brualdi and M. Newman, Proc. Cambridge Phil. Soc. **61,** Pt. 3, 741–746 (Jan. 26, 1965).

Mortality patterns in eight strains of flour beetles, D. B. Mertz, T. Park, and W. J. Youden, Biometrics **21,** No. 1, 99–144 (Mar. 1965).

On the binary collision expansion of the classical *N*-body Green's function, J. Weinstock, Phys. Rev. **126,** No. 1, 341–344 (Apr. 1, 1962).

On matching problems, J. Edmonds, A. J. Goldman, C. Witzgall, C. T. Zahn, Jr., Proc. ARO Working Group on Computers, ARO–D Report 65–1, pp. 46–50 (Office Chief Res. and Develop., Feb. 1964).

Paths, trees, and flowers, J. Edmonds, Can. J. Math. **17,** 449–467 (1965).

Plasma oscillations with collective correlations, C. M. Tchen, Proc. 6th Intern. Conf. Ionization Phenomena in Gases, Paris, France, July 8–13, 1963, I, 195–199 (P. Hubert Assoc., EURATOM–CEA Centra-d-Etudes Nucleaires de Fontenay-aux-Roses, Paris, France, 1963).

Realization of semimultipliers as multipliers, H. Fell and A. J. Goldman, Am. Math. Mo. **72,** No. 6, 639–641 (June–July 1965).

Some remarks on certain generalized Dedekind sums, H. Rademacher, Acta Arithmetica **9,** Sec. 1, 97–105 (1964).

Stochastic theory of diffusion in a plasma across a magnetic field, C. M. Tchen, Proc. Intern. Symp. Diffusion, Feldafing, Germany, June 29–July 3, 1964, pp. 118–123 (1964).

Comments on "Application of experimental design to the study of a test method", R. T. Thaxter and P. D. Hubbe. J. Mandel, Tappi **46,** No. 12, 193A–194A (Dec. 1963).

Educating metrologists, T. R. Young, Ordnance **XLIX,** No. 268, 432–435 (Jan.–Feb. 1965).

Measurement–R & D looks to future, W. A. Wildhack, Control Eng. **12,** No. 1, 75–76 (Jan. 1965).

Atomic scattering factors for the lithium and beryllium isoelectronic sequences from accurate analytic Hartree-Fock wave functions, C. M. Womack, Jr., and J. N. Silverman, Z. Kryst. **118,** No. 5–6, 422–433 (Sept. 1963).

Calculation of electronic energies in HCO_2^+, HCO_2 and HCO_2^-, W. H. Kirchhoff, J. Farren, and J. W. Linnett, J. Chem. Phys. **42,** No. 4, 1410–1422 (Feb. 15, 1965).

Calculations of the hyperfine splitting for the lithium atom, J. B. Martin and A. W. Weiss, J. Chem. Phys. Letter **39,** No. 6, 1618–1620 (Sept. 15, 1963).

Calculation of the radiative tail in the inelastic scattering of electrons, L. C. Maximon and D. B. Isabelle, Proc. Intern. Conf. Nuclear Physics, Paris, France, July 2–8, 1964, **2,** 1031–1033 (1964).

Coupling of particle-hole states and two particle-two hole states: splitting, W. Greiner and M. Danos, Compt. Rend. Congres Intern. Physique Nucleaire, ed. P. Gugenberger, **II,** 617 (Editions du Centre National de la Recherche Scientific, Paris, France, 1964).

Connection between shielding and stability in a collisionless plasma, F. Engelmann, M. Feix, and E. Minardi, Il Nuovo Cimento, Serie X **30,** 830–836 (Nov. 1963).

Dynamic theory of the nuclear collective model, M. Danos and W. Greiner, Phys. Rev. **134,** B285 (1964).

Electromagnetic properties of a quantized relativistic electron-positron gas, L. A. Steinert, Il Nuovo Cimento, Serie X **36,** 935–953 (Apr. 1965).

Experimental verification of the WLF superposition technique, A. J. Bur, Proc. Electrical Insulation Conf., Cleveland, Ohio, Oct. 1964, Natl. Acad Sci.-Natl. Res. Council Publ. 1238, pp. 70–71 (1965).

General report on fundamental spectroscopic data, C. E. Moore, (Proc. Intern. Astronomical Union Commission 14 Meeting, Hamburg, Germany, Aug. 1964), Trans. Intern. Astron. Union **XIIA,** 156 (July 1965).

Hypervelocity cratering data and a crater depth model for the regime of partical fluidity, O. G. Engel, Proc. 6th Hypervelocity Impact Symp., Cleveland, Ohio, Apr. 30–May, 1, 1963, pt. II, 337–366 (U.S. Army Ballistics Res. Lab., Aberdeen Proving Ground, Md., Aug. 1963).

Laboratory measurement of the rate of the reaction $O^+ + O_2 \rightarrow O_2^+ + O$ at thermal energy, F. C. Fehsenfeld, P. D. Goldan, A. L. Schmeltekopf, and E. E. Ferguson, Planet. Space Sci. **13,** 579–582 (Mar. 1965).

Minutes of the Meeting at Tokyo, Japan, of the Triple Commission for Spectroscopy, September 9, 1962, C. E. Moore, J. Opt. Soc. Am. **53,** No. 7, 883–893 (July 1963).

On the possibility of the measurement of the nuclear 2^4-pole deformation, M. Danos, W. Greiner, and C. G. Kohr, Physics Letters **12,** No. 4, 344 (1964).

Optical constants in the vacuum ultraviolet and electron energy losses, L. L. Marton, J. Quant. Spectr. Radiative Transfer **2,** 671–678 (May 1964).

Preliminary studies on the characterization of solution-grown ADP crystals, R. D. Deslattes, J. L. Torgensen, B. Paretzkin, and A. T. Horton, Advan. X-Ray Anal. **8,** 315–324 (1965).

Relation of the stacking fault energy to segregation at stacking faults and to the occurrence of phase boundaries in F. C. C. binary alloys, R. DeWit and R. E. Howard, ACTA Met. **13,** 655–661 (June 1965).

The determination of work function from the ratio of positive to negative surface ionization of an alkali halide, J. Fine, T. E. Madey and M. D. Scheer, Surface Sci. **3,** 227 (1965).

The gamma-ray distribution from oriented cerium-141 and its application to thermal contact at low temperature, J. F. Schooley and D. D. Hoppes (Proc. 8th Intern. Conf. Low Temperature Physics, Queen Mary College, London, England, Sept. 1963), Book, Low Temperature Physics, ed. R. O. Davies, pp. 435–436 (Butterworth, Inc., Washington, D.C., 1963).

The spin lattice relaxation time of some paramagnetic dispersions, P. H. Fang (Proc. XI Colloque Ampere, Eindhoven, The Netherlands, June 1962), Book, Magnetic and Electric Resonance and Relaxation, pp. 123–128 (1963).

Theoretical aspects of polymer crystallization with chain folds: bulk polymers, J. D. Hoffman, SPE Trans. 4, No. 4, 315–362 (Oct. 1964).

Utility of the Tait equation relating volume and pressure in the study of transitions in polymers, L. A. Wood, J. Polymer Sci. **B2,** No. 7, 703–707 (July 1964).

Unorthodoxy in science, L. A. Wood, J. Wash. Acad. Sci. **51,** 30 (Mar. 1961).

Vapor-phase growth kinetics of potassium and mercury crystals, R. L. Parker and S. C. Hardy (Proc. Intern. Symp. Condensation and Evaporation of Solids, Dayton, Ohio, Sept. 12–14, 1962), Book, Condensation and The Evaporation of Solids, Section II, Condensation of Solids, p. 649 (Gordon and Breach, New York, N.Y., 1964).

Volume relaxation of As_2O_3 in the glass transformation, A. B. Bestul, Proc. Intern. Conf. on Physics of Non-Crystalline Solids, Delft, The Netherlands, July 1964, pp. 426–435 (North-Holland Publ., Amsterdam, The Netherlands, 1965).

Wave functions for anharmonic oscillators by perturbation methods, A. M. Shorb, R. Schroeder, and E. R. Lippincott, J. Chem. Phys. **37,** 1043 (Sept. 1, 1962).

Dependence of the critical frequency of the ionospheric *E*-layer on solar zenith angle and the annual variation in *E*-layer ionization, T. Shimazaki, Nature **205,** No. 4974, 889–891 (Feb. 27, 1965).

Justification for neglecting the compressibility of the ionosphere in VLF radio propagation, J. R. Wait, IEEE Trans. Ant. Prop. **AP–13,** 480–481 (May 1965).

National Bureau of Standards Central Radio Propagation Laboratory, Boulder, C. G. Little, Astron. J. **69,** No. 9, 698–700 (Nov. 1964).

Natural electromagnetic phenomena below 30 kc/s, R. M. Gallet, NATO Advanced Study Institute, Bad Hamberg, pp. 167–204 (Plenum Press, Inc., New York, N.Y., 1964).

Propagation and technical factors in radio spectrum utilization, J. W. Herbstreit, Radio Spectrum Utilization, ed. J. W. Herbstreit, A report of the Joint Tech. Adv. Comm. of Inst. Elec. Electron. Eng., Inc., and the Electron Ind. Assoc., Chapt. III, pp. 30–208 (1964).

Representation of diurnal and geographic variations of ionospheric data by numberical methods. II. Control of stability, W. B. Jones and R. M. Gallet, Telecommun. J., pp. 1–12 (Place des Nations, Geneva, Switzerland, Jan. 1965).

The ionosphere; new guide, how to listen to the world, A. H. Shapley, World Publ. **11,** 15–18 (Hellerup, Denmark, Mar. 1965).

Crystal growth as chemical research, H. S. Peiser and J. L. Torgesen, Chemistry **38,** 15–20 (1965).

Infrared spectrum of the free radical NCN, D. E. Milligan, M. E. Jacox, J. J. Comeford, and D. E. Mann, J. Chem. Phys. **43,** No. 2, 756–757 (July 15, 1965).

Mass spectrometric study of the reaction of nitrogen atoms with ethylene, J. T. Herron, J. Phys. Chem. **69,** No. 8, 2736–2740 (Aug. 1965).

Frequency-dependent transport coefficients in fluid mechanics, R. Zwanzig, J. Chem. Phys. **43,** No. 2, 714–720 (July 15, 1965).

Thermal decomposition of 2,3-dimethylbutane in a single-pulse shock tube, W. Tsang, J. Chem. Phys. **43,** No. 2, 352–359 (July 15, 1965).

Xenon photosensitized formation of metastable nitrogen, M. D. Scheer and W. M. Jackson, Science **148,** 3678 (1965).

The temporal dimensional stability of surface-hardened steels, M. R. Meyerson, Metal Treating **15,** No. 6, 5 (Dec. 1964–Jan. 1965).

Analysis of the spectrum of triply ionized praseodymium (Pr IV), J. Sugar, J. Opt. Soc. Am. **55,** No. 9, 1058–1061 (Sept. 1965).

A one-dimensional model of polymer adsorption, E. A. DiMarzio and F. L. McCrackin, J. Chem. Phys. **43,** No. 2, 539–547 (July 1965).

Drift mobility and diffusion for impurities in ionic crystals, J. R. Manning, Phys. Rev. **139,** No. 6A, A2027–A2034 (Sept. 13, 1965).

Energy levels of polarons in a magnetic field, D. M. Larsen, Phys. Rev. **135,** No. 2A, A419–A426 (July 20, 1964).

Excitation of optically forbidden states in the ionization continuum by electron impact, J. A. Simpson, G. E. Chamberlain, and S. R. Mielczarek, Phys. Rev. **139,** No. 4A, A1039–A1041 (Aug. 1965).

Experiments in electron scattering, L. L. Marton, Lab. Invest. **14,** No. 6, pt. II, 754 (1965).

Investigation of the anomaly in the response of silicon semiconductor radiation detectors at low temperatures, W. R. Dodge, S. R. Domen, A. T. Hirshfeld, and D. D. Hoppes, IEEE Trans. Nuclear Sci. **NS–12,** 295 (Feb. 1965).

Letter to the Editor "Physical significance of the Fulcher equation", A. B. Bestul, Phys. Chem. Glasses **6,** No. 3, 108–110 (June 1965).

Localized-introduction concept on a curved vortex and motion of an elliptic vortex ring, R. J. Arms and F. R. Hama, Phys. Fluids **8,** No. 4, 553–559 (Apr. 1965).

Matter transport in solids, R. E. Howard and A. B. Lidiard, Rept. Progr. Phys. **XXVII,** 161–240 (1964).

Optical properties of beryllium in the ultraviolet from electron energy absorption, R. E. LaVilla and H. Mendlowitz, Appl. Opt. **4,** No. 8, 955–960 (Aug. 1965).

Thermal diffusion of substitutional impurities in metals, R. E. Howard and A. B. Lidiard, Acta Met. **13,** No. 4, 433–444 (1965).

**Publications for which a price is indicated are available by purchase from the Superintendent of Documents, U.S. Government Printing Office, Washington, D.C., 20402 (foreign postage, one-fourth additional). Reprints from outside journals and the NBS Journal of Research may often be obtained directly from the authors.*

U.S. GOVERNMENT PRINTING OFFICE : 1966 OL—794–732

jrnl-C/JUNE 46129
UNIVERSITY MICROFILMS INC
SERIALS SECTION
313 NORTH FIRST ST
ANN ARBOR MICH

UNITED STATES
GOVERNMENT PRINTING OFFICE
DIVISION OF PUBLIC DOCUMENTS
WASHINGTON, D.C. 20402

OFFICIAL BUSINESS

POSTAGE AND FEES PAID
U.S. GOVERNMENT PRINTING OFFICE

JOURNAL OF RESEARCH of the National Bureau of Standards
C. Engineering and Instrumentation

Vol. 70C, No. 1 January–March 1966

Contents

	Page
Coulometric calibration of microvolumetric apparatus. George Marinenko and John K. Taylor.	1
Effect of temperature and notch geometry on the tensile behavior of a titanium alloy. William D. Jenkins and William A. Willard.	5
Measurement standards for low and medium peak pulse voltages. A. R. Ondrejka and P. A. Hudson.	13
Temperature coefficient of rf permeability measurement using an impedance bridge as an equality indicating device. A. L. Rasmussen.	19
A test apparatus for the study of forced air-mixing devices. T. K. Faison, J. C. Davis, and P. R. Achenbach.	25
Publications of the National Bureau of Standards.	33

Library of Congress Catalog Card Number: 62-3900

For sale by the Superintendent of Documents, U.S. Government Printing Office, Washington, D.C., 20402. Price 75 cents (single copy). Subscription price: $2.75 a year; 75 cents additional for foreign mailing.
UNITED STATES GOVERNMENT PRINTING OFFICE, WASHINGTON : 1966